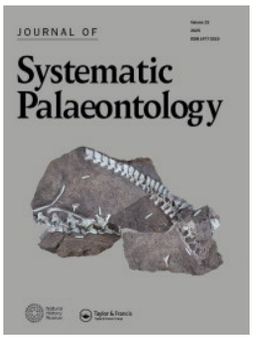

Journal of Systematic Palaeontology

ISSN: 1477-2019 (Print) 1478-0941 (Online) Journal homepage: www.tandfonline.com/journals/tjsp20

The enigmatic ailurid *Magerictis imperialensis* (Mammalia: Carnivora) unveiled: a systematic approach to the early Ailuridae

Jorge Morales, Juan Abella, Oscar Caballero, Daniel DeMiguel, Pablo Peláez-Campomanes & Alberto Valenciano

To cite this article: Jorge Morales, Juan Abella, Oscar Caballero, Daniel DeMiguel, Pablo Peláez-Campomanes & Alberto Valenciano (2025) The enigmatic ailurid *Magerictis imperialensis* (Mammalia: Carnivora) unveiled: a systematic approach to the early Ailuridae, Journal of Systematic Palaeontology, 23:1, 2571254, DOI: 10.1080/14772019.2025.2571254

To link to this article: https://doi.org/10.1080/14772019.2025.2571254

Journal of Systematic Palaeontology, 2025
Vol. 23, No. 1, 2571254
http://dx.doi.org/10.1080/14772019.2025.2571254

The enigmatic ailurid *Magerictis imperialensis* (Mammalia: Carnivora) unveiled: a systematic approach to the early Ailuridae

Jorge Morales[a]*, Juan Abella[b,c,d], Oscar Caballero[a], Daniel DeMiguel[c,e], Pablo Peláez-Campomanes[a] and Alberto Valenciano[f,g]*

[a]*Departamento de Paleobiología, Museo Nacional de Ciencias Naturales – CSIC, Madrid, Spain;* [b]*Grup d'Investigació en Paleontologia de Vertebrats del Cenozoic (PVC-GIUV), Departament of Botànica i Geologia, Universitat de València, Valencia, Spain;* [c]*Paleodiversity & Phylogeny Research Group, Institut Català de Paleontologia Miquel Crusafont, Universitat Autònoma de Barcelona, Edifici ICTA-ICP, c/Columnes s/n, Campus de la UAB, 08193 Cerdanyola del Vallès, Barcelona, Spain;* [d]*Instituto Nacional de Biodiversidad, Quito, Ecuador;* [e]*Departamento de Ciencias de la Tierra and Instituto Universitario de Investigación en Ciencias Ambientales de Aragón (IUCA), Área de Paleontología, Universidad de Zaragoza, Spain;* [f]*Departamento de Geodinámica, Estratigrafía, y Paleontología, Faculty of Geological Sciences, Universidad Complutense de Madrid, Madrid, Spain;* [g]*Research and Exhibitions Department, Iziko Museums of South Africa, Cape Town, South Africa*

(Received 21 November 2024; accepted 30 August 2025)

We present a detailed description of the craniodental and postcranial remains of the enigmatic *Magerictis imperialensis*, a basal Ailuridae previously known only from a single m2 from the Middle Miocene of the Madrid Basin (Spain). The discovery of new specimens from eight Middle Miocene (MN5–MN6) localities in Madrid has yielded comprehensive information on the dentition, mandibular morphology, and postcranial skeleton of this species. These new fossils provide an excellent opportunity to revise the phylogenetic relationships of *Magerictis* and related musteloids from the Oligocene and Miocene of Eurasia and North America. Our phylogenetic analysis indicates that *Magerictis* and *Rothictis* gen. nov. are the most basal members of the Aiuluridae. Both genera, together with *Alopecocyon*, *Actiocyon*, and *Protursus*, underwent a limited adaptive radiation during the Middle and Late Miocene in Eurasia and North America. This radiation potentially includes the ancestors of the most specialized ailurids (*Simocyon*, and the ailurines *Parailurus*, *Pristinailurus* and *Ailurus*). The postcranial elements attributed to *Magerictis*, particularly the astragalus and calcaneus, exhibit a morphological pattern comparable to that of *Ailurus*, thereby distinguishing it from other Musteloidea. A systematic rearrangement of the primitive Holartic musteloids from the Oligocene and Miocene is proposed. The Ailuridae are divided into three subfamilies: (i) Ailurinae for *Ailurus*, *Parailurus* and *Pristinailurus*; (ii) Simocyoninae, which includes *Simocyon*, *Protursus*, *Alopecocyon* and *Actiocyon*; and (iii) Magerictinae nov. rank for *Magerictis* and *Rothictis* gen. nov. (type species *Rothictis wintershofensis* comb. nov.). The family Amphictidae Winge, 1895 is revalidated for *Amphictis* and *Bonisictis* gen. nov. (type species *Bonisictis ambiguus* comb. nov.).

https://zoobank.org/urn:lsid:zoobank.org:pub:15D893D5-0C61-4652-8919-DAEF998F3953

Keywords: Iberian Peninsula, Miocene; Musteloidea; red panda

Introduction

The family Ailuridae Gray, 1843, is currently represented by a single genus, *Ailurus* Cuvier, 1825, which comprises one or two species (Glatston et al., 2022; Groves, 2022; Hu et al., 2022). Since the discovery in the early nineteenth century of *Ailurus fulgens* Cuvier, 1825 (red panda), this species has been the subject of considerable scientific interest due to its herbivorous adaptations as a bamboo-feeder, similar to that of the ursid *Ailuropoda melanoleuca* (David, 1869) (giant panda), with which it shows some convergences (Hu et al., 2017). However, *Ailurus* has an unusual dentition among extant carnivorans, since it does not resemble that of any other living species. For this reason, for a long time its systematic position within the Carnivora was unclear. It is with the works of Schmidt-Kittler (1981) and Wolsan (1993), based on fossil and extant species, that the Ailuridae was identified as a group closely related to other Musteloidea, occupying a basal position in their cladogenesis, a phylogenetic framework still accepted today.

Since the last decade of the twentieth century, with the emergence of molecular phylogenies, Ailuridae have been included in the superfamily Musteloidea Gray, 1843 together with Mustelidae, Procyonidae and

*Corresponding authors. Emails: jorge.morales@mncn.csic.es; albvalen@ucm.es

Published online 01 Dec 2025

Mephitidae (see Morlo & Peigné, 2010 for an overview). Despite this, there is no consensus regarding the phylogenetic relationships among these four families. Koepfli et al. (2017, and references therein) presented three different hypotheses: (i) *Ailurus* separates first from the rest of the families and Mephitidae appears to be a sister group to Procyonidae + Mustelidae; (ii) Mephitidae separates first and Ailuridae is the sister group of Procyonidae + Mustelidae; (iii) Ailuridae and Mephitidae are sister groups. Koepfli et al. (2017) indicated that the second hypothesis would be the most likely, with additional support provided by more recent studies (Law et al., 2018; Wang et al., 2023). However, Hassanin et al. (2021) and Winter et al. (2023) presented alternative evidence in favour of the third hypothesis.

Although the fossil record of the Ailuridae is scarce, it provides valuable insights into the systematic position of this family within the order Carnivora. Species exhibiting strong molarization of the premolars and structural complexity of the molars comparable to that of the extant *A. fulgens* have been identified in the basal Pliocene of North America, including *Pristinailurus bristoli* Wallace and Wang, 2004 (Wallace, 2011, Wallace & Lyon, 2022) and three species of *Parailurus* Schlosser, 1899, which dispersed throughout the Northern Hemisphere continents during the Pliocene (Dawkins, 1888; Fejfar, 1964; Fejfar & Sabol, 2004; Kormos, 1934; Kundrát, 2022; Morlo & Kundrat, 2008; Morlo & Peigné, 2010; Newton, 1890; Ogino et al., 2009; Sotnikova, 2008; Tedford & Gustafson, 1977; Wallace & Lyon, 2022). The cranial morphology and hypocarnivorous adaptation of the dentition of the Ailurinae identify them as a monophyletic clade. According to a recent phylogenetic analysis by Wallace and Lyon (2022), this clade comprises two tribes: Ailurini, which includes the extant *Ailurus*, and Pristinailurini, which includes the extinct *Parailurus* and *Pristinailurus*.

The relationship between Ailurinae and *Simocyon* as a sister group, based on a series of cranial characters proposed by Wang (1997) and later supported by additional evidence (Antón et al., 2006; Peigné et al., 2005; Salesa et al., 2006, 2008, 2011), has significantly altered the concept of Ailuridae. This has resolved the controversy about the systematic position of *Simocyon* (e.g. Beaumont, 1964, 1986; Pilgrim, 1931; Thenius, 1949b; Viret, 1951; Wolsan, 1993; Zdansky, 1924). Nevertheless, there are important interpretative systematic difficulties due to the hypocarnivorous dental adaptation of *Ailurus*, which is morphologically distant from the hypercarnivorous dentition of *Simocyon.* Both dentitions are autapomorphic within the Ailuridae clade. For this reason, the plesiomorphic forms attributed to this family, such as *Alopecocyon* Camp and Vanderhoof, 1940, *Actiocyon* Stock, 1947, *Protursus* Crusafont and Kurtén, 1976, *Magerictis* Ginsburg, Morales, Soria, and Herráez 1997, and *Amphictis* Pomel, 1853 (see Morlo & Peigné, 2010; Salesa et al., 2011), are clearly mesocarnivorous and therefore capable of evolving towards opposite dental adaptations. The divergence between Ailurinae and *Simocyon* was already established during the beginning of the Late Miocene (Vallesian mammalian age), as evidenced by the presence of *Simocyon diaphorus* (Kaup, 1832) in Central European localities such as Eppelsheim and Rudabánya (Kullmer et al., 2008; Werdelin, 2005), or even older if the determination of *Simocyon* sp. from the Chinese Middle Miocene of the Lower Halamagai Formation is confirmed (Wang et al., 1998).

Protursus was considered a synonym of *Simocyon* by Thenius (1977), a hypothesis not shared in later works (Peigné et al., 2005). Recently, Kargopoulos et al. (2022) have indicated a possible presence of *Protursus* in the early late Miocene of Hammerschmiede (Germany) and Rudánbanya (Hungary). *Alopecocyon* from the Middle Miocene of Europe has been commonly related to *Simocyon* (e.g. Beaumont, 1964, 1976; Morlo & Peigné, 2010; Thenius, 1949b; Viret, 1951), except for Wolsan (1993) who synonymized it with *Amphictis*. Its presence in the Middle Miocene of China is doubtful (Wang et al., 1998). *Actiocyon* from the Middle and Late Miocene of North America (K. Smith et al., 2016; Stock, 1947) has a similar morphological dental pattern to *Alopecocyon*. Webb (1969) considered *Actiocyon* and *Alopecocyon* synonymous, while Baskin (1998b) interpreted them as closely related but generically separated. Morlo and Peigné (2010) also regarded them as synonyms, a view not shared in the present work.

Amphictis antiquus Pomel, 1853, the type species of the genus, has a controversial history due to difficulties in interpreting its diagnosis, which has been the subject of considerable debate (Beaumont, 1976; de Bonis, 1973; Dehm, 1950; Schlosser, 1887; Teilhard de Chardin, 1915; Viret, 1929b). The quality of new fossils attributed to *Amphictis ambiguus* (Gervais, 1872) from the Quercy sites (Late Oligocene) (e.g. de Bonis, 1976; Cirot, 1992; Cirot & de Bonis, 1993) has led to this species being considered more representative of *Amphictis*. However, the paraphyletic nature of this genus (Morlo & Peigné, 2010) obscures our understanding of the origin of the Ailuridae clade and complicates the systematics of the cladogenesis of the Musteloidea. A rearrangement of the species included in *Amphictis* has been deemed necessary for the systematic interpretation

of *Magerictis imperialensis* Ginsburg, Morales, Soria, and Herráez, 1997.

Magerictis imperialensis was defined on the basis of a single m2 from the Estación Imperial site, from the Middle Miocene of the Madrid Basin, Spain (Middle Aragonian, local biozone Dc) (Ginsburg et al., 1997). The morphology of the m2 is highly derived. It is characterized by the remarkable elongation of the talonid due to the strong development of the hypoconulid, which forms a third lobe, similar to what is observed in both extant and extinct ailurids (Ogino et al., 2009; Wallace & Lyon, 2022) and some procyonids (Baskin, 1998b). In addition, the arrangement of the trigonid cuspids on the periphery, which is associated with the loss of the internal cristids of the protoconid and metaconid, results in the union of the valleys of the trigonid and the talonid, representing the singular features of *M. imperialensis.* The authors of this species have demonstrated the ailurid character of this molar and placed it at the base of the radiation of the family. Subsequent authors have accepted this relationship, but the limited availability of material has hindered further investigations (Salesa et al., 2011; Wallace & Lyon, 2022). Recent palaeontological finds in the urban area of Madrid, including associated maxillae and mandibles, have enabled us to expand our understanding of this species. This work aims to conduct a taxonomic and systematic analysis of *M. imperialensis* and its relationship with other musteloids related to the origin of Ailuridae.

Geological setting

The fossil sites containing *M. imperialensis* are located within the metropolitan area of Madrid, near the northwestern edge of the Cenozoic Madrid Basin in Spain (Fig. 1). During most of the Miocene, this region was predominantly occupied by marsh and lacustrine environments, fed by fluvial currents from the Sistema Central highlands (Calvo et al., 1989). These processes led to the accumulation of significant sediment thicknesses. The fossiliferous sediments in the study area are found at altitudes ranging from 570 to 635 m, dating back to the Middle Miocene, approximately 15.5–13.55 Ma (Fig. 2).

Remains of *Magerictis* have been found within two of the main lithostratigraphical units recognized in the Madrid Basin: the upper part of the Lower Unit and the lower part of the Intermediate Unit (Hernández-Ballarín & Peláez-Campomanes, 2017). Localities including Estación Imperial (E. Imperial, MN5), Embajadores (EMB-PG3, MN5), Los Nogales (NOG, MN5), Príncipe Pio-2 (PP-2, MN5), and Fábrica de Mahou (FMH, MN5), are situated within the Lower Unit and are correlated to local biozone Dc. The localities of the

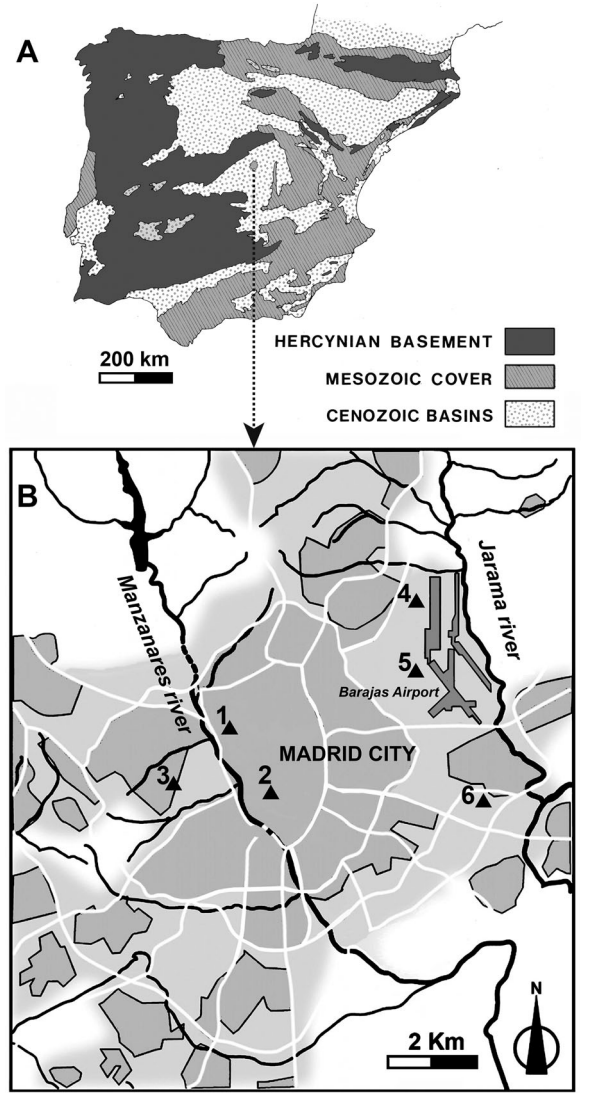

Figure 1. Location of the fossil sites with *Magerictis imperialensis*. **A**, Simplified geological map of the Iberian Peninsula with the location of the urban area of the city of Madrid. **B**, Fossil localities with *Magerictis imperialensis*: **1**. Príncipe Pío-2; **2**. Estación Imperial (type locality), Fábrica de Mahou, Los Nogales and Embajadores; **3**. Alhambra-Túneles; **4**. Barajas-17; **5**. Barajas-3; **6**. El Cañaveral.

Intermediate Unit belong to three local biozones. The sites Barajas-3 (BAR-3, MN5) and Barajas-17 (BAR-17, MN5) are correlated with local biozone Dd. In contrast, the site of El Cañaveral (CAÑ, MN5) belongs to the local biozone E, whereas the site of Alhambra-Túneles (ALH-TU, MN6) belongs to the local biozone F (Fig. 2) (Hernández-Ballarín & Peláez-Campomanes, 2017). The boundary between the two units is marked by a stratigraphical discontinuity dated by magnetostratigraphy to chron C5ADn, calibrated by interpolation to approximately 14.4 Ma (Montes et al., 2006). Biozone Dd,

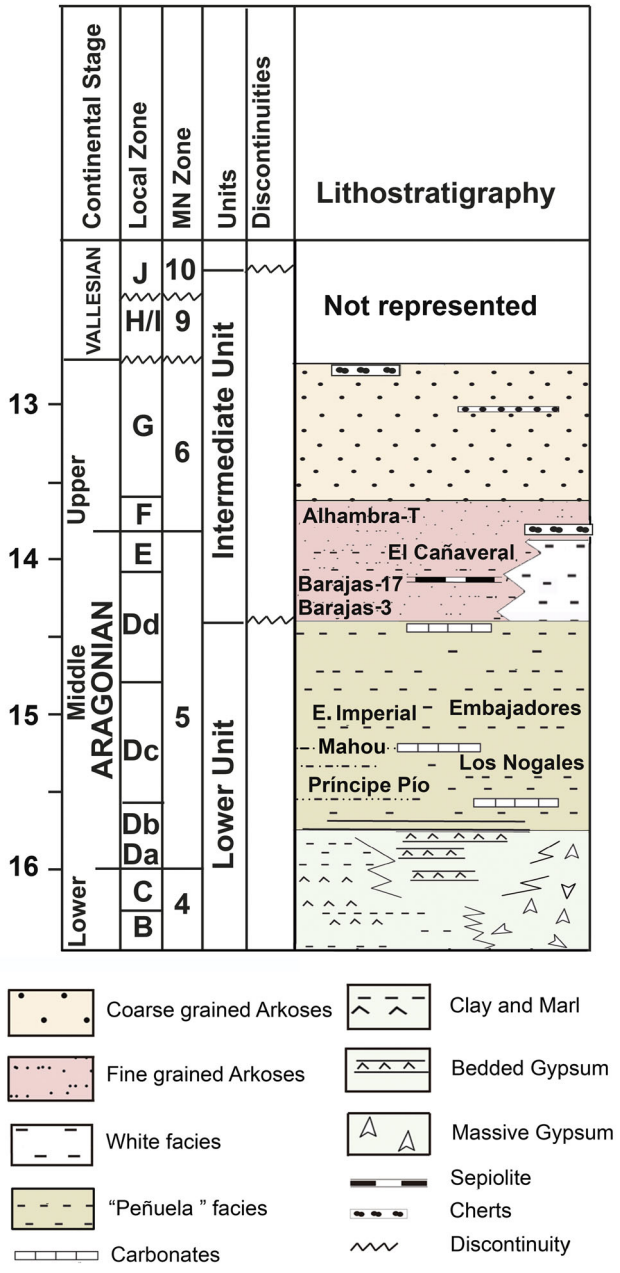

Figure 2. Biostratigraphy and lithostratigraphy of the Miocene localities with *Magerictis imperialensis*. The lithostratigraphical scheme is modified from Calvo et al. (1993), López-Martínez et al. (1987) and Peláez-Campomanes et al. (2003). Local zonation from Daams et al. (1999). MN zones from Bruijn et al. (1992) and Mein (1975). **Abbreviations: E,** Estación; **MN,** Mammal Neogene zones, **T**, Túneles.

which included the boundary between the two units, was dated by Van der Meulen et al. (2012) to 14.81–14.09 Ma in the Aragonian type area. This correlation has been confirmed by Hernández-Ballarin and Peláez-Campomanes (2017) based on the rodent sequence in the Madrid Basin. The deposits containing *M. imperialensis* span a time range of approximately 2 My (15.5–13.55 Ma). This interval coincides with the Middle Miocene Climate Transition (MMCT), marking the end of the high temperatures of the Miocene Climatic Optimum (MCO) and the beginning of the cooling trend of the Neogene (Domingo et al., 2012; García-Paredes et al., 2016).

The *Magerictis* localities dated as biozone Dc, Estación Imperial, Embajadores, Los Nogales, Príncipe Pío-2, and Fábrica de Mahou (Figs. 1–2) are situated on the eastern bank of the Manzanares River, within the historic city centre of Madrid, near the classic sites of San Isidro and Puente de Toledo, known since the mid-nineteenth century (Peláez-Campomanes et al., 2003). The fossil sites of Los Nogales (Herráez et al., 2006) and Embajadores (Hernández-Ballarín & Peláez-Campomanes, 2017) are located in the so-called 'Peñuela' facies, which consists of dark greenish-brown plastic clays with sepiolite levels. In contrast, the sites of Príncipe Pío-2, Fábrica de Mahou and Estación Imperial are somewhat more detritic facies, representing lateral changes within the Peñuela facies (Ginsburg et al., 1997; Pickford & Morales, 2016; Roca et al., 2009; Salesa et al., 2024).

The biozone Dd localities of Barajas-3 and Barajas-17 are located at the Madrid-Barajas International Airport and were discovered during various runway extension projects (Esteban, 2004). The fossils are found in arkosic sediments interbedded with brown clays and sands.

The El Cañaveral site (biozone E) was discovered during the construction of a new residential area south of Barajas airport. Fossils here are preserved within brown clay sediments, containing organic material and silex nodules, at the top of a sequence of green and white clays with silex nodules. The fossils show signs of prolonged exposure to the external environment prior to burial, including fractures, deformations and various degrees of corrosion (Pesquero et al., 2008).

The site of Alhambra-Túneles (biozone F) was discovered on the west bank of the Manzanares River less than 2 km from the classic site of San Isidro, during the construction of a new road (Herráez et al., 2000). The fossiliferous sediments consist of massive brown clays and sands.

The large mammals from biozones Dc and Dd localities associated with *Magerictis* correspond to the typical fauna found in the Tagus basin during much of the Middle Aragonian. Antunes (1979) referred to this fauna as 'Faunas with *Hispanotherium*', referencing the abundance of this medium-sized hornless Elasmotheriini rhinoceros, interpreted as a species suited to arid and warm environments (Cerdeño & Nieto, 1995; Sanisidro et al., 2012). Large ruminants such as *Tricheromeryx*

(Palaeomerycidae) are also common, while the abundance of *Anchitherium* (Equidae) varies among localities. It is abundant at Los Nogales, scarce at Estación Imperial and Barajas-3 and 17, and very rare in Príncipe Pío-2.

El Cañaveral (biozone E) and Alhambra-Túneles (biozone F) exhibit a markedly different large mammal composition from that the other *Magerictis*-bearing sites. *Anchitherium* remains abundant in Alhambra, but is represented by a different species than in the Dc–Dd biozones (Sánchez et al., 1998). This new faunal assemblage is characterized by the disappearance of *Hispanotherium* and the substantial renewal of the ruminant assemblage, with palaeomerycids becoming very rare and cervids and bovids becoming abundant. Bunodont suids also disappear, coinciding with the appearance of the first tetraconodont suids represented by *Retroporcus* and *Conohyus* (see Pickford & Laurent, 2014; Pickford & Morales, 2016).

Materials and methods

Nomenclature and measurements

Dental nomenclature follows Ginsburg (1999) and J. B. Smith and Dodson (2003). The nomenclature of the m2 is explained in Figure 3 and the nomenclature for the tarsals is explained in Figure 4. Anatomical descriptions are based primarily on Barone (1999, 2000), Evans and de Lahunta (2010, 2013) and Schaller (2007). The terminology conforms to the standard of the Nomina anatomica veterinaria (NAV; Waibl et al., 2005). Measurements were taken using Mitutoyo Absolute digital callipers to the nearest 0.1 mm (Supplemental material 1, S1).

Institutional abbreviations

AMNH, American Museum of Natural History, New York, USA; **B and Bat-1**, Batallones-1 temporarily housed in MNCN (Madrid, Spain); **ETMNH**, East Tennessee Museum of Natural History, Johnson City, USA; **FMNH**, Field Museum of Natural History, Chicago, USA; **FS-LPVP**, Faculté Sciences; Laboratoire de Paleontologie des Vertébrés, Poitiers, France; **FSM**, Faculté des Sciences de Marseille, France; **IPS**, collection of the Institut Català de Paleontologia Miquel Crusafont, Barcelona, Spain; **LACM**, Natural History Museum of Los Angeles County, Los Angeles, USA; **MACN**, Museo Argentino de Ciencias Naturales 'Bernardino Rivadavia', Buenos Aires, Argentina; **MDC**, Musée des Confluences, Lyon, France; **MNCN**,

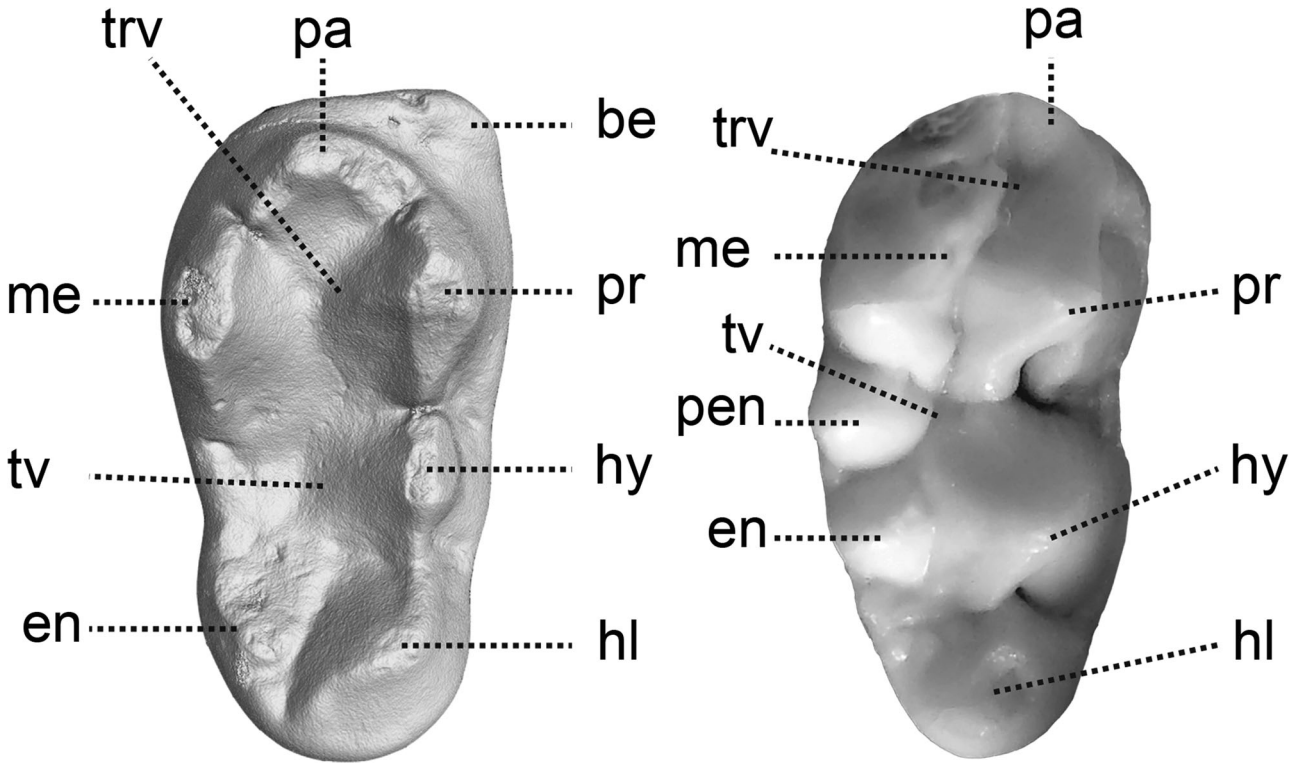

Figure 3. Dental nomenclature of the right m2 of Ailuridae. **Left**, *Magerictis imperialensis*; **right**, *Ailurus fulgens* (mirrored). **Abbreviations**: **be**, basal expansion (mesiobucal); **en**, entoconid; **hl**, hypoconulid; **hy**, hypoconid; **me**, metaconid; **pa**, paraconid; **pen**, pre-entoconid; **pr**, protoconid; **trv**, trigonid valley; **tv**, talonid valley.

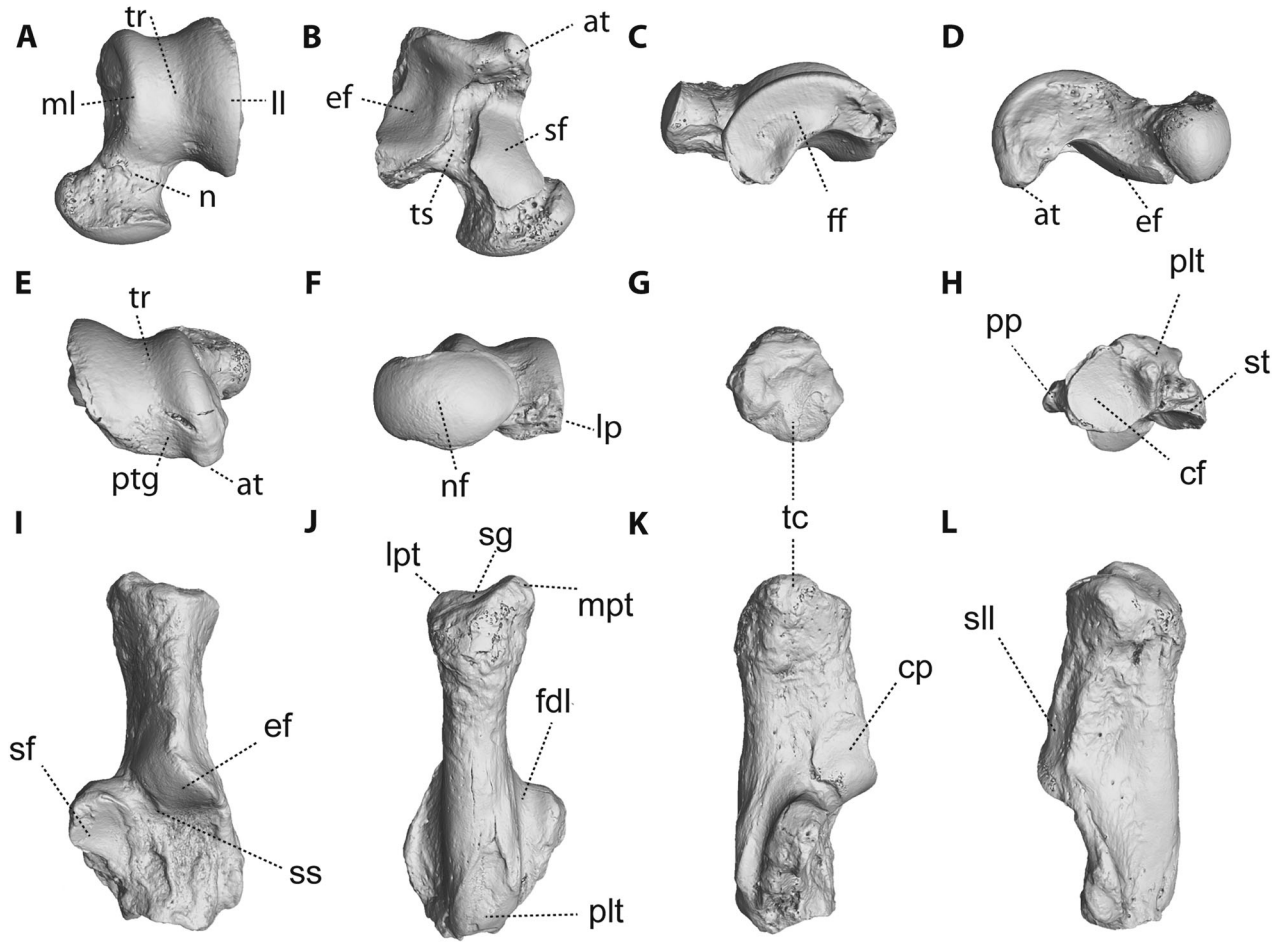

Figure 4. *Magerictis imperialensis* from Fábrica de Mahou locality. Tarsal nomenclature used for the astragalus and calcaneum. **A–F**, astragalus: **A**, dorsal view; **B**, plantar view; **C**, medial view; **D**, lateral view; **E**, proximal view; **F**, distal view. **G–L**, calcaneum: **G**, proximal view; **H**, distal view; **I**, dorsal view; **J**. plantar view; **K**, medial view; **L**, lateral view. **Abbreviations**: **at**, astragalar tubercle (proximomedial plantar tuberosity); **cf**, cuboid facet; **cp**, coracoid process; **ef**, ectal facet; **fdl**, groove for the tendon of m. flexor digitorum lateralis; **ff**, fibular facet; **ll**, lateral lip; **lp**, lateral process; **lpt**, lateral process of tuber; **ml**, medial lip; **mpt**, medial process of tuber; **n**, neck; **nf**, navicular facet; **plt**, plantar tubercule; **pp**, peroneal process; **ptg**, plantar tendon groove; **sf**, sustentacular facet; **sg**, sagittal groove; **sll**, groove for the insertion of the short lateral-collateral ligament; **ss**, sustentacular sulcus; **st**, sustentaculum tali; **tc**, tuber calcis; **tr**, trochlea (astragalar tibial facet); **ts**, tarsal sinus.

Museo Nacional de Ciencias Naturales-CSIC, Madrid, Spain; **MNHN**, Muséum national d'Historie naturelle, Paris, France; **NHMW**, Naturhistorisches Museum Wien, Vienna, Austria; **NRM**, Naturhistoriska rikmuseet, Stockholm, Sweden; **SMNS**, Staatliches Museum für Naturkunde Stuttgart, Stuttgart, Germany; **SNSB-BSPG**, Staatliche Naturwissenschaftliche Sammlungen Bayerns, Munich, Germany; **UCBL-FSL**, Université Claude Bernard Lyon 1, Faculté des Sciences de la Terre, Lyon, France; **UCMP**, University of California Museum of Paleontology, Berkeley, USA; **YPM-PU**, Peabody Museum of Natural History at Yale University, Connecticut, USA.

Studied material

The fossil remains of *M. imperialensis* are stored in the collections of the Department of Paleobiología of MNCN. For specific details of each specimen, see the studied material in the section on Systematic palaeontology.

Comparative material

The primary comparative sample of cranial material is based on a direct study of the original fossils. When the analysis is based on casts or photographs, this is noted. *Pseudobassaris riggsi* Pohle, 1917, from Quercy (Oligocene, France) (hemimandibles determined by

Wolsan, 1993, SNSB-BSPG 1879 XV 713, 716, 718; skull, AMNH 117488, cast of the original YPM-PU 11455; as well as the original publication of Wolsan & Lange-Badré, 1996); *Plesictis robustus* Pomel, 1853 from Quercy (Late Oligocene, France) (maxilla, MNHN.F. QU-9117; mandible UCBL-FSL 7223); *Plesictis genettoides* Pomel, 1846, from Peublanc (Late Oligocene, MP30, France) (cranial and postcranial bones, AMNH 11001); *Amphictis schlosseri* Heizmann and Morlo, 1994, from Ulm-Westtangente (Early Miocene, MN2, Germany) (skull, SMNS-45756; hemimandible SMNS-45758, 45759, M1 SMNS-45757), and from Eggingen (Early Miocene, MN2, Germany) (hemimandible, SNSB-BSPG 1881 IX 571; M1, SNSB-BSPG 1881 IX 572); *Amphictis ambiguus* Gervais, 1872, from Quercy (Late Oligocene, France) (hemimandible MNHN-F QU-9244), and from Pech du Fraysse, Quercy (Late Oligocene, MP28, France) (skull, FS-LPVP PFRA28, photographs); *Amphictis borbonica* Viret, 1929b, from Coderet (Late Oligocene, MP30, France) (maxilla, UCBL-FSL 97711); *Amphictis antiquus* Pomel, 1853, from Saint Gérand le Puy (Early Miocene, MN2, France) (hemimandibles UCBL-FSL-213845, 213846, 213849, 213847 [cast, original figured in Viret, 1929b], and two maxillae UCBL-FSL-213850 and 213860 [casts, originals figured in Viret, 1929b]); *Amphictis aginensis* de Bonis, 1973, from Laugnac (Early Miocene, MN2, France) (mandible, cast of FSM Lg M-14); *Amphictis wintershofensis* Heizmann and Morlo, 1994, from Wintershof-West (Early Miocene, MN3, Germany) (hemimandibles SNSB-BSPG 1937 II 13126, 13132, 13138/9, 13147, 13191); *Alopecocyon leptorhynchus* (Filhol, 1881) from La Grive (Middle Miocene, MN7/8, France) (maxilla fragment, UCBL-FSL 213788; M1, UCBL-FSL 213789; maxilla fragment, AMNH 100028, cast, original figured in Gaillard, 1899), from Sansan (Middle Miocene, MN6, France) (hemimandible, cast of MNHN-San 345), from Göriach (Middle Miocene, MN5 to MN6, Austria) (association of upper and lower dentition, NHMW 470/1963); Devínská Nová Ves (= Neudorf an dem March) (Middle Miocene, MN6, Slovakia) (m2, NHMW N5); *Alopecocyon getti* Mein, 1958, from Vieux-Collonges (Middle Miocene, MN5, France) (M1, UCBL-FSL 65695; M2, UCBL-FSL 65694; m2, UCBL-FSL 65758); *Actiocyon leardi* Stock, 1947, from Apache Canyon (Middle–Late Miocene, Clarendonian, California, USA) (maxilla fragment, AMNH 6843, cast of LACM 2747); *Actiocyon parverratis* K. Smith et al., 2016, from Monarch Mill (Middle Miocene, Barstovian, Nevada, USA) (hemimandibles, UCMP 141928, photographs; maxilla fragment with P4, UCPM 141911, photographs); *Simocyon batalleri* (Viret, 1929a) from Batallones-1 (Late Miocene, MN10, Spain) (skull, B – 3620; skull, B – 3458; hemimandible, B – 5430; hemimandibles from the same individual B – 3392 and Bat – 1 – D7 – 7–2001; M2, B – 3235; m2 B – 4733; m2 B – 3238); *Protursus simpsoni* Crusafont and Kurtén, 1976, from Can Llobateres (Late Miocene, MN9, Spain) (m2, IPS-1976); *Parailurus tedfordi* Wallace and Lyon, 2022, from White Bluffs (Early Pliocene, Washington, USA) (M1, cast of LACM 10808); extant *Ailurus fulgens*, skulls and mandibles (MNCN M-142311, AMNH M146682, 35433, 35495, 119676, 169496, 164121, 164148, NRM-MA582386, 584529, 584903, 585304, 609530). Finally, we studied from their original publications *Amphictis milloquensis* (Helbing, 1928a) from La Milloque (Late Oligocene, MP29, France, Helbing [1928a], Cirot & Wolsan [1995]); and *Pristinailurus bristoli* Wallace & Wang, 2004, from Gray Fossil Site (Early Pliocene, Tennessee, USA; Wallace & Wang [2004]; Wallace & Lyon [2022]).

For descriptions and comparisons of the postcranial bones we used the following extinct and extant species of Musteloidea housed in the collections of FMNH, MACN, MNCN, NRM: Ailuridae (*Ailurus fulgens*; *Simocyon batalleri* from Batallones-1 see Salesa et al., 2008); Procyonidae (*Procyon lotor* Storr, 1780); Mustelidae (*Meles meles* [Linnaeus, 1758], *Gulo gulo* [Linnaeus, 1758], *Martes foina* [Erxleben, 1777], *Mustela putorius* Linnaeus, 1758, and *Taxidea taxus* Waterhouse, 1838); Mephitidae (*Mephitis mephitis* [Schreber, 1776], *Conepatus chinga* [Molina, 1782], *Conepatus leuconotus* [Lichtenstein, 1832], *Spilogale gracilis* Merriam, 1890, *Mydaus javanensis* [Desmarest, 1820]).

Cladistic analysis

We performed a cladistic analysis to elucidate the phylogenetic position of *M. imperialensis* and other European and North American extinct taxa with musteloid affinities from the Eocene to the Pliocene, as well as the extant *Ailurus fulgens*. We analysed 13 operational taxonomic units (OTUs) and 54 cranial, mandibular and dental characters based on Baskin (1998a, 2004), Bryant et al. (1993), Morlo and Peigné (2010), Valenciano et al. (2016), Wallace and Lyon (2022), Wolsan (1993) and this work. The extinct forms analysed are *Pseudobassaris riggsi* from Quercy (France); *Amphictis schlosseri* from Ulm-Westtangente and Eggingen (Germany); *Amphictis ambiguus* from Quercy and Pech du Fraysse (France); *Amphictis milloquensis* from La Milloque (France); *Amphictis antiquus* from Saint Gérand le Puy (France); *Amphictis wintershofensis* from Wintershof-West (Germany); *M. imperialensis* from Estación Imperial, Los Nogales, Príncipe Pio-2, Barajas-3, Barajas-17, El Cañaveral, Embajadores and Alhambra-Túneles (Spain); *Alopecocyon leptorhynchus* from La Grive, Sansan (France), Göriach (Austria) and

Devínská Nová Ves (Slovakia); *Actiocyon leardi* from Apache Canyon (California, USA); *Actiocyon parverratis* from Monarch Mill (Nevada, USA); *Simocyon batalleri* from Batallones-1 (Spain); *Pristinailurus bristoli* from Gray Fossil Site (Tennessee, USA). All characters were equally weighted and unordered. The complete list of taxa, characters and the character–taxon matrix are available in Supplemental materials 1 and 2. The data supporting the findings of this study is openly available through MorphoBank at https://doi.org/10.7934/P6014 (Morales et al. 2025a). The selected outgroup was *Pseudobassaris riggsi*. Cladistic analysis was performed using PAUP*4.0b10 (Swofford, 2002). Clade support was calculated using bootstrap analysis with 10,000 replicates and Bremer support values.

Micro CT scans

The acquisition of three-dimensional reconstructions was performed using computed axial tomography (CT) employing a NIKON XT H-160 µCT-SCAN provided by the Non-Destructive Techniques Service at the National Museum of Natural Sciences (MNCN-CSIC). The virtual reconstructions were processed and the final images were generated using the VGStudio MAX software v. 3.0. The data supporting the findings of this study is openly available through MorphoSource, where the full media list can be found at https://doi.org/10.17602/M2/L780594 (Morales et al. 2025b)

Systematic palaeontology

Order **Carnivora** Bowdich, 1821
Suborder **Caniformia** Kretzoi, 1943
Superfamilia **Musteloidea** Kretzoi, 1929
Family **Amphictidae** Winge, 1895

Type genus. *Amphictis* Pomel, 1853.

Diagnosis. In Cirot and Wolsan (1995).

Included genera. *Amphictis* and *Bonisictis* gen. nov.

Differential diagnosis. Amphictidae differs from Ailuridae by the simple morphology of their m2, characterized by moderate length, trigonid larger than the talonid, hypoconid placed buccally and hypoconulid vestigial or absent. As a result, the third lobe of the m2 that characterizes the Ailuridae is not fully developed in Amphictidae.

Genus ***Amphictis*** Pomel, 1853

Type species. *Amphictis antiquus* Pomel, 1853 (= *Viverra antiqua* de Blainville 1842 (pars). pp.72–73. vol. 2, pl. XIII).

Type locality. St-Gérand-le-Puy (Early Miocene, MN2, France).

Diagnosis. In Pomel (1853, pp. 63–64); see Viret (1929b).

Emended diagnosis. Amphictidae with high premolars; p4 with strong accessory distal cuspid; m1 with high and large trigonid and short talonid; robust m2 with short talonid with a well-developed hypoconid and small talonid valley placed lingually; Large P4 with strong protocone; M1 trigone with a well-developed postprotocrista, metaconule present or absent; M2 is small compared to M1.

Occurrence. Early Miocene, biozone MN2, Western Europe.

Remarks. All species previously classified in *Amphictis* are excluded from the genus, except *Amphictis antiquus* Pomel, 1853, and *Amphictis schlosseri* Heizmann and Morlo, 1994. *Amphictis ambiguus* Gervais, 1872, and *Amphictis milloquesis* (Helbing, 1928a) are included herein in *Bonisictis* gen. nov. (Amphictidae), whereas *Amphictis wintershofensis* Heizmann and Morlo, 1994, and *Amphictis prolongata* Morlo, 1996, are classified herein in *Rothictis* gen. nov. (Ailuridae). *Amphictis borbonica* Viret, 1929b, *Amphictis ageniensis* de Bonis, 1973, *Amphictis cuspida* Nagel, 2003, and *Amphictis timicua* Baskin, 2017, have an indeterminate generic status.

Amphictis antiquus Pomel, 1853

1842 *Viverra antiqua* de Blainville (pars): 72–73, pl. 13.
1853 *Amphictis antiquus* Nob. (*Viverra antiqua*, mandible, Blain.) Pomel: 63.
1859 *Viverra antiqua* Pomel in Gervais: 223, pl. 28, figs. 7–8.
1872 *Amphictis* Pomel in Gervais: 266.
1879 *Plesictis robustus* Pomel in Filhol: 124, pl. 22, fig. 9.
1879 *Plesictis robustus* (var, gracilis) Pomel in Filhol: 128, pl. 22, fig. 5.
1879 *Amphictis antiquus*, Pomel in Filhol: 171, pl. 24, figs. 1–4.
1885 *Amphictis antiquus*, Pomel in Lydekker: 102–103.
1929b *Amphictis antiquus* Pomel in Viret: 196, pl. 14, figs. 8–17.
1976 *Amphictis antiquus* (Pomel, 1853) in De Beaumont: 173, figs. 1a–2a.
1994 *Amphictis antiqua* Pomel in Heizmann and Morlo: 9–10.

Neotype. UCBL-FSL 213846, right mandible with p3–m2 (Fig. 5A–C). Based on the original publication (Pomel, 1853) it is impossible to identify the syntype of the species within Saint Gérand le Puy material (Viret, 1929b). We therefore choose one of the best-preserved

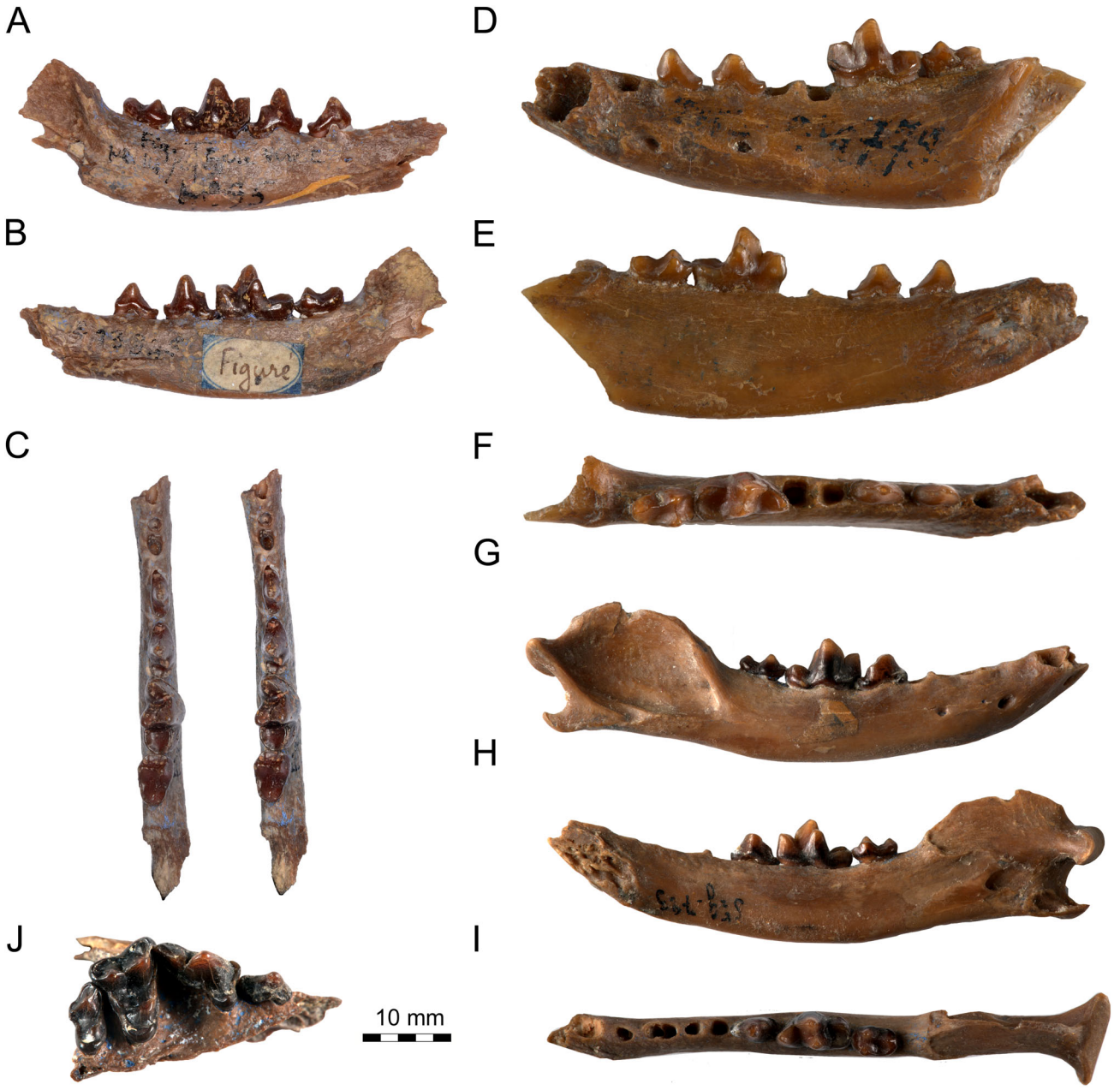

Figure 5. Lower and upper dentition of *Amphictis antiquus* from Saint Gérand le Puy (Early Miocene, MN2, France). **A–C**, UCBL-FSL 213846 (neotype), right hemimandible (figured in Viret 1929b, pl. XIV, fig. 9): **A**, buccal view; **B**, lingual view; **C**, occlusal view (stereo pair). **D–F**, MDC-StG 779, left hemimandible (figured in Viret 1929b, pl. XIV, fig. 10): **D**, buccal view; **E**, lingual view; **F**, occlusal view. **G–I**, MDC-StG 783, left hemimandible (figured in Viret 1929b, pl. XIV, fig. 11): **G**, buccal view; **H**, lingual view; **I**, occlusal view. **J**, MDC-StG 809, left maxilla in occlusal view.

specimens from this locality (UCBL-FSL 213846; Viret, 1929b, pl. XIV, fig. 9) and elevate it to the rank of neotype. The designation of this specimen appears necessary for the objective definition of the species.

Type locality. Terrain tertiaire à Lagny (France) (equivalent name for Saint Gérand le Puy).

Diagnosis. *Amphictis* with elongate P4 with strong protoconid, M1 with sub-rectangular occlusal shape, complete trigonid with metaconule attached to protoconid. M2 unreduced, buccolingually wide. m1 with very high and voluminous metaconid, basined talonid with small hypoconid, and entoconid and hypoconulid united in a

peripheral cristid. m2 elongated, with reduced paraconid and valley of talonid occupied almost entirely by a voluminous hypoconid.

Occurrence. Early Miocene, biozone MN2, Western Europe.

Remarks. *Amphictis antiquus* has been regarded as a problematic species, largely due to the paucity of information contained in the earliest figured materials (Blainville, 1842; Filhol, 1879; Gervais, 1859) and the low precision of the information provided by these authors (Schlosser, 1887, 1888). In this study (Fig. 5), we follow the approach taken by Viret (1929b) who conducted the first review of *Am. antiquus* from the type locality of Saint Gérand le Puy. Much of the debate surrounding the taxonomic status of this species has been centred on the interpretation of the m2 morphology (Schmidt-Kittler, 1981). In particular, de Bonis (1973) and Beaumont (1976) were highly critical in this aspect, proposing that the majority of the dentognathic material attributed by Viret (1929b) to *Am. antiquus* should have been determined as *Plesictis robustus* Pomel, 1853. Nevertheless, despite the necessity for a comprehensive revision of the species attributed to the genus *Plesictis* Pomel, 1853, *Am. antiquus* can be distinguished from *P. robustus*, both defined in the same locality of Saint Gérand le Puy. The diagnoses of Pomel (1853) clearly delineated the distinction between the two taxa. *Plesisctis robustus* is distinguished from *Am. antiquus* by a more sectorial m1 with a sharp talonid and smaller m2 (Teilhard de Chardin, 1915, fig. 10). In *Am. antiquus*, the talonid of m1 has low cusps and a well-developed central valley. The m2 is not reduced, although the talonid is almost exclusively formed by the hypoconid. Morlo and Peigné (2010) consider that the m2 morphology of *Am. antiquus* and *Am. schlosseri* represents the plesiomorphic condition in musteloids.

Description of the neotype. UCBL–FSL 213846 is a right mandible with p3–m2 and alveoli of p1 and p2 (Fig. 5A–C). Measurements (mm): p3 (5.6×2.3), p4 (7.1×3.3), m1 (9.6×5.4), m2 (6.1×4.4). The ascending ramus of the mandible has mostly broken and only preserves the most anterior part of the masseteric fossa. The mandibular body is high and robust. The p1 has a single oval alveolus and the p2 has two alveoli, the posterior one somewhat more developed. The p3 has a single cuspid that is relatively high and narrow, with the extended distal cristid ending in a reduced cingulid. The p4 is tall, robust and distally widened. The mesial accessory cuspid is low and narrow, while the distal accessory one is high, relatively large, and lingually displaced. The distal part of the tooth is surrounded by a crowned distal cingulid. The m1 is robust with a trigonid larger than the talonid. In occlusal view, the cuspids of the trigonid are arranged in a relatively open V. The height of the protoconid is notably high, while the metaconid is of a similar height to the paraconid but less developed. The two cusps are joined basally. The talonid is broad and formed by an extended hypoconid and a distolingual cristid corresponding to the hypoconulid and entoconid, which are poorly differentiated. The valley of the talonid is small. The m2 is large, with the trigonid being wider and larger than the talonid. It is formed by a well-developed protoconid and metaconid, with the protoconid being slightly higher and larger. Both cusps are connected by internal cristids. A rudimentary paraconid is included in the mesial cingulid. The mesial valley of the trigonid is relatively wide. The talonid is narrower than the trigonid and is formed almost exclusively by the hypoconid. A small distolingual cingulid occupies the position of the hypoconulid and the entoconid.

Amphictis schlosseri (Heizmann & Morlo, 1994)

1887 *Amphictis antiquus* Pomel in Schlosser: pl. 8, figs. 47, 56, 62.
1888 *Amphictis antiquus* (Pomel) in Schlosser: 119 f. (pars).
1976 *Amphictis antiquus* (Pomel, 1853) in de Beaumont: 173, fig. 1b.

Holotype. SMNS 45756, composed of a marl slab with a skull and mandibular fragments.

Type locality. Ulm-Westtangente, Baden-Württemberg, Germany (Early Miocene, MN2).

Diagnosis. In Heizmann and Morlo (1994, p. 4).

Differential diagnosis. It differs from *Am. antiquus* by its longer and more slender m2, the absence of M1 metaconule and the greater development of the M1 postprotocrista.

Other localities. Weisenau, Germany; Wiesbaden-Amöneburg, Germany; Eggingen, Germany; Michelserg bei Ulm, Germany (see Heizmann & Morlo, 1994).

Occurrence. Early Miocene, biozone MN2 of Western Europe.

Genus ***Bonisictis*** **gen. nov.**

Type species. *Bonisictis ambiguus* (Gervais, 1872).

Etymology. Named after Dr Louis de Bonis in recognition of his valuable contribution to the study of Caenozoic carnivorans.

Diagnosis. Schmidt-Kittler (1981, p. 776). Skull: Alisphenoid canal present. Middle ear amphictid. Tympanic bulla without ossified external auditory canal and laterally less deeply incised than in *Mustelictis*. Mastoid and paroccipital processes more pronounced; bony shelf between these and the bulla wider than in *Mustelictis*. Dentition: M2 three-rooted, larger than in *Mustelictis*; m2 distinctly elongated, with a reduced paraconid and closed trigonid.

Differential diagnosis. *Bonisictis* differs from *Amphictis* in the basined m2 morphology, characterized by a smaller hypoconid placed buccally, and a larger centrolingual talonid valley. It also differs in M1 more robust, with wider lingual wall and with an absent metaconule and postprotocrista.

Included species. *Bonisictis ambiguus* (Gervais, 1872) (Fig. 6), and *Bonisicts milloquensis* (Helbing, 1928a).

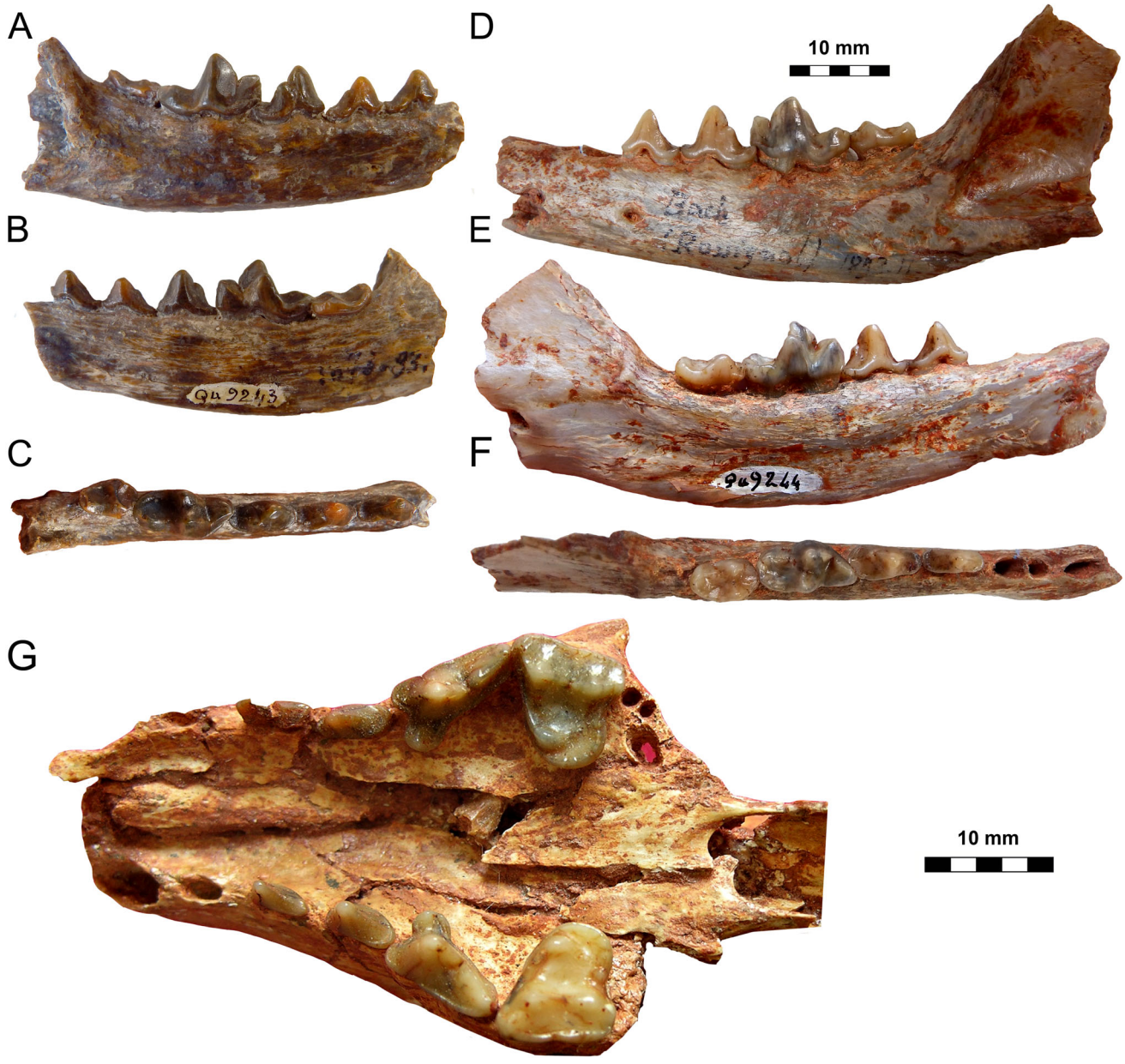

Figure 6. Lower and upper dentition of *Bonisictis ambiguus* from Quercy (Late Oligocene, France). **A–C**, MNHN-F-Qu 9243 (holotype), right hemimandible: **A**, buccal view; **B**, lingual view; **C**, occlusal view. **D–F**, MNHN-F-Qu 9244, left hemimandible: **D**, buccal view; **E**, lingual view; **F**, occlusal view. **G**, FS-LPVP PFRA-28, skull from Pech du Freysse, Quercy in occlusal view.

Occurrence. Late Oligocene, MP28 to MP29, Western Europe.

Remarks. Gervais (1872) included *Am. ambiguus*, even "provisionally", in the genus *Amphictis*, together with *Am. antiquus*, merging two temporally distant species with different m2 morphological patterns into a single genus. The definition of a new genus for *Am. ambiguus* seems justified, resolving the systematic problem of *Amphictis*.

Bonisictis ambiguus (Gervais, 1872)

1872 *Viverra* (*Amphictis*) *ambigua* Gervais: 266.
1873 *Viverra* (*Amphictis*) *ambigua* Gervais: 373, pl. 1, fig. 1.
1876 *Amphictis antiguus* Gervais: 51, pl. 13, figs. 10–10a.
1888 *Amphictis Gervaisi* Schlosser: 9, figs. 46, 47 (not fig. 18).
1915 *Amphictis ambiguus* Gervais 1872 in Teilhard de Chardin: 47, pl. 4, fig. 12, pl. 5, fig. 11, pl. 6, figs. 8, 10, 11, pl. 7, figs. 2, 6, 8.
1976 *Amphictis ambiguus* Gervais 1872 in de Bonis: 1327, figs. 1–2.
1976 *Plesictis milloquensis* Helbing 1928a, in Crouzel et al: 224, figs. 22–24
1981 *Amphictis ambiguus* Gervais 1867–1869 in Schmidt-Kittler: 776.
1992 *Amphictis ambiguus* (Gervais) 1872 in Cirot: 107, pl. 13, figs. 4–9, pl. 14, figs. 1–2, pl. 15, figs. 1–7.
1995 *Amphictis ambigua* (Gervais, 1872) in Cirot and Wolsan: 765, fig. 4.

Holotype. MNHN F.QU 9243, right mandible with p2-m2 (Fig. 6A–C).

Type locality. Concots, Quercy (France).

Diagnosis. In Cirot (1992).

Emended diagnosis. *Bonisictis* with robust lower premolars with low crowns, m2 with short trigonid and elongated talonid, smaller hypoconid placed buccally, hypoconulid vestigial or absent. M1 sub-quadrangular occlusal shape (mesiodistal length smaller than the buccolingual) due to the widening of the distal wall. However, the posterior crista of the protocone (postprotocrista) is poorly developed or even absent and the metaconule is weaker or absent.

Occurrence. Late Oligocene, Western Europe.

Other localities. Pech Desse (Late Oligocene, MP28), Pech du Fraysse (Late Oligocene, MP28) and Dieupentale (Late Oligocene, MP29) (France; Cirot, 1992; Crouzel et al., 1976).

Bonisictis milloquensis (Helbing, 1928a)

1928 *Plesictis milloquensis* n. sp. Helbing: 46, pl. 4, figs. 4–6.
1995 *Amphictis milloquensis* (Helbing, 1928a), Cirot and Wolsan: 758, figs. 1–2

Holotype. NMB LM 554, fragmentary left mandible with m1-m2 (Helbing, 1928a, p. 46, pl. 4, figs. 4–6).

Type locality. La Milloque, Late Oligocene, MP29, France.

Differential diagnosis. It differs from *B. ambiguus* by the lower premolars with higher crowns, shorter m2 talonid, and M1 with narrower lingual wall.

Occurrence. Late Oligocene, Western Europe.

Remarks. *Bonisictis* is considered a basal member of the Musteloidea based on its cranial morphology (Cirot & de Bonis, 1993; de Bonis, 1973; Schmidt-Kittler, 1981; Wolsan, 1993). The molars, particularly the morphology of the m2 and M1, distinguish it from *Amphictis* (Supplemental material 1, S3). Other basal musteloids, such as *Mustelictis* Lange, 1969 (Lange, 1970; de Bonis, 1997) and *Plesictis*, differ from *Bonisictis* by the relatively smaller size of the m2, which also has a shortened talonid with a prominent hypoconid and a reduced talonid valley. Therefore, these genera are more closely related to *Amphictis* than to *Bonisictis* in terms of m2 morphology. Furthermore, the proposed phylogenetic analysis excludes a direct relationship between *Bonisictis* and the Ailuridae.

Family **Ailuridae** Gray, 1843

Diagnosis. In Morlo and Peigne, 2010.

Included subfamilies: Ailurinae Gray, 1843; Simocyoninae Dawkins, 1868; and Magerictinae nov. rank.

Subfamily **Ailurinae** Gray, 1843

Type genus. *Ailurus* Cuvier, 1825.

Diagnosis. In Morlo and Peigne, 2010.

Included genera. *Ailurus* Cuvier, 1825; *Parailurus* Schlosser, 1899; and *Pristinailurus* Wallace and Wang, 2004.

Occurrence. Pliocene to present, North America, Asia and Europe.

Remarks. *Magerictis* was previously considered an Ailurinae by Morlo and Peigne (2010), Salesa et al. (2011) and Wallace and Lyon (2022). The new fossils of *Magerictis* described here lead to the exclusion of this genus from this subfamily.

Subfamily **Simocyoninae** Dawkins, 1868

Type genus. *Simocyon* Wagner, 1858.

Diagnosis. In Wolsan (1993), and Morlo and Peigné (2010).

Emended diagnosis. Ailuridae with not molarized teeth; m1 with elongated trigonid; P4 with reduced protocone; M1 with sub-quadrate occlusal shape.

Included genera. *Simocyon* Wagner, 1858; *Alopecocyon* Camp and Vanderhoof, 1940; *Actiocyon* Stock, 1947; and *Protursus* Crusafont and Kurtén, 1976.

Genus ***Simocyon*** Wagner, 1858

Type species. *Simocyon primigenius* Roth and Wagner, 1854.

Diagnosis. In Wolsan (1993).

Differential diagnosis. In Morlo and Peigné (2010).

Included species. *S. diaphorus*; *S. primigenius*; *S. batalleri*; *Simocyon hungaricus* Kadić and Kretzoi, 1927; *Simocyon marshi* Thorpe, 1921.

Occurrence. Late Miocene (MN9 to MN13) of Europe, Asia and North America.

Remarks. *Simocyon* is characterized by more hypercarnivorous adaptations, such as the reduced premolars, strengthened carnassial teeth, a buccolingually shortened M1 with well-developed buccal cusps, and smaller M2/m2 compared to the M1/m1 (Peigné et al. 2005; Wang, 1997).

Genus ***Alopecocyon*** Camp and Vanderhoof, 1940

Type species. *Alopecocyon leptorhynchus* (Filhol, 1881).

Diagnosis. In Morlo and Peigné (2010).

Emended diagnosis. Ailurid of small size; ascending ramus of the mandible projected backwards; lower premolars not reduced; p1 present; m1 with low trigonid, strong metaconid, and short talonid with moderate hypoconid; m2 elongated, with reduced trigonid, hypoconid and hypoconulid well developed, talonid valley lingually placed; P4 with poorly differentiated protocone similar to a widened cingulum; M1 robust, with sub-quadrate occlusal shape, and strong metaconule; M2 not reduced in comparison to the M1.

Occurrence. Middle Miocene (MN5 to MN7/8) Western Europe.

Alopecocyon leptorhynchus (Filhol, 1881)

1881 *Viverra leptorhyncha* Filhol: 67, pl. 4, figs. 16–19.
1884 *Cynodictis* (*Elocyon*?) *Göriachensis* n. spec, Toula: 386, figs. 1–10
1899 *Cephalogale* sp., Gaillard: 50, fig. 26
1899 *Viverra leptorhyncha* (Filhol) Gaillard: 58, pl. 2, fig. 8
1913 *Cephalogale Gaillardi* Wegner: 227, fig. 24, pl. 12, fig. 23
1928b Canidae cf. *Galecynus oeningensis* Owen, Helbing: 238, fig. 5
1933 *Alopecodon gaillardi* Wegner, Viret: 1, 2, 9, figs. 1–4
1947 *Viretius* Kretzoi: 286
1949b *Alopecodon leptorhynchus* (Filhol), Thenius: 799, figs. 1–2
1951 *Alopecocyon goriachensis* Toula, Viret: 23, pl. 1, figs. 8–9

Holotype. LG 1274, left maxilla with P3-M1 (Gaillard, 1899, fig. 26).

Type locality. La Grive Saint Alban, MN7/8, France.
Diagnosis. As for the genus.

Other localities. Savigné, Pontigné, Dénezé and Lublé (France, MN5; Ginsburg, 2001), Sansan (France MN6; Ginsburg, 1961; Peigné, 2012), Opole (Poland, MN7; Wegner, 1913), Leoben (Austria, MN5; Beaumont, 1982), Göriach (Austria, MN6; Thenius, 1949a; Toula, 1884), Hammerschmiede (Germany, MN7/8; Kargopoulos et al., 2022), Devinska Nova Ves (Slovaquia, MN6; Zapfe, 1950), Schlieren-Uetiko (Swiss, MN6; Helbing, 1928b).

Occurrence. Middle Miocene, MN 5–8 of Western Europe.

Remarks. *Alopecocyon* is one of the best-recorded ailurids during the Middle Miocene in Europe. However, the findings are limited exclusively to dentognathic remains. *Alopecocyon leptorhynchus* (= *Al. goriachensis*) has also been recognized in Duolebulejin, China, based on a m1 (Wang et al., 1998). The authors highlight differences between this specimen and the European species, particularly in the taller trigonid and hypoconid of the m1 in the Chinese form. Additionally, the Chinese m1 has a shorter talonid compared to the trigonid. While it is plausible that this m1 belongs to the Ailurinae subfamily, classifying it as *Alopecocyon* is debatable.

Genus ***Actiocyon*** Stock, 1947

Type species. *Actiocyon leardi* Stock, 1947.

Diagnosis. After Stock (1947; generic and specific characters).

Included species. *Actiocyon leardi* and *Actiocyon parverratis* K. Smith, Czaplewski and Cifelli, 2016.

Occurrence. Barstovian to Late Clarendonian (Cl3) Land Mammal Age from North America (c. MN 5–10).

Actiocyon leardi Stock, 1947

Holotype. LACMlCIT 2747, fragment of a skull.

Type locality. CC17H, Cuyama beds, Apache Canyon, California, USA.

Diagnosis. In Baskin (1998b).

Occurrence. Late Miocene, Late Clarendonian (Cl3) (Tedford et al., 2004), North America.

Remarks. *Actiocyon leardi* was defined based on a skull fragment with the complete right C, P2–M1, and a lingually broken M2, besides the left P4–M1. Webb (1969) regarded *Actiocyon* and *Alopecocyon* as synonyms, while Baskin (1998b) saw them as very closely related, but generically separated. Morlo and Peigné (2010) also considered them to be synonyms. Despite the paucity of available material, the differences between *Ac. leardi* and *Al. leptorhynchus* are sufficiently pronounced to warrant the retention of a generic distinction. The P4 of *Ac. leardi* is characterized by a short metastyle and a markedly broadened paracone, which has a convex buccal wall comparable to that of the P4 of *Simocyon*. However, in *Ac. leardi* the parastyle is not well developed. The P4 of *Al. leptorhynchus* is more graceful, and its buccal wall is rectilinear. The occlusal sub-triangular shape of the M1 of *Ac. leardi* is similar to that of both *Alopecocyon* and *Simocyon* (Supplemental material 1, S3). However, it is distinguished from both by the strongly developed metaconule, which brings it closer to Ailurinae.

Actiocyon parverratis K. Smith, Czaplewski and Cifelli, 2016

Holotype. UCMP 141928, associated right and left hemimandibles with p2–m2.

Type locality. UCMP V74103 (OMNH V973), Eastgate, Churchill County, Nevada, USA.

Diagnosis. In K. Smith et al. (2016).

Differential diagnosis. Differs from *Ac. leardi* in the P4 having a less well-developed and undivided small protocone on the internal cingulum, as well as the rectilinear buccal wall.

Occurrence. Barstovian (c. MN5–6).

Remarks. The authors of this species have recognized that its assignment to *Actiocyon* is hypothetical with the current material. The mandibular morphology of *Ac. parverratis* differs from that of *Al. leptorhynchus* by the ascending ramus being positioned at a more vertical angle. Additionally, the premolars of *Ac. parverratis* are shorter and higher than those of the mandible of *Al. leptorhynchus* from the Sansan site (Peigné, 2012). Moreover, the m2 of *Ac. parverratis* differs from that of the European species due to the more central position of the hypoconid and hypoconulid and the greater development of the buccal cingulum. *Actiocyon parverratis* and *Al. leptorhynchus* exhibit the same dental morphological grade, with unreduced premolars and carnassials, and a more conservative morphology that is far from the hypercanivorous pattern observed in *Simocyon.*

Genus ***Protursus*** Crusafont and Kurtén, 1976

Type species. *Protursus simpsoni* Crusafont and Kurtén, 1976.

Diagnosis. In Crusafont and Kurtén (1976, p. 22, figs. 16–17).

Protursus simpsoni Crusafont and Kurtén, 1976

Holotype. IPS-1976, left m2 (Fig. 7).

Type locality. Can Llobateres, Late Miocene (MN9), Barcelona, Spain.

Diagnosis. As for the genus.

Differential diagnosis. In Morlo and Peigné (2010).

Emended diagnosis. Medium-sized member of the Simocyoninae; m2 elongated with reduced trigonid, large talonid with a hypertrophied hypoconulid and a deep valley lingually placed.

Other localities. Hammerschmiede, MN7/8 Germany (Kargopoulos et al., 2022), Rudabànya, MN9, Hungary (Werdelin, 2005).

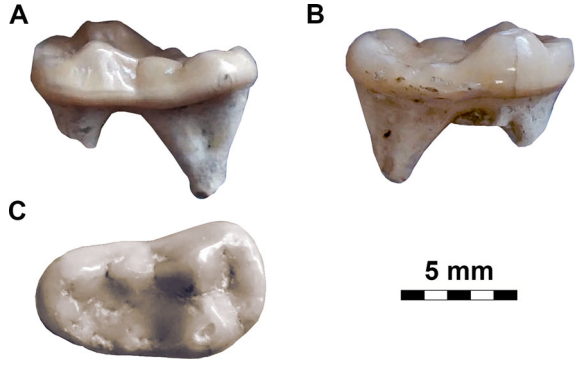

Figure 7. Holotype of *Protursus simpsoni* (IPS-1976) from Can Llobateres (Late Miocene, early Vallesian, MN9, Barcelona, Spain), left m2. **A**, buccal view; **B**, lingual view; **C**, occlusal view.

Occurrence. Early Late Miocene of Western Europe.

Remarks. Kargopoulos et al. (2022) identified an m2 from Hammerschmiede, Germany, as Simocyoninae indet. and related it to *Protursus simpsoni* Crusafont and Kurtén, 1976. The species was initially described from an isolated m2 in the Late Miocene of Can Llobateres, Spain (MN9), and was initially classified as belonging to the Ursinae. Thenius (1977) correctly dismissed this potential relationship and proposed its inclusion in the genus *Simocyon*. Peigné et al. (2005) considered it to be a Simocyoninae, but they maintain its generic validity. Kargopoulos et al. (2022) proposed that some fossils from the Rudabànya site described by Werdelin (2005) could be classified as *Protursus simpsoni* (specimens 1989/142: mandible fragment with m1–m2; 1990/103: m1; 1989/219 and 1990/54: M1). The specimen 1989/230 M2 determined as Melinae gen. et sp. indet., could also be added to this group. The taxonomic reassignment proposed by Kargopoulos et al. (2022) is solidly argued. Although the Rudabànya material attributed to *Protursus* is quite limited, it provides very relevant information about its dentition. The Rudabànya teeth have a less specialized morphology compared to *Simocyon*; the m1 is less sectorial, the m2 has a deep talonid valley, and the M1 has a comparatively larger crestiform metaconule. In summary, *Protursus simpsoni* lacks the hypercarnivores adaptations of *Simocyon*. An incomplete M1 from the middle Miocene site of Four (MN7/8), France, was determined by Ginsburg et al. (2001) as Ailurinae indet. The sub-quadrangular occlusal morphology, the development of the metaconule and the size of this molar are comparable to the M1 of Rudabànya reassigned to *Protursus* by Kargopoulos et al. (2022).

Subfamily **Magerictinae Subfam. nov.**

Type genus. *Magerictis* Ginsburg, Morales, Soria, and Herráez, 1997.

Diagnosis. Ailuridae with non-reduced and simple premolar dentition; m1 with high trigonid and short talonid; m2 with very long talonid compared to the trigonid, and a well-developed hypoconulid; P4 elongated, with a robust protocone located mesially to the paracone; M1 gracile, with a central protocone with postprotocrista attached to metaconule, and a very broad lingual area; M2 of medium size compared to M1, and buccolingualy large.

Included genera. *Rothictis* gen. nov., and *Magerictis*.

Genus ***Rothictis* gen. nov.**

Type genus. *Rothictis wintershofensis* (Roth, 1987) in Heizmann and Morlo (1994).

Etymology. Named after Dr Claudia Roth in recognition of her contribution to the study of European Miocene carnivorans.

Diagnosis. Small-sized Magerictinae, characterized by a tall ascending ramus; elongated lower premolars, p3–4 with distal accessory cuspids; and elongated m2 talonid with a large hypoconulid already distinct from the hypoconid.

Differential diagnosis. *Rothictis* differs from *Amphictis* by the talonid morphology of the m2, whose hypoconid and hypoconulid of similar size are placed buccally, while the lingual area is basined. *Rothictis* differs from *Magerictis* by its smaller size, the retention of the internal cristids that join the protoconid and metaconid in the m2, lower premolars elongated, p3 with accessory distal cuspid, and the coronoid process high and verticalized.

Included species. *Rothictis wintershofensis* (Heizmann & Morlo, 1994) comb. nov. (Fig. 8) and *Rothictis prolongata* (Morlo, 1996) comb. nov.

Occurrence. Early Miocene, MN2 to MN3, Western Europe.

Rothictis wintershofensis (Heizmann & Morlo, 1994) comb. nov.

1950 *Amphictis* aff. *antiquus* Pomel, Dehm: 112
1976 *Amphictis* aff. *antiquus* Dehm, Beaumont: 177
1976 *Plesictis humilidens* Dehm, 1950, Beaumont: 177
1993 *Amphictis* Pomel, 1853, Wolsan: 347
1994 *Amphictis wintershofensis* Roth nov sp., Heizmann and Morlo: 10–11
1996 *Amphictis wintershofensis* Roth in Heizmann and Morlo, Morlo: 213
2010 *Amphictis wintershofensis* Roth in Heizmann and Morlo, Morlo and Peigné: 123

Holotype. BSP 1937 II 13132, right mandible with c–m2, Dehm (1950, fig. 112) (Fig. 8A–C).

Type locality. Wintershof-West, Germany.

Diagnosis. Heizmann and Morlo (1994, p. 18).

Occurrence. Early Miocene (MN3).

Rothictis prolongata (Morlo, 1996)

1996 *Amphictis prolongata* nov. sp., Morlo: 214, fig. 9.

Holotype. SMF M 5791, left mandible fragment with p3–m2.

Type locality. Wiesbaden-Amöneburg, Germany.

Diagnosis. In Morlo (1996, p. 214).

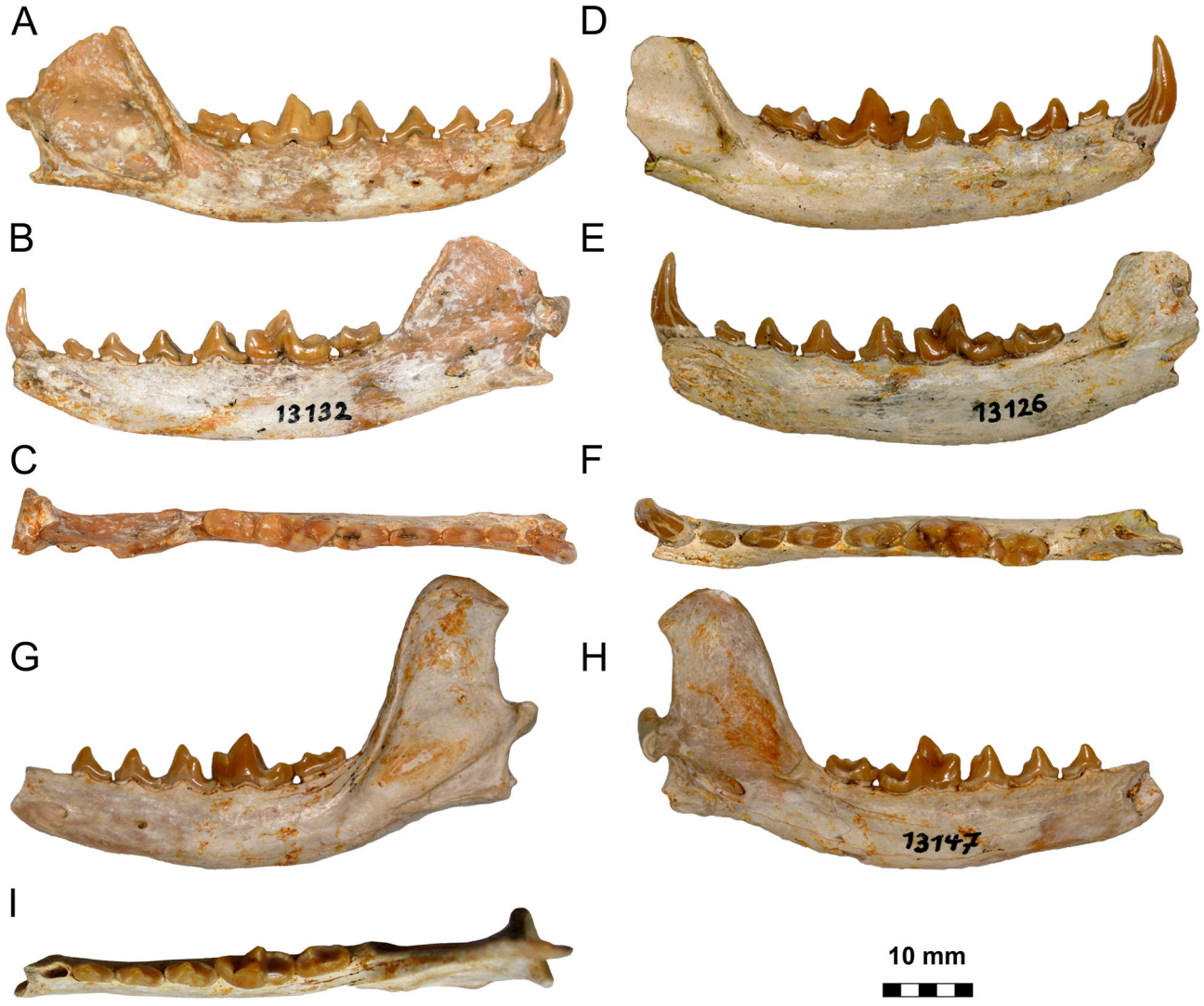

Figure 8. Lower dentition of *Rothictis wintershofensis* from Wintershof-West (Early Miocene, MN3, Germany). **A–C**, SNSB-BSPG 1937 II 13132 (holotype) right hemimandible: **A**, buccal view; **B**, lingual view; **C**, occlusal view. **D–F**, SNSB-BSPG 1937 II 13126 right hemimandible: **D**, buccal view; **E**, lingual view; **F**, occlusal view. **G–I**, SNSB-BSPG 1937 II 13147 left hemimandible: **G**, buccal view; **H**, lingual view; **I**, occlusal view.

Occurrence. Early Miocene (MN2).

Genus ***Magerictis*** Ginsburg, Morales, Soria, and Herráez, 1997

Diagnosis. In Ginsburg *et al.* 1997 (translated from French). Primitive Ailuridae of size comparable of *Ailurus fulgens*. m2 with low trigonid, with protoconid and metaconid elongated, in a very peripheral position, and separated from one to the other by a longitudinal valley directly connected to the valley of the talonid. Low and very elongated talonid, mainly due to the very significant elongation of the hypoconulid.

Emended diagnosis. Magerictinae of medium size, with non-reduced and simple premolar dentition. m1 with high trigonid and short talonid; m2 with very long talonid compared to the trigonid. Absence of the internal cristids of the union between the protoconid and metaconid, resulting in a continuity between the valleys of the trigonid and the talonid. Hypoconulid larger than hypoconid. P4 elongated, with a strong protocone mesial to paracone. M1 slender, with a central protocone and a postprotocrista attached to a well-developed metaconule; large lingual area between protocone and the lingual cingulum; M2 of moderate size compared to M1, and elongated buccolingually.

Included species. *Magerictis imperialensis* Ginsburg, Morales, Soria, and Herráez, 1997.

Occurrence. Middle Miocene (MN5 to MN6) of Madrid (Spain).

Magerictis imperialensis Ginsburg, Morales, Soria, and Herráez, 1997
(Figs. 9–15; Tables 1–5)

Holotype. MNCN69462, right m2.
Type locality. Estación Imperial, Madrid, Spain (Middle Miocene, MN5, local biozone Dc).

Diagnosis. As for the genus.

Other localities. Los Nogales (NOG, MN5), Príncipe Pio-2 (PP-2, MN5), Fábrica de Mahou (FMH, MN5), Barajas-3 (BAR-3, MN5), Barajas-17 (BAR-17, MN5), El Cañaveral (CAÑ, MN5), Alhambra-Túneles (ALH-TU, MN6), Embajadores (EMB-PG3, MN5).

Studied material. The fossil remains of *M. imperialensis* are stored in the collections of the Department of Paleobiología of MNCN. They come from the localities of Estación Imperial: MNCN69462, right m2 (holotype); Barajas 3: BAR-3-54, right m1, BAR-3-41, left m1; Barajas 17: BAR-17-03-8, right mandible with p4 and alveoli of p3, m1 and m2; El Cañaveral: CAÑ-506, skull fragment with premaxillae, left maxillae with C–M1 and M2 alveolus, and the anterior part of the right maxilla with C–P1. CAÑ-458, right P4. CAÑ-1026, right M1. CAÑ-742/743, association of a single individual comprising isolated left P4 (CAÑ-743d), left maxilla fragment with M1 and incomplete M2 (CAÑ-743b), right maxilla fragment with I3, C, P2, P3 (CAÑ-743a) and isolated right M1 (CAÑ-743c), as well as a left mandible with broken p3–p4, and complete m1–m2 (CAÑ-742a), a right mandible with complete p3 and m1 (CAÑ-742b), and a right isolated m2 (CAÑ-742c). CAÑ-1050, skull and mandible fragments (poor preservation). CAÑ-974, right mandible with p4–m1. CAÑ-1140, left astragalus. CAÑ-998, left calcaneus. CAÑ-1168, left calcaneus; Fábrica de Mahou: FMH'14-5162, left astragalus. FMH'14-1703, left calcaneus. FMH'14-1292, right metacarpal I. FMH'14-1478, left metatarsal I; Los Nogales: NOG-103, left m1; Embajadores: EMB-PG3-55, left M2; Príncipe Pío-2: PP-2-3623, left mandible with m1–p4, alveoli of p2 and m2. PP-2-3624, association of right m1–m2, left p4 and right p2; Alhambra-Túneles: ALH-TU-718 right maxilla fragment with P4 and incomplete P3. ALH-TU-686 right edentate mandible (Tables 1–2; Supplemental material 1, S4).

Redescription of the holotype. MNCN69462, right m2 (Fig. 9). The tooth is markedly elongated, with low trigonid and talonid cuspids encircling an elongated and continuous central valley. Consequently, both the protoconid and the metaconid have lost the internal cristids

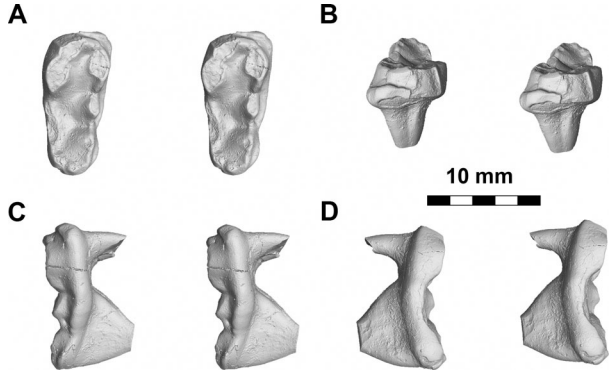

Figure 9. Holotype of *Magerictis imperialensis* (MNCN69462) from Estación Imperial, (Middle Miocene, Aragonian, MN5, Madrid, Spain). **A**, occlusal view (stereo pair); **B**, mesial view (stereo pair); **C**, buccal view (stereo pair); **D**, lingual view (stereo pair).

that separate the trigonid from the talonid. The trigonid is formed by three elongated worn cuspids. The protoconid is placed at the mesiobuccal edge of the tooth, slightly mesially to the metaconid. The two cuspids are of comparable size and are joined mesially by a robust paraconid, which encloses the anterior part of the trigonid in a semicircular wall. The talonid is very elongated, exhibiting a narrower width than the trigonid. The buccal wall has two well-developed cuspids, which may correspond to the hypoconid and hypoconulid (Fig. 9). The lingual aspect of the specimen exhibits substantial wear, particularly in the region distal of the metaconid. The presence of two small, low, and elongated cuspids (entoconid and pre-entoconid) can be discerned solely through observation of their wear surface. Furthermore, two minor cuspids, the entoconulid at the distolingual angle and the post-hypoconulid, are situated in the distal position, completely enclosing the talonid. The tooth is encircled by a robust basal cingulid, which is especially strong at the base of the protoconid, where it is mesially projected.

Description of the new material

Upper dentition. CAÑ-506. Skull fragment that includes almost complete premaxillae, a fragment of the right maxilla with C–P1, and the left maxilla with C–M1 and alveolus of M2 (Fig. 10A–F). The incisors are arranged in a gentler curve than that shown in *A. fulgens*. I1–I2 are small, close in size, with a low crown, and their buccolingual length is greater than mesiodistal. The I3 is slightly larger than the central incisors. It also has a low crown, a thickened base, and an almost circular cross-section. The diastema between I3 and C is short, and the premaxillary-maxillary separation is

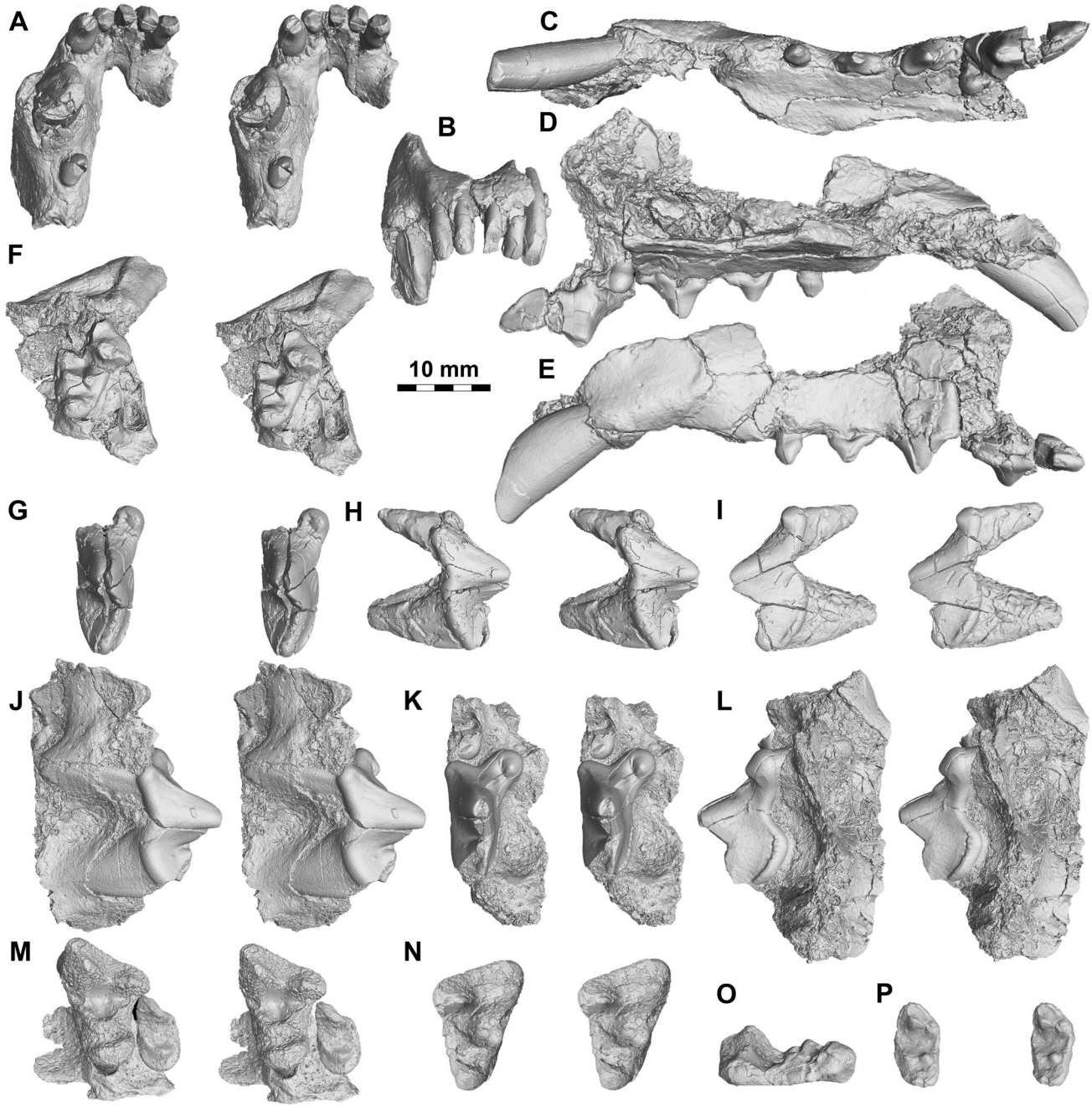

Figure 10. Cranial and upper dentition remains of *Magerictis imperialensis* from the Middle Miocene localities of El Cañaveral, Alhambra-Túneles, and Embajadores (Madrid, Spain). **A–F**, CAÑ-506, skull fragment of a single individual from El Cañaveral. **A–B**, CAÑ-506a, left I1–3, right I2–3 and C–P1: **A**, occlusal view (stereo pair); **B**, mesial view. **C–E**, CAÑ-506b, left maxilla with C–P4: **C**, occlusal view; **D**, lingual view; **E**, buccal view. **F**, CAÑ-506c, left M1 and M2 alveolus, occlusal view (stereo pair). **G–I**, CAÑ-458, right P4 from El Cañaveral: **G**, occlusal view (stereo pair); **H,** buccal view (stereo pair); **I**, lingual view (stereo pair). **J–L**, ALH-TU-718, right maxilla fragment with P4 and P3 distal portion from Alhambra-Túneles: **J**, buccal view (stereo pair); **K**, occlusal view (stereo pair); **L**, lingual view (stereo pair). **M**, CAÑ-743b, left maxilla with M1 and M2 (buccally broken) from El Cañaveral, occlusal view (stereo pair). **N–O**, CAÑ-1026, right M1 from El Cañaveral, Madrid (Spain): **N**, occlusal view (stereo pair); **O**, distal view. **P**, EMB-PG3-55, left M2 from Embajadores, Madrid (Spain), occlusal view (stereo pair).

marked by a pronounced depression. Despite the poor state of preservation, it can be inferred that the snout was considerably longer than that of *Ailurus*. In the left row, the canine has a markedly large root and a heavily worn mesial area. Its cross-section is sub-circular and displays a relatively weak distal crista. The complete left premolar series consists of a unicuspid P1, separated from the canine and P2 by two diastemata. The P2 is longer, low, and has an extended distal crista, as well as a small distolingual projection thickens a very weakly differentiated talonid. The P3 has a high cusp, the distal crista is much extended, ending in a well-marked talonid, lingually delimited by a small basal expansion. The P4 is poorly preserved, its mesial portion is partially displaced, and the metastyle area is broken. The M1 has the paracone broken and the metacone is placed distolingually. The paraconule is well defined, the protocone is small and has a posterior crista that connects to a developed metaconule. The lingual cingulum is strong and well separated from the base of the protocone. The alveoli of the M2 indicate that this molar was short with a large mesial alveolus and a second tiny one attached distolingually to the anterior, a third lingual alveolus is large and elongated buccolingually. These alveoli of M2 are similar to those of the specimen CAÑ-743c, with a very short buccal length, but buccolingually elongated. In the distal part of the maxilla of CAÑ-506, at the level of the P4, the bone is thick and has a deep groove in the area of the jugal-maxillary ventral suture. This structure is partly due to the strong development of insertion of the muscle masseter superficialis, but also to the thickness of the ventral margin of the infraorbital foramen, which appears to be quite developed.

CAÑ-458, right P4 (Fig. 10G–I). Its preservation is poor, with two deep fractures, one running mesiodistally in the middle of the crown, and another affecting the paracone. A third fracture is observed only in the lingual wall of the metastyle, at the level of the carnassial notch. These fractures have slightly displaced the buccal wall from the lingual and have fractured the mesial base of the paracone so that the protocone appears to be slightly more mesial than it was originally. The protocone is large and well separated from the lingual wall of the paracone. The metastyle is short and slightly compressed similar to that of the paracone.

ALH-TU-718, right maxillary fragment with P4 and the distal part of the P3 (Fig. 10J–L). The buccomesial root of the M1 is located within the bone. The P3 is broken and only retains a well-developed distobasal cusp. The P4 has a carnassial notch. The protocone is robust and situated quite mesial to the parastilar area. The mesial wall displays a very pronounced flexed morphology, accentuating the separation of the protocone from the paracone. The paracone is robust, exhibiting a moderate buccomesial crista that joins the protocone. A small mesiolingual conule is situated in that crista. The parastyle is barely discernible. The metastyle is distally broken, showing a strong and high lingual cingulum.

CAÑ-743, association of a left P4 (CAÑ-743d), left maxilla fragment with M1 and incomplete M2 (CAÑ-743b) (Fig. 10M), right maxilla fragment with I3, C, P2, P3 (CAÑ-743a) and an isolated right M1 (CAÑ-743c). The left P4 although complete is poorly preserved, including enamel loss and superficial corrosion. The most remarkable feature is the presence of a protocone that is distinctly separated from the paracone by a long neck, similar to the other P4s described herein. The left and right M1 are molars with a sub-triangular occlusal shape. The labial wall is rectilinear and elongated mesiodistally, while the lingual part of the molar is narrowed. The paracone is highly developed in comparison to the metacone, occupying approximately two-thirds of the buccal wall. The parastyle is placed in the mesiobuccal corner. A moderately developed mestatyle is present. There is a moderate buccal cingulum that delineates a central buccal platform between the two main buccal cusps. The metaconule and the protocone are of a similar size, and together with a well-developed paraconule, form a broad and deep trigone valley. The lingual cingulum is high and robust, separated from the metaconule-protocone by a markedly deep valley. The left M2 is not reduced but it is smaller than M1. The buccal cusps are not preserved. The trigone valley is deep, bordered lingually by a semicircular ridge that consists of a poorly differentiated protocone, paraconule and metaconule. The lingual cingulum is low, and comparatively less developed than in M1. The lingual root is robust and occupies the basal mid-lingual part of the crown. CAÑ-1026, right M1 (Fig. 10M–O) with the same morphology as the M1 CAÑ-743. EMB PG3-53, left M2 with a quadrangular occlusal shape, except for the buccomesial projection of the parastylar area (Fig. 10P). The paracone is larger than the metacone. The central valley of the trigone is wide and deep. The protocone is eroded mesially and joins distally with a large metaconule. As with the M1, there is a notable separation between the lingual wall of the protocone and the lingual cingulum.

Mandible and lower dentition. PP-2-3623, left mandible with complete m1–p4, the distal alveolus of p2 and alveoli for p3 and m2 (Fig. 11A–C). The fossil is well preserved, although the mandible is broken at the symphysis and exhibits both angular and articular processes embedded in a carbonate crust. There is a large diastema mesial to the p3 roots. However, the p2 roots are observable in the CT scan images, which suggests that this premolar may have broken during the individual's lifetime, resulting in the obliteration of the roots. The caudal part of the mandibular body presents a protrusion at the level of the muscle digastricus attachment area, similar to that observed in many arctoid carnivorans. The area with both angular and articular processes is very bad

preserved. The coronoid process is wide, robust, relatively tall and curved backwards. The masseteric fossa is deep particularly near its ventral border where the mandibular bone is thickened. The p4 is a robust tooth with an elliptical occlusal shape, a high main cuspid, a weak distal accessory cuspid, and a small talonid. The mid-lingual area of the tooth exhibits a broadening. The m1 is robust, with a trigonid larger than the talonid. The paraconid is wide and low compared to the protoconid. It presents a buccal wear facet, and a weak mesiobuccal cristid, extending to a cingulid. The protoconid is very robust and has a pyramidal shape. The mesial cristid is not very sharp. The metaconid is highly developed, with a comparable height to that of the paraconid but a smaller size. It is somewhat displaced distally and very well individualized from the protoconid. The talonid is relatively short, extending for approximately one-third of the mesiodistal length of the tooth. The hypoconid is the most developed cuspid. It is elongated and occupies the entire buccal edge. It joins distally with a cristid that surrounds the talonid valley until reaching the distal base of the metaconid. The basal cingulid is weak, only somewhat thickened at the distobuccal base of the talonid.

PP-2-3624, association of isolated right p2, left p4, and right m1–m2 in an excellent state of preservation (Fig. 11D–O). The p2 is relatively tall and unicuspid. The p4 is almost identical to that of PP-2-3623, and it can be observed that the buccolingual cingulid is connected with a weak lingual cristid of the main cuspid. The m1is similar to that of PP-2-3623. However, in this specimen, the presence of a small hypoconulid is observed in the talonid, and the crestiform entoconid is slightly serrated.

CAÑ-742 (associated with CAÑ-743). The left mandible CAÑ-742a preserves alveoli for both p1 (uniradicular) and p2 (Fig. 12A–B). The p3 and p4 are severely damaged, while the m1 and m2 are complete but poorly preserved. The mandibular body is crushed. There is a mental foramen at the level of p1–p2. The masseteric fossa is wide, deep, and outwardly expanded at the base. The m1 has a stretched trigonid, with a low paraconid in relation to the protoconid, and a well-developed metaconid that is displaced distally. The talonid is short, with a central valley surrounded by a peripheral hypoconid somewhat more developed than the entoconid. Both cuspids join distally, although it cannot be known if they are fused. The general structure of the m2 is similar to that of the holotype, although its preservation is very poor. The right mandible CAÑ-742b (Fig. 12C–D) is better preserved than the left one, but only the p3 and m1 are present. There is a second mental foramen at the level of the distal root of the p3.

Table 1. Measurements (in mm) of the upper dentition of *Magerictis imperialensis*. *alveolus measurement. **approximate measurement

Specimens	L C	WC	LP1	WP1	LP2	WP2	LP3	WP3	LP4	WP4	LM1	WM1	LM2	WM2
CAÑ-506	9.3	6.9	4.1	3.1	8.1	3.2	9.7	4.7		8.6	10.9	14.2	3.6*	9.5*
CAÑ-506	9.3		4.7	3.2										
CAÑ-458									15.7	7.9				
CAÑ-1026											9.2	13.9		
CAÑ-743 a,c					9.3	3.3	9.5	3.9			10.5	13.7		
CAÑ-743 b,d									14.8**	9.5	9.9	13.9	5**	9.5
CAÑ-1050	9.8**						9.4**		13.8**				4.3**	9.3**
ALH-TU-718									12.8**	8.5**				
EMB-PG3-55													5.8	9.9

Abbreviations: L, mesiodistal length; W, buccolingual width.

Table 2. Measurements (in mm) of the lower dentition of *Magerictis imperialensis*.*alveolus measurement. **approximate measurement.

Specimens	Lp2	Wp2	Lp3	Wp3	Lp4	Wp4	Lm1	Wm1	Lm2	Wm2
MNCN69462									12.3	5.9
PP-2-3623			8.3*		9.2	4.6	14.4	6.4	10.2*	
PP-2-3624			6.9	3.1	9.6	5.1	15.5	7.21	11.9	6.2
NOG-103							14.5	7.2		
BAR-17-03-8			7.6*		10.9	5.4	15.2*		9.8*	
BAR-3-54							15.2	6.6		
BAR-3-41							15.8			
ALH-TU-686									10.2*	
CAÑ-974					11.4	5.5	17.0	7.5		
CAÑ-742 b,c	7.8*		8.8	4.2	10.2*		16.4	6.6	10.0	5.1
CAÑ-742 a							16.9	6.8	9.4	4.9
CAÑ-1050							15.3*		9.5*	

Abbreviations: L, mesiodistal length; W, buccolingual width.

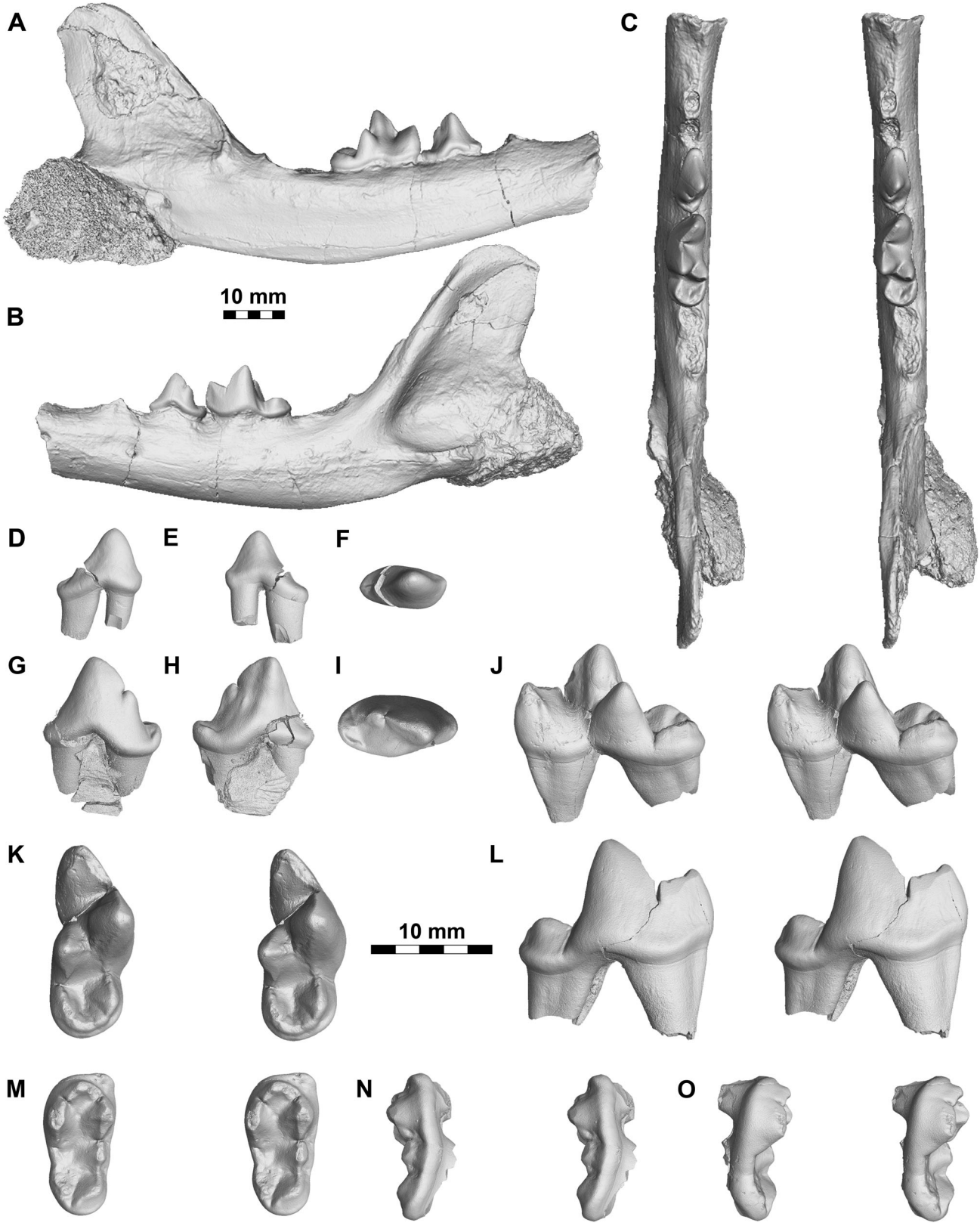
A
B
10 mm
C
D
E
F
G
H
I
J
K
10 mm
L
M
N
O

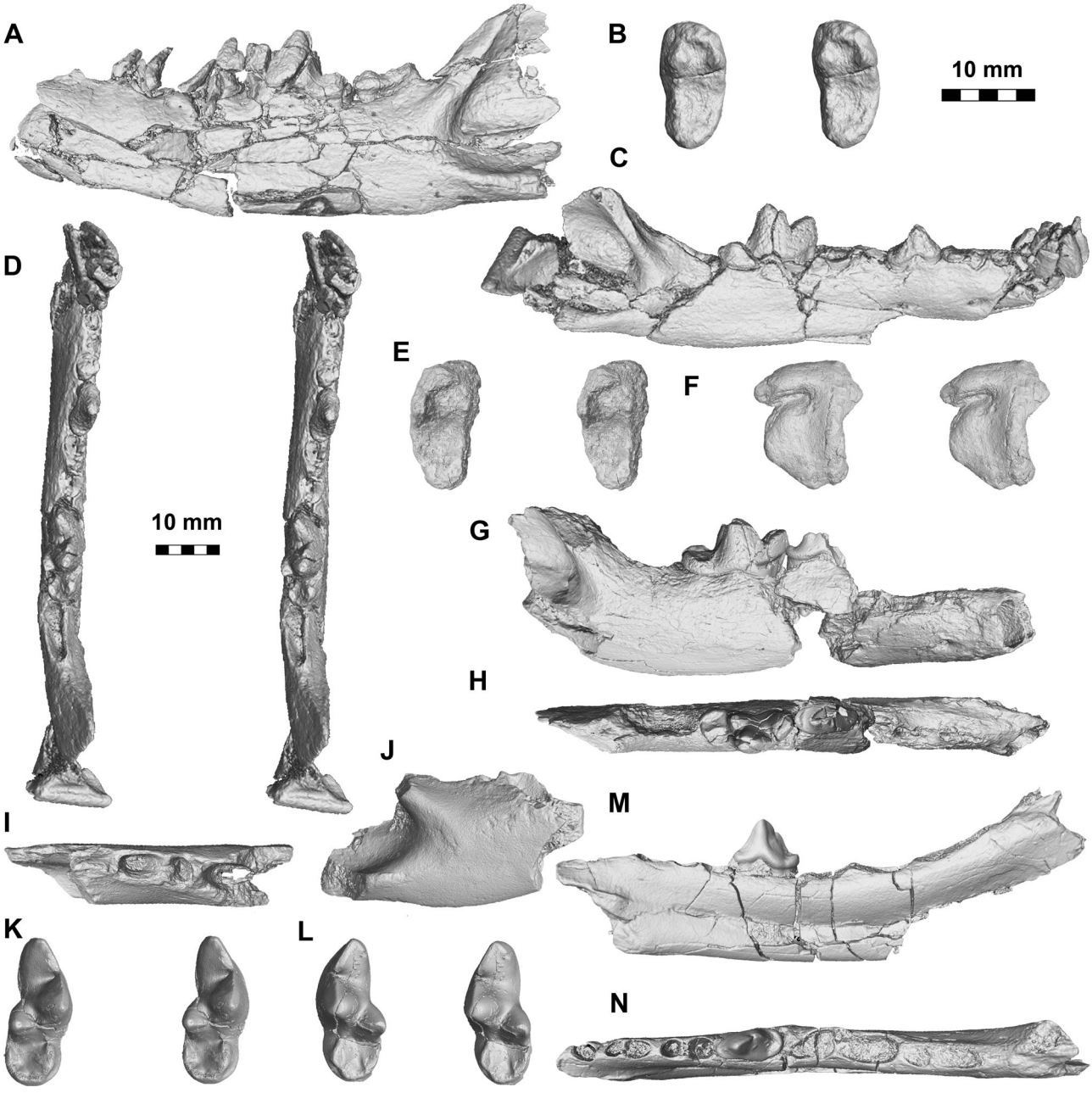

Figure 12. Mandibular and lower dentition remains of *Magerictis imperialensis* from El Cañaveral, Barajas-17, Barajas-3, Alhambra-Túneles and Nogales (Madrid, Spain). **A–B**, CAÑ-742a, left mandible with p4–m2 from El Cañaveral: **A**, buccal view; **B**, detail of the m2 in occlusal view (stereo pair). **C–D**, CAÑ-742b, right mandible with p3 and m1 from El Cañaveral; **C**, buccal view; **D**, occlusal view (stereo pair). **E–F**, CAÑ-742c, right isolated m2 from El Cañaveral: **E**, occlusal view (stereo pair); **F**, buccal view (stereo pair). **G–H**, CAÑ-974, right mandible with p4–m1 from El Cañaveral: **G**, buccal view; **H**, occlusal view. **I–J**, ALH-TU-686, right fragmentary mandible with m2 alveolus from Alhambra-Túneles: **I**, occlusal view; **J**, buccal view. **K**, BAR-3-54, right m1 from Barajas-3, occlusal view (stereo pair). **L**, NOG-103, left m1 from Nogales, occlusal view (stereo pair). **M–N**, BAR-17-03-8, right mandible with p4 and alveoli for p1–p3, and m1–m2 from Barajas 17, Madrid (Spain): **M**, lingual view; **N**, occlusal view. **A, C, D, G–J, M–N** share the scale bar and **B, E–F, K–L** share the same scale bar.

Figure 11. Mandibular and lower dentition remains of *Magerictis imperialensis* from Príncipe Pio-2 (Madrid, Spain). **A–C**, PP-2-3623, left mandible with complete p4–m1 and alveoli for p3 and m2: **A**, lingual view; **B**, buccal view; **C**, occlusal view (stereo pair). **D–O**, PP-2-3624, an association of isolated teeth. **D–F**, right p2: **D**, buccal view; **E**, lingual view; **F**, occlusal view. **G–I**, left p4: **G**, buccal view; **H**, lingual view; **I**, occlusal view; **J–L**, right m1: **J**, lingual view (stereo pair); **K**, occlusal view (stereo pair); **L**, buccal view (stereo pair). **M–O**, right m2: **M**, occlusal view (stereo pair); **N**, buccal view (stereo pair); **O**, lingual view (stereo pair). **A–C** share the same scale bar and **D–O** share the same scale bar.

The masseteric fossa is deep, the base of the coronoid process is broad and extends buccally, and the condylar process is gracile. The p3 is robust, wider distally, and apparently without a distal accessory cuspid. The m2 CAÑ-742c (Fig. 12E–F) was detached from the mandible, and most of the enamel is severely deteriorated. However, the overall structure has been preserved in its entirety, with trigonid and talonid cuspids arranged peripherally as in the holotype. The only notable difference is the greater development of the distal root, which merges with the mesial root of the molar.

CAÑ-974, right mandible broken in three fragments, with the alveolus of the c, roots of p1–p3 and m2, and complete p4–m1 (Fig. 12G–H). This specimen is larger and more robust than the previous ones, though it is less compressed buccolingually. In lingual view, the mandibular symphysis is notably rough and reaches the height of the mesial alveolus of the p2. The anterior mental foramen lies below the mesial root of the p2. The masseteric fossa is strongly developed. The p4 is robust, there is no mesial accessory cuspid, the area of the distal accessory cuspid is broken, and a distolingual cingulum is well developed. The m1 is poorly preserved. The paraconid and metaconid have lost part of the lingual enamel, and the metaconid is well developed and slightly distal to the protoconid. The talonid is relatively short, with the hypoconid extending almost to the buccal half, and joining a peripheral entoconid distally. The alveoli of the m2 are partially broken and it is likely they were long, as observed in other specimens from this site.

BAR-17-03-8, right mandible with complete p4, as well as the alveoli of p1–p3, and m1–m2 (Fig. 12M–N). Only the anterior part of the mandibular body has been preserved, with the posterior part and the ascending ramus missing, except for a small part of the masseteric fossa. The p4 is morphologically identical to that described in Príncipe Pío 2, although it is somewhat less robust. The alveoli of p3 and p2 are close in size and are separated by a small diastema from the uniradicular alveolus of p1. The alveoli of the m2 are composed of an almost circular mesial alveolus and another distal, longer alveolus with an elliptical shape. ALH-TU-686 (Fig. 12I–J) left mandible fragment with part of the masseteric fossa, which is quite deep, as well as the alveoli for the m2 and the distal alveolus for the m1. The morphology and size of the alveoli of m2 are similar to those of BAR-17-03-8.

Other isolated teeth are: NOG-103, left m1 (Fig. 12L). It is morphologically close to the m1 of Príncipe Pío 2. It is robust with a strong metaconid placed distally, and a short talonid with a peripherical hypoconid, hypoconulid and entoconid enclosing the talonid valley. BAR-3-54, right m1 (Fig. 12K). It is also morphologically similar to the specimen from Príncipe Pío 2, but somewhat more graceful. The mesiolingual cristid of the paraconid is very weak. The paraconid and protoconid have a smooth wear facet in the buccal wall. The hypoconid is high, occupying the entire talonid buccal wall, and is distally attached to the entoconid by a minuscule hypoconulid, so that the distal edge of the talonid is completely closed. BAR-3-41, is a right m1 almost identical to the latter but with the broken metaconid.

Postcranial. Astragalus. FMH'14-5162, left talus (Fig. 13A–F; Table 3). It has a low dorsoplantar body. The trochlea is broad and somewhat flattened, with the lateral lip not very pronounced and the medial lip somewhat sharper. Proximally, the trochlea maintains its width, resulting in a poorly defined groove for the

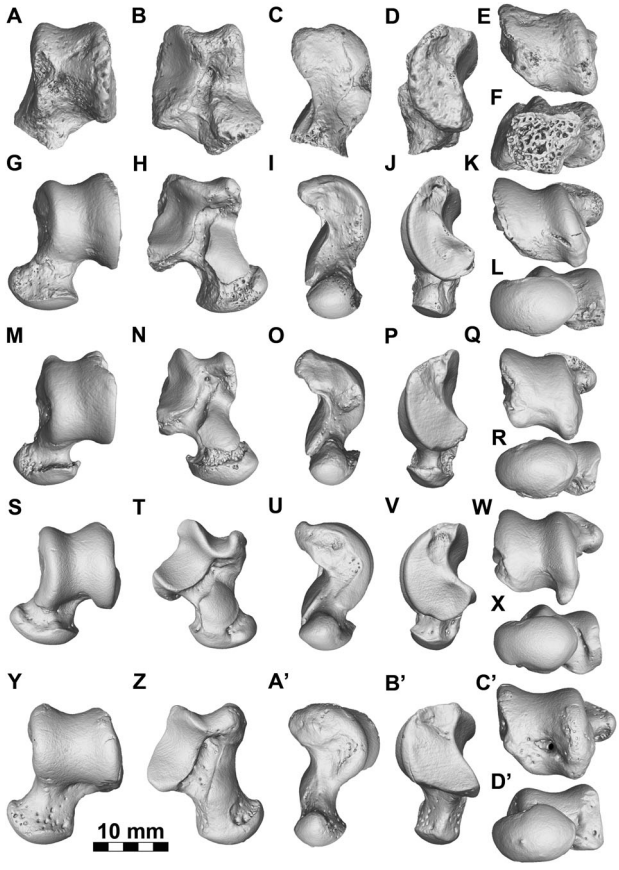

Figure 13. Astragalus of *Magerictis imperialensis* from El Cañaveral and Fábrica de Mahou, Madrid (Spain) and selected extant Musteloidea (*Ailurus fulgens*, *Procyon lotor*, *Meles meles*). **A–F**, *M. imperialensis* CAÑ-1140, left talus from El Cañaveral: **A**, dorsal view; **B**, plantar view; **C**, medial view; **D**, lateral view; **E**, proximal view; **F**, distal view. **G–L**, *M. imperialensis* FMH'14-5162, left talus from Fábrica de Mahou: **G**, dorsal view; **H**, plantar view; **I**, medial view; **J**, lateral view; **K**, proximal view; **L**, distal view. **M–R**, *A. fulgens* MNCN M-14231, left talus: **M**, dorsal view; **N**, plantar view; **O**, medial view; **P**, lateral view; **Q**, proximal view; **R**, distal view. **S–X**, *Pr. lotor* MNCN M-19501, left talus: **S**, dorsal view; **T**, plantar view; **U**, medial view; **V**, lateral view; **W**, proximal view; **X**, distal view. **Y–D'**, *Me. meles* MNCN M-21763 left talus: **Y**, dorsal view; **Z**, plantar view; **A'**, medial view; **B'**, lateral view; **C'**, proximal view; **D'**, distal view.

Table 3. Measurements (in mm) of the astragalus of the ailurids *Magerictis imperialensis*, *Simocyon batalleri* and *Ailurus fulgens*. See Supplemental Figure S1 to see how the measurements were taken.

Specimens	1	2	3	4	5	6	7	8
Magerictis imperialensis CAÑ-1140		11.2	14.1	14.7	10.5	11		
Magerictis imperialensis FMH'14-5162	18	9	13.2	12.6	8	9.5	9.9	6.7
Simocyon batalleri B-5450	33.1	17.1	21.8	24.8	16.4	17.3	18.9	11.5
Simocyon batalleri B-39	32.5	17.5	22.4	24.6	16.6	17.8	18.2	11.9
Ailurus fulgens MNCN M-14231 (r)	17.3	8.4	11.5	12.3	7.5	8.5	9.2	7
Ailurus fulgens MNCN M-14231 (l)	17.9	7.9	11.6	12.3	6.9	9	8.9	6.6

Abbreviations: l, left; r, right; 1, proximodistal length; 2 lateromedial diameter of the trochlea; 3, proximodistal length of the lateral lip; 4, proximodistal length of the medial lip; 5, dorsoplantar diameter of the medial lip; 6, dorsoplantar diameter of the lateral lip; 7, lateromedial diameter of the navicular facet; 8, dorsoplantar diameter of the navicular facet.

Table 4. Measurements (in mm) of the calcaneus of the ailurids *Magerictis imperialensis, Simocyon batalleri* and *Ailurus fulgens*. See Supplemental Figure S1 to see how the measurements were taken.

Specimens	1	2	3	4	5	6	7
Magerictis imperialensis FMH'14-1703	30.1	14.5	11.7	9.4	10.1	8.9	7.7
Simocyon batalleri B-2497	51.1	29.4	20.8	16.3	17.3	14.9	15.2
Ailurus fulgens MNCN M-14231 (r)	27.3	13.9	10.4	8.5	10.2	7.6	6.7

Abbreviations: r, right; 1, proximodistal length; 2, lateromedial diameter of the articular facets; 3, maximum dorsoplantar diameter; 4, lateromedial diameter of the tuber calcis; 5, dorsoplantar diameter of the tuber calcis; 6, lateromedial diameter of the cuboid facet; 7, dorsoplantar diameter of the cuboid facet.

Table 5. Measurements (in mm) of the metacarpal-I (Mc-I) and the metatarsal-I (Mt-I) of the ailurids *Magerictis imperialensis*, *Simocyon batalleri* and *Ailurus fulgens*. See Supplemental Figure S1 to see how to take the measurements.

Mc-I	1	2	3	4	5
Magerictis imperialensis FMH'14-1298	25.9	5.4	5.7	4.5	4.5
Simocyon batalleri B-90	30	9.6	13.9	7.6	9.5
Ailurus fulgens MNCN M-14231	17	4.5	6.2	4.3	5
Mt-I					
Magerictis imperialensis FMH'14-1478	32.5	7.8	6.4	4.7	5.7
Simocyon batalleri B-1793	44	10.7	12.9	7.2	9.6
Ailurus fulgens MNCN M-14231	24.7	6.5	6.2	4.3	6.2

Abbreviations: 1, proximodistal length; 2, lateromedial diameter of the proximal epiphysis; 3, dorsopalmar/plantar diameter of the proximal epiphysis; 4, lateromedial diameter of the distal epiphysis, 5; dorsopalmar/plantar diameter of the distal epiphysis.

plantar tendon that hardly protrudes plantarly. The lateral process and the astragalar tubercle are of a moderate size. In plantar view, the ectal facet is slightly inclined in the dorsoplantar direction and has a smooth concavity. The sustentacular facet covers a substantial portion of the plantar surface of the neck and nearly two-thirds of the plantar surface of the body. The most proximal part is curved, but does not reach the proximal border. The two plantar facets are separated by the tarsal sinus, which extends in an arc from the lateral border, below the lateral process, to the distal border of the body of the talus, between the beginning of the neck and the distal border. The talus has a short and broad neck with an elliptical facet for the navicular. This facet is positioned transversely and compressed dorsoplantarly. CAÑ-1140, left talus (Fig. 13G–L; Table 3). The body and the basal part of the neck are preserved. The only significant difference compared to the Fábrica de Mahou talus is its size, which is approximately 20% larger than El Cañaveral.

Calcaneus. FMH'14-1703, left calcaneus (Fig. 14A–F; Table 4). The size and morphology of the articular surfaces of the calcaneus correspond exactly to those of the plantar articular surfaces of the Fábrica de Mahou talus. The proximal epiphysis of the tuber calcanei is subrounded, with the lateral and medial processes not prominent and the sagittal groove shallow. Distally, the shaft of the calcaneum is strongly compressed lateromedially. It shows on the laterodorsal edge an elongated groove for the insertion of the short lateral-collateral ligament. The ectal facet is elongated and extends distally in the coracoid process, having a well-defined and strongly convex morphology. The talar facet of the sustentaculum is almost circular but continues in a narrow band to the dorsal edge of the cuboid facet. The sustentacular sulcus is wide and deep. The plantar tubercle is elongated but moderately developed. Proximally, the lateral surface broadens dorsally, forming a soft depression that culminates in a peroneal tubercle of moderate size. This is associated with the insertion of the tendons of the fibularis (peroneus) longus and brevis muscles. The facet for the cuboid (tarsal IV) is almost circular, quite concave, with a groove associated with the plantar tubercle marked on its dorsal edge. Two calcaneal

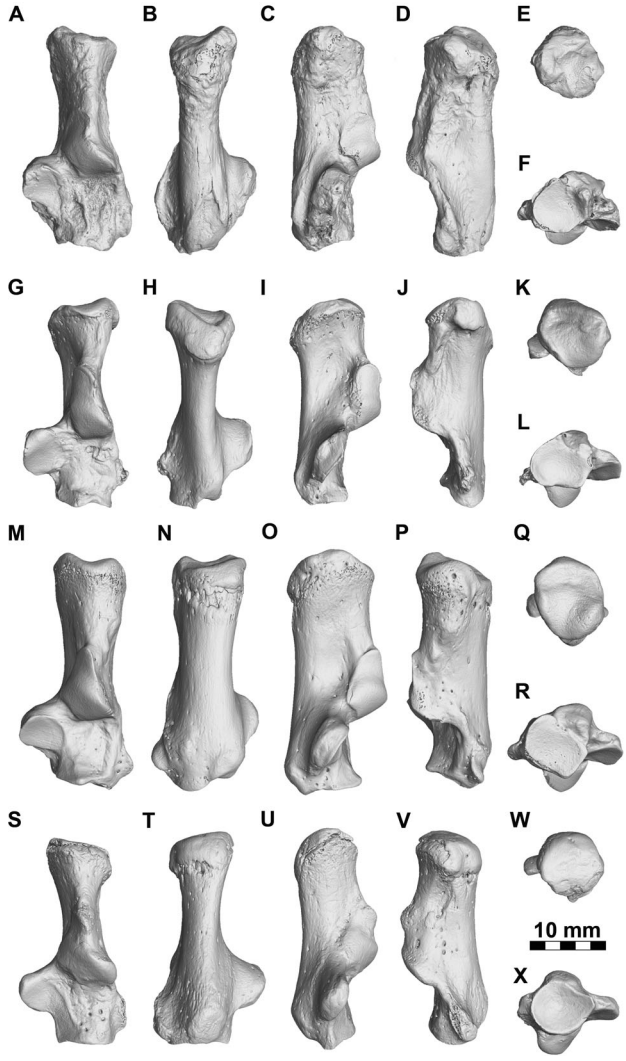

Figure 14. Calcaneus of *Magerictis imperialensis* from Fábrica de Mahou, Madrid (Spain) and selected extant Musteloidea (*Ailurus fulgens*, *Procyon lotor*, *Meles meles*). **A–F**, *M. imperialensis* FMH'14-1703, left calcaneus from Fábrica de Mahou: **A**, dorsal view; **B**, plantar view; **C**, medial view; **D**, lateral view; **E**, proximal view; **F**, distal view: **G–L**, *A. fulgens* MNCN M-14231, left calcaneus: **G**, dorsal view; **H**, plantar view; **I**, medial view; **J**, lateral view; **K**, proximal view; **L**, distal view. **M–R**, *Pr. lotor* MNCN M-19501, left calcaneus: **M**, dorsal view; **N**, plantar view; **O**, medial view; **P**, lateral view; **Q**, proximal view; **R**, distal view. **S–X**, *Me. meles* MNCN M-21763, left calcaneus: **S**, dorsal view; **T**, plantar view; **U**, medial view; **V**, lateral view; **W**, proximal view; **X**, distal view.

fragments from the site of El Cañaveral (CAÑ-998 and CAÑ-1168) are in a very poor state of preservation but can be attributed to the species.

Metapodials. FMH'14-1292, right metacarpal- I (Mc-I) (Fig. 15A–F; Table 5). It is slender and slightly curved dorsopalmarly. The proximal articulation for the trapezium is triangular and located on a dorsally inclined plane. The medial process is well developed and possesses a smooth process for the attachment area of the abductor digiti I longus. The articulation with the Mc-II is poorly marked. The distal epiphysis is asymmetrical, and the keel is well marked palmarly.

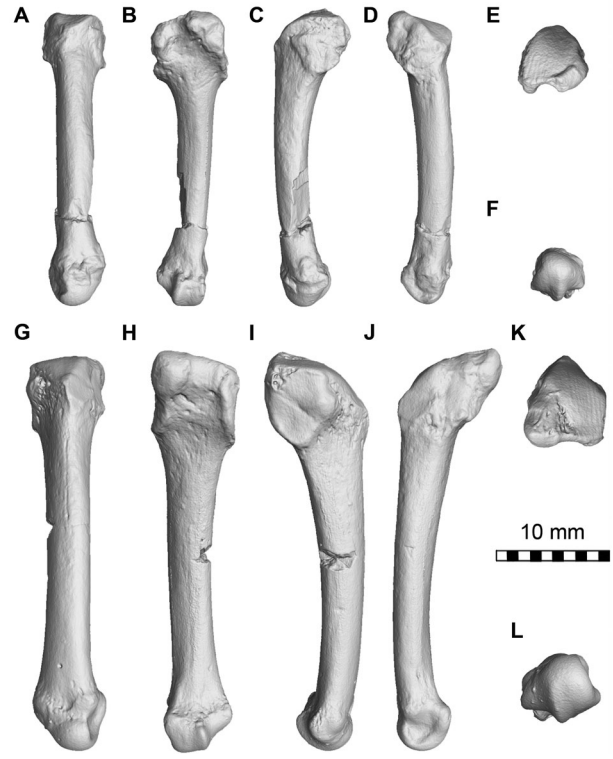

Figure 15. Metapodials of *Magerictis imperialensis* from Fábrica de Mahou (Madrid, Spain). **A–F**, FMH'14-1292, right metacarpal I: **A**, dorsal view; **B**, palmar view; **C**, medial view; **D**, lateral view; **E**, proximal view; **F**, distal view. **G–L**, FMH'14-1478 left metatarsal I: **G**, dorsal view; **H**, plantar view; **I**, medial view; **J**, lateral view; **K**, proximal view; **L**, distal view.

FMH'14-1478, left metatarsal-I (Mt-I) (Fig. 15G–L; Table 5). It is slender and slightly curved dorsoplantarly. The proximal articulation for the entocuneiform is trapezoidal. The lateral process is large and rough, being the attachment for the muscle peroneus longus. The medial one is well defined and has a tuberosity for the tibialis cranialis muscle. Palmarly, below the proximal epiphysis, a small depression develops between the lateral and medial processes. The distal epiphysis is asymmetrical, and the keel is plantarly well defined.

Discussion

Magerictis imperialensis has a distinctive dentition. Some of its characteristics are primitive and similar to

those of Amphictidae (*Amphictis* and *Bonisictis*), in particular the mandibular morphology, high premolar teeth, P4 with a strong protocone and high m1 trigonid. Other features are closer to *A. fulgens*, as evidenced by the elongated and complex m2 and the well-developed M1 paraconule. The remarkable elongation of the m2, which is related to the strong development of the hypoconid and hypoconulid, forming a third lobe, is one of the synapomorphies that characterize the Ailuridae family (Fig. 16). This trait is present in the European fossil record from the Early Miocene in Wiesbaden-Amöneburg (MN2, Germany) with *R. prolongata* (Morlo, 1996) and Wintershof-West (MN3, Germany) with *R. wintershofensis* (Beaumont, 1976; Dehm, 1950; Heizmann & Morlo, 1994). *Magerictis imperialensis* differs from *Rothictis* in the loss of the internal cristids' connection between the metaconid and the protoconid in the m2, the main cuspids of which have an incipient selenodont morphology and are separated by a continuous mesiodistal valley. It is the specific morphology of the m2 that serves to distinguish *Magerictis* and *Rothictis* from *Am. antiquus*. In the latter, the m2 exhibits a larger and more robust trigonid than the talonid, which is almost entirely occupied by the hypoconid (Beaumont, 1976). Furthermore, an elongation of the m2 is also observed in other species such as *B. ambiguus*, *B. milloquensis* and *Am. schlosseri* (Fig. 16). However, the m2 in these species is comparatively smaller and not correlated with an increase in the hypoconulid size. The morphology of the M1 of *Rothictis* and *Magerictis* is similar to that of *Am. antiquus* (Viret, 1929b), with the buccolingual length greater than the mesiodistal length (Supplemental material 1, S3). The M1 trigone arrangement in these species is primitive for the Carnivora, with the distal crista of the protocone (postprotocrista) in contact with the metaconule. This is also a common feature in the Simocyoninae, but not in the Ailurinae. In the latter subfamily, the upper molars have undergone a loss of the postprotocrista, resulting in the metaconule becoming isolated from the protocone. This has resulted in a modification towards an advanced bunoselenodont pattern. Therefore, *Rothictis* and *Magerictis* represent the most primitive taxa within the Ailuridae, and *R. wintershofensis* is identified as the stem species of this family (Fig. 17). Consequently, *Amphictis* and *Bonisictis* should be placed in a different family, Amphictidae, due to the distinct morphology of the m2. This does not preclude *B. ambiguus* from being the ancestral taxon of the ailurids and other Musteloidea (de Bonis, 1976; Cirot & de Bonis, 1993; Schmidt-Kittler, 1981; Wolsan, 1993). The species *B. ambiguus* and *B. milloquensis* have been dated to the Late Oligocene (MP 28–29), which places these species in close proximity to the inferred age for the divergence of the Ailuridae and Procyonidae (e.g. Eizirik et al., 2010; Sato & Wolsan, 2012; Sato et al., 2009; Wang et al., 2023).

Regarding the postcranial skeleton, the talus (astragalus) of *M. imperialensis* from El Cañaveral and Fábrica de Mahou exhibits a similar morphology to that of *A. fulgens* (Fig. 13). They are significantly low dorsoplantarly and have a flattened trochlea that is comparatively narrower in the extant species in the lateromedial direction. The strong dorsoplantar compression influences the morphology of the ectal facet, which appears more flattened and extends proximally in plantar view. Consequently, the groove for the plantar tendon is poorly defined and does not protrude plantarly. This morphology is also observed in *S. batalleri*. The sustentacular facet is more developed in *Magerictis* than in *Ailurus* and is arranged almost parallel to the plantar plane, similar to *S. batalleri*. In contrast, in *A. fulgens* it is curved medially. The navicular facet in both *Magerictis* and *Ailurus* is elliptical, transverse and dorsoproximal compressed, as in *S. batalleri*. The calcaneus of Fábrica de Mahou exhibits a high degree of similarity to that of *A. fulgens*. However, they differ in the arrangement of the talar sustentaculum, which in *Ailurus* is rotated towards a more dorsoproximal position, with the articular facet situated farther from the ectal facet. The lateromedial length of the articular area is relatively greater (Fig. 14). In *S. batalleri* the position of the sustentaculum tali is comparable to that observed in *Ailurus*, yet the lateromedial length of the articular area is markedly more developed. In *Magerictis* the peronian process is not particularly prominent. However, in dorsal view, there is a notable widening of the lateral surface. In contrast, this widening and the peronian process are relatively small in *Ailurus*. *Simocyon batalleri* is similar to *A. fulgens*, but the peronian process appears to be relatively more developed. Both genera are also distinguished from *Magerictis* by the greater development of the coracoid process. While comparison with other extinct Ailurinae is possible, it is limited. Although *P. bristoli* is known from postcranial materials that include two nearly complete skeletons, a detailed description is still lacking (Wallace & Lyon, 2022). *Parailurus hungaricus* Kormos, 1934 from the Hajnácka site, Slovakia, includes dental material and some postcranial remains, such as a talus and two calcanei (Fejfar & Sabol, 2004). The size of the Hajnácka astragalus is intermediate between that of *A. fulgens* and *Simocyon batalleri*, but its robustness is closer to that of the latter species. The astragalus of Hajnácka has a deeper trochlea and more pronounced lips in comparison to *A. fulgens*, displaying similarities to those observed in *Simocyon* and *Magerictis*. The facet for the navicular is more rounded

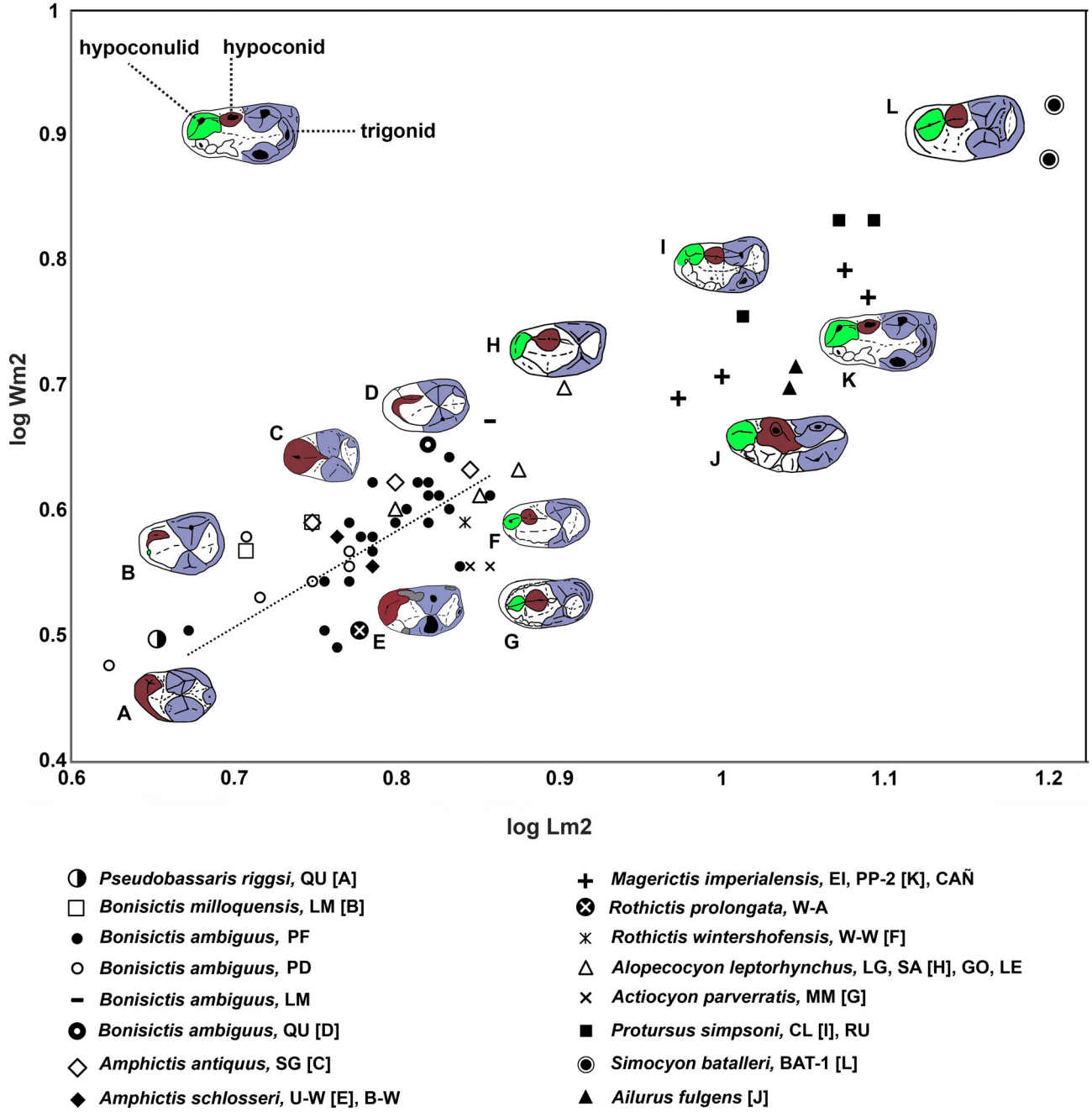

Figure 16. Bivariate plot comparing the length (L) and width (W) of the m2 of *Magerictis imperialensis* with other Ailuridae and Musteloidea. **Locality abbreviations**: **Bat-1**, Batallones-1; **CA**, Cañaveral; **CL**, Can Llobateres; **EI**, Estación Imperial; **EG**, Eggingen**; GO**, Göriach; **LE**, Leöben; **LG**, La Grive; **LM**, La Milloque; **MM**, Monarch Mill; **PD**, Pech Desse; **PF**, Pech du Fraysse; **PP**, Prín4cipe Pío-2; **QU**, Quercy; **RU**, Rudabánya; **U-W**, Ulm-Westtangente; **W-A**, Wiesbaden-Amöneburg; **W-W**, Wintershof-West. **m2** schemes based on: **A**, *Pseudobassaris riggsi* from Quercy (SNSB-BSPG 1879 XV 716); **B**, *Bonisictis milloquensis* from La Milloque (FS-LPVP LM 1969 MC-2); **C**, *Amphictis antiquus* from Saint Gérand (FSL 213846); **D**, *Bonisictis ambiguus* from Quercy (MNHN. F. QU-9244); **E**, *Amphictis schlosseri* from Ulm-Westtangente (SMNS-45758); **F**, *Rothictis wintershofensis* from Wintershof-West (SNSB-BSPG 1937 II 13138); **G**, *Actiocyon parverratis* from Monarch Mill (UCMP 141828); **H**, *Alopecocyon leptorhynchus* from Sansan (MNHN-F-345); **I**, *Protursus simpsoni* from Can Llobateres (IPS-1976); **J**, *Ailurus fulgens* (extant, MNCN M-142311); **K**, *M. imperialensis* from Príncipe Pío-2 (PP-2-3624); **L**, *Simocyon batalleri* from Batallones-1 (B-3238). The trend line represents the specimens of *Bonisisctis ambiguus* from Pech du Freysse. Data from Cirot (1992), Cirot and Wolsan (1995), Heizmann and Morlo (1994), Morlo (1996), Peigné (2012), Peigné et al. (2005), K. Smith et al. (2016), Viret (1929b).

and less compressed dorsoplantarly, resembling that of *Ailurus*. The calcaneus of Hajnácka is comparable to that of *Simocyon* because of the highly developed coracoid process, although as in *Magerictis*, the peronian process is relatively small. The metapodials of *M. imperialensis* Mc-I and Mt-I are relatively longer proximodistally and more slender than those of *Ailurus* (Table 5), similar to what can be observed when compared to the even more robust metapodials of *S. batalleri*. The proximal epiphyses of these two metapodials are narrower lateromedially, due to the poor development of the lateral process, which is more developed in *Ailurus*. In contrast, *Simocyon* has developed more lateral processes but also enlarged the proximal articular surface, especially in the Mc-I (Salesa et al., 2006). The attachment area for the abductor digiti I longus in *Magerictis* is quite large and widened medially. This would imply that the development of this muscle would be considerable (Abella et al 2015, 2016; Salesa et al, 2006). Unfortunately no radial sesamoid was found, so no comparison can be made to discuss the capability of this species to grasp using the radial sesamoid complex. However, following Abella et al. (2015, 2016) we could expect this species to have a well-developed and functional false thumb.

In summary, the postcranial morphology of *M. imperialensis* appears to be closer to *Ailurus* than to *Simocyon*. The morphology of the calcaneo-talar joint is a defining feature that links these three genera to *Parailurus*, allowing for the clear distinction of the Ailuridae family from other families within Musteloidea. The most notable contrasts are evident when comparing to the Mustelidae (*Mustela*, *Martes*, *Gulo*, *Meles* and *Taxidea*) (Figs. 14–15) and Mephitidae (*Mephitis*, *Conepatus*, *Spilogale*, and *Mydaus*). In Mustelidae, the talus has a very strong lateral process and the trochlea extends proximally. This results in the groove for the talonid tendon projecting plantarly, thereby enclosing the tarsal groove. The body of the talus is high and compressed lateromedially. There is some variability in the shape of the neck, which is more elongated and the ectal facet is highly inclined to the plantar plane. The astragalus of the Mephitidae differs from that of the Ailuridae in the shallow depth of the trochlea in which the lips are barely discernible, and consequently by the very shallow dorsal surface, which is somewhat more marked proximally. The ectal facet is notably broad, reflecting the widening of the trochlea. The body of the talus is distinguished by a higher body, a pronounced astragalar groove, and a more robust neck. In Mephitidae, the calcaneal shaft is relatively short in comparison to the articular area. The distinctions between the Ailuridae and Procyonidae are relatively minor (Figs. 14–15). In *Procyon*, the trochlea of the talus is wider, its surface is deeper, and the lips are more prominent. The body is tall, with the lateral surface as high as in *Meles*. The talar neck is wider, with a short sustentacular facet touching the articular surface for the navicular. The ectal facet is wider. Proximally, the groove for the plantar tendon is higher and very well defined (canalized) and the astragalar tubercle is stronger and more individualized.

Phylogenetic relationships

The phylogenetic relationships within Ailuridae are strongly influenced by the close evolutionary

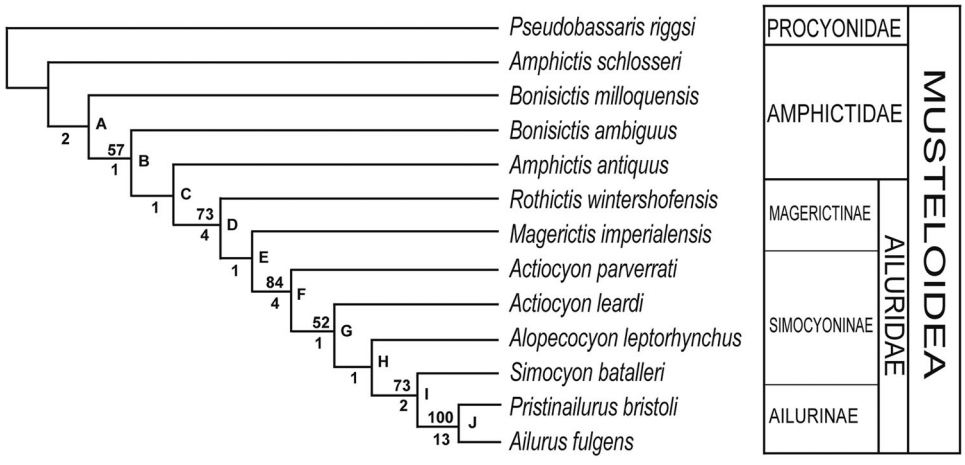

Figure 17. Phylogenetic relationship of *Magerictis imperialensis* within Ailuridae (node D) and of some extinct Musteloidea carnivorans. *Pseudobassaris riggsi* is the outgroup. Searches were performed using the Branch and Bound and a Bootstrap analysis through 10,000 replicates. A single tree is obtained (length 107 steps, consistency index [CI] = 0.6355, homoplasy index [HI] = 0.3645, and retention index [RI] = 0.7090). The numbers below nodes are Bremer indices, and the numbers above nodes are bootstrap support percentages (only shown if >50). The synapomorphies are shown in Supplemental material 1 (S5).

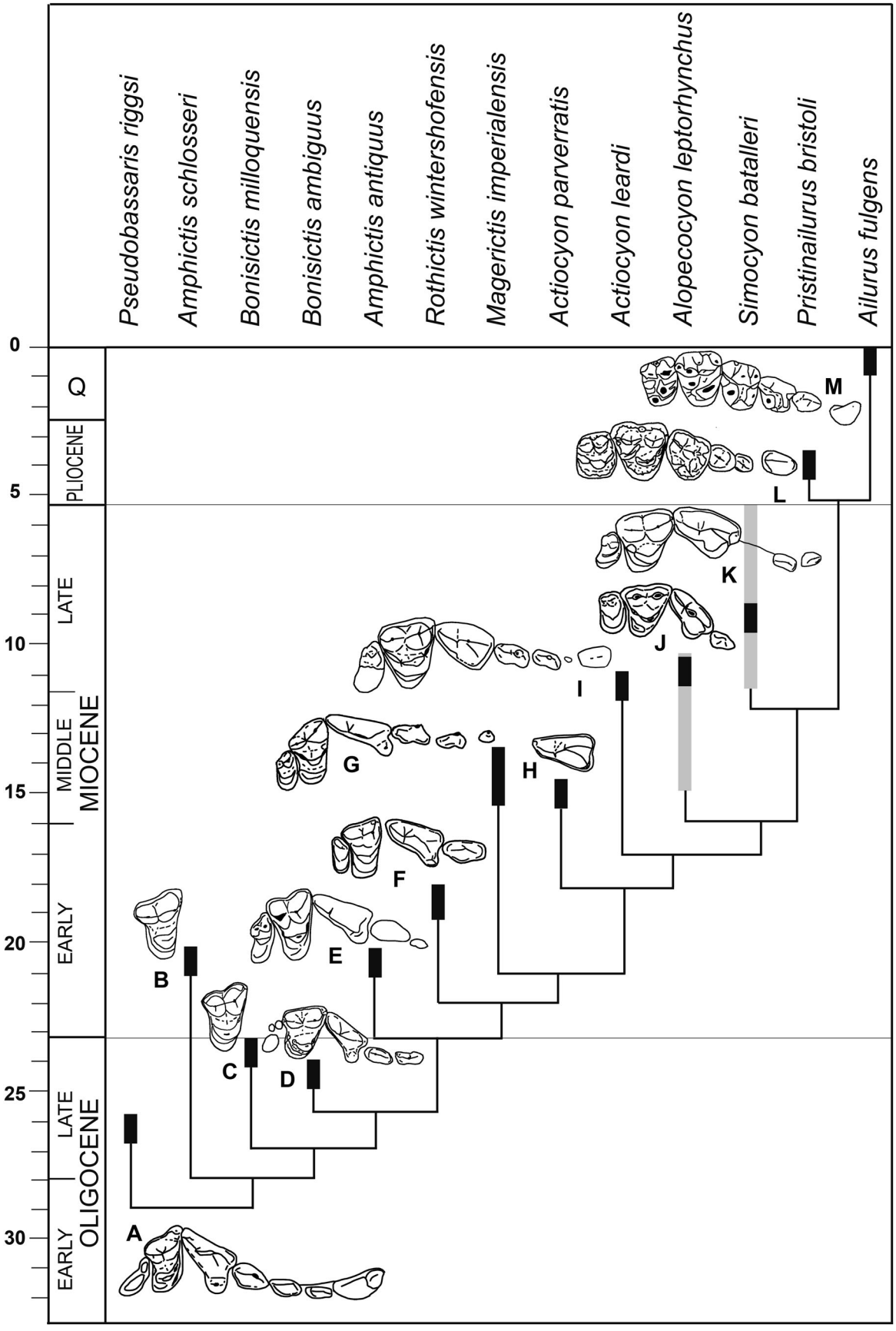
Pseudobassaris riggsi
Amphictis schlosseri
Bonisictis milloquensis
Bonisictis ambiguus
Amphictis antiquus
Rothictis wintershofensis
Magerictis imperialensis
Actiocyon parverratis
Actiocyon leardi
Alopecocyon leptorhynchus
Simocyon batalleri
Pristinailurus bristoli
Ailurus fulgens
0
5
10
15
20
25
30
Q
PLIOCENE
LATE
MIDDLE
MIOCENE
EARLY
LATE
OLIGOCENE
EARLY
A
B
C
D
E
F
G
H
I
J
K
L
M

relationship between *Simocyon* and *Ailurus*. The two genera share cranial, mandibular and postcranial characteristics that support a sister group relationship (Peigné et al., 2005; Salesa et al., 2006, 2011; Wang, 1997). However, the significant differences in dental morphology suggest that the split between the two genera occurred before the Middle–Late Miocene boundary. During the Middle Miocene, a modest adaptive radiation occurred in Western Europe and North America, with the appearance of *Alopecocyon* and *Actiocyon* (Figs. 17–18). These genera are characterized by a mesocarnivorous dentition, which is prone to alteration in opposite directions, such as hypercarnivorous or hypocarnivorous. However, the majority of authors have concluded that they are more closely associated with *Simocyon* than *Ailurus* (Morlo & Peigné, 2010; Salesa et al., 2011). This is supported by the temporal continuity in the European fossil record between *Rothictis*, *Alopecocyon* and *Simocyon*, and the gradual changes towards a more robust dentition, with the protocone reduction of the P4 and an M1 with the buccolingual width shortened (Fig. 18). In addition to the reduction of the P4 protocone, the strengthening of the dentition and the shortening of the M1 are derived characters that are shared with the Ailurinae. However, the absence of any signs of molarization in the premolars and the maintenance of a simple morphology of molars, except for m2, influence the conclusion that these taxa are more closely related to *Simocyon* than to *Ailurus*. This group of mesocarnivorous ailurids is present in North America (K. Smith et al., 2016; Stock, 1947), where it is represented by *Ac. leardi* and *Ac. parverratis*. Both species have a comparable morphological dental grade to that of the European *Alopecocyon*, yet exhibit notable distinctions that justify their classification as distinct genera. As with *Alopecocyon*, establishing a link with the Ailurinae is challenging, apart from the observed trend towards stronger dentitions. These two genera are included in the Simocyoninae, despite this being a paraphyletic taxon. In our cladogram, *Alopecocyon* and *Actiocyon* are shown as a sister group to *Simocyon* and Ailurinae (Fig. 17). *Magerictis* is placed between the clade constituted by the Symocyoninae-Ailurinae and the stem species *R. wintershofensis* (Fig. 17). It presents a plesiomorphic dentition, whereby the m2 differs from all other Ailuridae species. The m2 of *Magerictis* displays a distinctive arrangement of buccal and lingual cuspids, which are positioned in parallel and separated by a continuous trigonid-talonid valley. This central continuous valley is present in the m2 of the Ailurinae species, but it is almost obliterated due to the significant development of the cuspids. Accordingly, the dental morphological distance between *Magerictis* and *Ailurus* seems too great to consider a direct relationship. Nevertheless, the process of premolar molarization associated with a molar specialization in carnivorans is well known in both fossil and extant species, and known cases that illustrate the quick molarization of premolars and the high molar specialization occur, such as that of the family Lophocyonidae, a group of bunoselenodont feliform carnivorans that evolved from primitive Hyaenidae (Fejfar et al., 1987; Morales et al., 2019). Additionally, the morphology of certain postcranial elements suggests that *Magerictis* was very closely related to *Ailurus* in terms of the proximal tarsal articulation, although the two preserved metapodials exhibit primitive proportions in comparison to the homologous bones of *Ailurus*. Thus, *Magerictis* provides evidence of an alternative pathway for the acquisition of the ailurid morphology, independent of the Simocyoninae species.

Conclusions

Based on their dental characteristics, *M. imperialensis* and *R. wintershofesis* are considered the most basal Ailuridae taxa. They can be distinguished from the more primitive Amphictidae (*Amphictis* and *Bonisictis*) by the derived m2 morphology, characterized by the strong development of the hypoconid and hypoconulid forming a third lobe. These synapomorphies characterize the Ailuridae family.

Our phylogenetic analysis indicates that *M. imperialensis* is the sister group to the Simocyoninae and the

Figure 18. Biochronology and hypothesis of phylogenetic relationships of the species of Ailuridae and other Musteloidea based on our cladistic analysis (Fig. 15). The upper dentition schemes are based on: **A**, *Pseudobassaris riggsi* from Quercy (AMNH-17488); **B**, *Amphictis schlosseri* from Eggingen (SNSB-BSPG 1881 IX 572); **C**, *Bonisictis milloquensis* from La Milloque (FS-LPVP LM 1969 MC-4); **D**, *Bonisictis ambiguus* from Pech du Fraysse (FS-LPVP PFRA-28); **E**, *Amphictis antiquus* from Saint Gérand le Puy (UCBL-FSL 212860); **F**, *Rothictis wintershofensis* from Wintershof-West (composed by SNSB-BSPG 1937 II 13402, 13707 and 14488); **G**, *Magerictis imperialensis* from El Cañaveral (composed by CAÑ-506, 743); **H**, *Actiocyon parverratis* from Monarch Mill (UCPM-141911); **I**, *Actiocyon leardi* from Apache Canyon (LACM-2747); **J**, *Alopecocyon leptorhynchus* from La Grive (modified from Thenius, 1949a); **K**, *Simocyon batalleri* from Batallones-1 (composed by B-3620, 3235); **L**, *Pristinailurus bristoli* from Gray Fossil Site (ETMNH 15000); **M**, *Ailurus fulgens*. The drawings of the specimens are not scaled and have all been considered as the right side. **Abbreviation**: **Q**, Quaternary.

Ailurinae, and is placed in a distinct subfamily, Magerictinae, together with *Rothictis*. The mesocarnivore genera *Alopecocyon*, *Actiocyon* and *Protursus* underwent a limited adaptative radiation during the Miocene in Eurasia and North America. It is likely that the potential ancestors of *Simocyon* and Ailurinae can be found within this group. However, the dental morphological gap between these Ailurinae and their hypothetical Miocene ancestors remains to be documented. This is because all members of the Ailurinae present a highly advanced bunoselenodont molar morphology that is not found in any other ailurid species. Furthermore, there is evidence of molarization of the premolars, a process that has reached the P4/p4 in *Pristinailurus* and is incipient in the P3/p3 but is completed in *Parailurus* and *Ailurus*. Therefore, the links between Ailurinae and the rest of the Ailuridae are waiting to be discovered, probably in Asia.

Acknowledgements

We thank the following curators and collection managers for granting access to comparative material under their care: J. Galkin, J. Flynn, J. Meng and R. O'leary (AMNH), J. Robles and J. Galindo J.M. (ICP), B. Patterson (FMNH), S. Fraile and A. Garvia (MNCN), C. Argot, G. Billet (MNHN), U.B. Göhlich (NHMW), D.C. Kalthoff (NRM), E. Amson (SMNS), G. Rössner (SNSB-BSPG), and E. Robert (UCBL-FSL). We also thank the authors of the photographs we used to study some of the taxa considered: Q. Jiangzuo (Chinese Academy of Sciences) for *Actiocyon parverratis* from Monarch Mill, D. Berthet (MDC) for *Amphictis antiquus* from Saint Gérand le Puy, S. Mayda (Ege University) for the occlusal view of the specimen 13147 of *Rhoticitis wintershofensis* from Wintershof-West, M.D. Ercoli (INECOA) and J. Tarquini (CICYTTP, CONICET-Gob. ER-UADER) for tarsals of extant mephitids, and L. de Bonis for *Bonisictis ambiguuus* from Pech du Fraysse. We express our gratitude to Dirección General de Patrimonio Histórico de la Comunidad de Madrid and the directors of the excavations from the Madrid urban area where *M. imperialensis* was found. We further thank S.C. Wallace (ETMNH) for sharing the character matrix descriptions from Wallace and Lyon (2022), E. Cantero (MNCN-CSIC) for the preparation of the fossils of *M. imperialensis*, and C. Paradela (Servicio de Técnicas No Destructivas from MNCN-CSIC). O. Caballero is a pre-doctoral FPI (PRE2019-091348) of the project PGC2018-094122-B-100 (MICU/AI/FEDER, EU). A. Valenciano received support for his research through the project SYNTHESYS3, http://www.synthesys.info/ (SYNTHESYS; AT-TAF-5457), financed by the European Community Research Infrastructure Action under the FP7 'Capacities' Programme, and the European Union's Seventh Framework Programme (FP7/2007-2013) under grant agreement no. 226506 (SYNTHESYS; SE-TAF-3637), a Visiting Scholarship of the Chicago Field Museum of Natural History (2016), as well as funding from AMNH by a Collection Study Grant Program 2022 and Theodore Roosevelt Memorial Grant 2022. This study was supported by the Research Group UCM910607, and the projects PID2023-151089NB-I00 and PID2024-160207NB-I00 funded by MCIU/AEI/10.13039/501100011033/FEDER, UE. Lastly, we thank the Editor-in-Chief I. Rahman as well as the three anonymous reviewers for their valuable comments and suggestions.

Supplemental material

Supplemental material for this article can be accessed here: https://doi.org/10.1080/14772019.2025.2571254.

Disclosure statement

The authors report there are no competing interests to declare.

Funding

The study was funded by the Research Group UCM910607, and the projects PID2023-151089NB-I00 and PID2024-160207NB-I00 funded by MCIU/AEI/10.13039/501100011033/FEDER, UE.

ORCID

Juan Abella http://orcid.org/0000-0002-3433-6093
Oscar Caballero http://orcid.org/0000-0002-5038-1388
Alberto Valenciano http://orcid.org/0000-0003-1633-2248

Data availability statement

The data supporting the findings of this study are openly available through MorphoBank at https://doi.org/10.7934/P6014 (Morales *et al.* 2025a) and through MorphoSource, where the full media list can be found at https://doi.org/10.17602/M2/L780594 (Morales *et al.* 2025b), consisting of:

https://doi.org/10.17602/M2/M773448;
https://doi.org/10.17602/M2/M773440;
https://doi.org/10.17602/M2/M773432;
https://doi.org/10.17602/M2/M773424;
https://doi.org/10.17602/M2/M773420;
https://doi.org/10.17602/M2/M773404;
https://doi.org/10.17602/M2/M773396;
https://doi.org/10.17602/M2/M773383;
https://doi.org/10.17602/M2/M773369c;
https://doi.org/10.17602/M2/M773361;
https://doi.org/10.17602/M2/M773333;
https://doi.org/10.17602/M2/M773326;
https://doi.org/10.17602/M2/M772914;
https://doi.org/10.17602/M2/M772883;
https://doi.org/10.17602/M2/M772869;
https://doi.org/10.17602/M2/M772849;
https://doi.org/10.17602/M2/M772844;
https://doi.org/10.17602/M2/M772835;
https://doi.org/10.17602/M2/M772826;
https://doi.org/10.17602/M2/M772822;
https://doi.org/10.17602/M2/M772709;
https://doi.org/10.17602/M2/M772663;
https://doi.org/10.17602/M2/M772659;
https://doi.org/10.17602/M2/M772640;
https://doi.org/10.17602/M2/M772631;
https://doi.org/10.17602/M2/M772522;
https://doi.org/10.17602/M2/M772463.

References

Abella, J., **Pérez-Ramos, A.**, **Valenciano, A.**, **Alba, D. M.**, **Ercoli, M. D.**, **Hontecillas, D.**, **Montoya, P., & Morales, J.** (2015). Tracing the origin of the panda's thumb. *The Science of Nature*, *102*(35). https://doi.org/10.1007/s00114-015-1286-3

Abella, J., **Ruiz-Sánchez, F. J.**, **Valenciano, A.**, **Hontecillas, D.**, **Pérez-Ramos, A.**, **Cornejo, M. H.**, **Santana Cabrera, J. A.**, **Román-Carrión, J. L.**, **Montoya, P., & Morales, J.** (2016). When cotton rats grasp like pandas. *Journal of Mammalian Evolution*, *23*(3), 309–317. https://doi.org/10.1007/s10914-015-9314-9

Antón, M., **Salesa, M. J**, **Pastor, J. F.**, **Peigné, S., & Morales, J.** (2006). Implications of the functional anatomy of the hand and forearm of *Ailurus fulgens* (Carnivora, Ailuridae) for the evolution of the 'false-thumb' in pandas. *Journal of Anatomy*, *209*(6), 757–764. https://doi.org/10.1111/j.1469-7580.2006.00649.x

Antunes, M. T. (1979). '*Hispanotherium* fauna' in Iberian middle Miocene, its importance and paleogeographical meaning. *Annales Géologiques du Pays Hellénique*, 25–33.

Barone, R. (1999). *Anatomie comparée des mammifères domestiques, Tome 1, ostéologie* (4th ed.). Éditions Vigot.

Barone, R. 2000. *Anatomie comparée des mammifères domestiques, Tome 2, antrologie et myologie* (4th ed.). Éditions Vigot.

Baskin, J. A. (1998a). Mustelidae. In C. M. Janis, K. M. Scott, & L. L. Jacobs (Eds.), *Evolution of Tertiary mammals of North America*, Volume *1: Terrestrial carnivores, ungulates, and ungulatelike mammals* (pp. 152–173). Cambridge University Press.

Baskin, J. A. (1998b). Procyonidae. In C. M. Janis, K. M. Scott, & L. L. Jacobs (Eds.), *Evolution of Tertiary mammals of North America*, Volume *1: Terrestrial carnivores, ungulates, and ungulatelike mammals* (pp. 144–151). Cambridge University Press.

Baskin, J. A. (2004). *Bassariscus* and *Probassariscus* (Mammalia, Carnivora, Procyonidae) from the early Barstovian (middle Miocene). *Journal of Vertebrate Paleontology*, *24*(3), 709–720. https://doi.org/10.1671/0272-4634(2004)024[0709:BAPMCP]2.0.CO;2

Baskin, J. A. (2017). Additional carnivorans from the early Hemingfordian Miller Local Fauna, Florida. *Journal of Vertebrate Paleontology*, *37*(2), 17.1293069. https://doi.org/10.1080/02724634.2017.1293069

de Beaumont, G.. (1964). Essai sur la position taxonomique des genres *Alopecocyon* Viret et *Simocyon* Wagner (Carnivora). *Eclogae Geologia Helvetica*, *57*, 829–836.

de Beaumont, G.. (1976). Remarques preeliminaires sur le genre *Amphictis* Pomel (Carnivore). *Bulletin du Société Vaudoise des Sciences Naturelles*, *350*(73), 171–180.

de Beaumont, G.. (1982). Qu'est-ce que le *Plesictis leobensis* Redlich (Mammifère, Carnivore)? *Archives des Sciences (Geneva)*, *35*(2), 143–152.

de Beaumont, G. (1986). Les Carnivores (Mammifères) du Néogène de Höwenegg/Hegau, Baden-Württemberg. *Carolinea*, *44*, 35–45.

de Blainville H. M. D.. (1842). *Ostéographie ou déscription iconographique comparée du squelette et du système dentaire des cinq classes d'animaux vertebras récents et fossils pour servir de base à la zoologie et à la géologie*. J. B. Baillière.

de Bonis, L. (1973). Contribution à l'étude des mammifères de l'Aquitanien de l'Agenais: Rongeurs, Carnivores, Perissodactyles. *Mémoires du Muséum national d'Histoire naturelle, Sér. C – Sciences de la Terre*, *28*, 1–192.

de Bonis, L.. (1976). Découverte d'un crâne d'*Amphictis* (Mammalia, Carnivora) dans l'Oligocène supérieur des Phosphorites du Quercy. *Comptes rendus de l'Académie des Sciences Paris*, *283*(4), 327–330.

de Bonis, L. (1997). Précisions sur l'âge géologique et les relations phyletiques de *Mustelictis olivieri* nov. sp. (Carnivora, Mustelidae), carnassier de l'Oligocéne inférieur (MP 22) des phosphorites du Quercy (France). *Geobios* M.S., *20*, 175–180. https://doi.org/10.1016/S0016-6995(97)80009-5

Bowdich, T. E. (1821). *An analysis of the natural classifications of Mammalia, for the use of students and travellers*. J. Smith.

de Bruijn, H., **Daams, R.**, **Daxner-Höck, G.**, **Fahlbusch, V.**, **Ginsburg, L.**, **Mein, P.**, & **Morales, J.** (1992). Report of the RCMNS working group on fossil mammals, Reisensberg 1990. *Newsletters on Stratigraphy*, *26*, 65–118. https://doi.org/10.1127/nos/26/1992/65

Bryant, H. N., **Russell, A. P., & Fitch, W. D.** (1993). Phylogenetic relationships within the extant Mustelidae (Carnivora): Appraisal of the cladistic status of the Simpsonian subfamilies. *Zoological Journal of the Linnean Society*, *108*(4), 301–334. https://doi.org/10.1006/zjls.1993.1028

Calvo, J. P., **Alonso Zarza, A. M., & García del Cura, M. A.** (1989). Models of Miocene marginal lacustrine sedimentation in response to varied depositional regimes

and source areas in the Madrid Basin (central Spain). *Palaeogeography, Palaeoclimatology, Palaeoecology*, *70*, 199–214. https://doi.org/10.1016/0031-0182(89)90090-4

Calvo, J. P., **Daams, R.**, **Morales, J.**, **López-Martínez, N.**, **Agustí, J.**, **Anadón, P.**, **Armenteros, I.**, **Cabrera, L.**, **Civis, J.**, **Corrochano, A.**, **Díaz-Molina, M.**, **Elizaga, E.**, **Hoyos, M.**, **Martín-Suárez, E.**, **Martínez, J.**, **Moissenet, E.**, **Muñoz, A.**, **Pérez-García, A.**, **Pérez-González, A.**, **… & Mein, P.** (1993). Up-to-date Spanish continental Neogene synthesis and Paleoclimatic interpretation. *Revista de la Sociedad Geológica de España*, *6*, 29–40.

Camp, C. L., & Vanderhoof, V. L. (1940). Bibliography of fossil vertebrates 1928–1933. *Geological Society of America*, Special Paper, *27*, 1–503.

Cerdeño, E., & Nieto, M. (1995). Changes on Western European Rhinocerotidae related to climatic variations. *Palaeogeography, Palaeoclimatology, Palaeoecology*, *114*, 325–338. https://doi.org/10.1016/0031-0182(94)00085-M

Cirot, E. (1992). *Étude phylogénétique de quelques genres d'Arctoidea de l'Oligocène Eurasiatique, comparaison des données morphologiques et moléculaires*. [PhD dissertation, Faculté des Sciences Fondamentales et Appliquées, Université de Poitiers].

Cirot, E., & de Bonis, L.. (1993). Le crâne d'*Amphictis ambiguus* (Carnivora, Mammalia): son importance pour la compréhension de la phylogénie des Muséloïdes. *Comptes rendus de l'Académie des Sciences Paris*, *316*, 1327–1333.

Cirot, E., & Wolsan, M. (1995). Late Oligocene amphictids (Mammalia: Carnivora) from La Milloque, Aquitaine Basin, France. *Geobios*, *28*(6), 757–767. https://doi.org/10.1016/S0016-6995(95)80072-7

Crouzel, F., **Ginsburg, L.**, & **Vidalenc, D.** (1976). Les carnivores fissipèdes du Stampien terminal de Dieupentale (Tarn-et-Garonne). *Bulletin de la Société d'Histoire Naturelle de Toulouse*, *112*, 207–229.

Crusafont Pairó M., & **Kurtén B.** (1976). Bears and bear-dogs from the Vallesian of the Vallés-Penedés Basin, Spain. *Acta Zoologica Fennica*, *144*, 1–29.

Cuvier, F. (1825). Panda. In: G. Saint-Hillaire (Ed.), *Histoire naturelle des Mammiferes, avec des figures originales, colorées, desinées d'après des animaux vivants* (pp. 1–3). Chez A. Belin.

Daams, R., **Van der Meulen, A. J.**, **Álvare-Sierra, M. A.**, **Peláez-Campomanes, P.**, **Calvo, J. P.**, **Alonso Zarza, M. A., & Krijgsman, W.** (1999). Stratigraphy and sedimentology of the Aragonian (Early to Middle Miocene) in its type area North-Central Spain. *Newsletters on Stratigraphy*, *37*, 103–139. https://doi.org/10.1127/nos/37/1999/103

David, A. (1869). Extrait d'une lettre du mem, datee de la Principaute Thibetaine (independente) de Mou-pin, le 21 Mars 1869. *Nouvelles Archives du Muséum d'Histoire Naturelle, Paris, 5*, 12–13.

Dawkins, W. B. (1868). Fossil animals and geology of Attica, by Albert Gaudry. (Critical summary). *Quarterly Journal of the Geological Society of London*, *24*, 1–7.

Dawkins, W. B. (1888). On *Ailurus anglicus*, a new carnivore from Red Crag, Q. J. *Quarterly Journal of The Geological Society of London*, *44*, 228–231. https://doi.org/10.1144/GSL.JGS.1888.044.01-04.20

Dehm, R. (1950). Die Raubtiere aus dem Mittel-Miocän (Burgidalium) von Wintershof-West bei Eichstätt in Bayern. *Abhandlungen der Bayerischen Akademie der Wissenschaften, Mathematisch-Naturwissenschaftliche Klasse Neue Folge*, *58*, 1–141.

Desmarest, A. G. (1820). *Mammalogie ou description des espèces de mammiferes*. Encyclopédie méthodique des mammifères. Veuve Agasse.

Domingo, L., **Koch, P. L.**, **Grimes, T. G.**, **Morales, J., & López-Martínez, N.** (2012). Isotopic paleoecology of mammals and the Middle Miocene Cooling event in the Madrid Basin (Spain). *Palaeogeography, Palaeoclimatology, Palaeoecology*, *339–341*, 98–113. https://doi.org/10.1016/j.palaeo.2012.04.026

Eizirik, E., **Murphy, W. J.**, **Koepfli, K.-P.**, **Johnson W. E.**, **Dragoo, J. W.**, **Wayne, R. K., & O'Brien, S. J.** (2010). Pattern and timing of diversification of the mammalian order Carnivora inferred from multiple nuclear gene sequences. *Molecular Phylogenetics and Evolution*, *56*(1), 49–63. https://doi.org/10.1016/j.ympev.2010.01.033

Erxleben, J. C. P. (1777). *Systema Regni Amimalis*, *per Classes*, *Ordines*, *Genera*, *Species*, *Varietates*, *Cum Synonymia et Historia Animalium*. *Classis I, Mammalia*. Weygand.

Esteban, M. C. (2004). Actuaciones arqueológicas y paleontológicas en el Plan Barajas. *Actas de las primeras jornadas de Patrimonio Arqueológico en la Comunidad de Madrid*, 55–67. Comunidad de Madrid, Consejería de Cultura y Deportes. Dirección General de Patrimonio Histórico.

Evans, H. E., & de Lahunta, A. (2010). *Miller's guide to the dissection of the dog* (4th ed). W. B. Saunders.

Evans, H. E., & de Lahunta, A. (2013). *Miller's anatomy of the dog* (4th ed). W. B. Saunders.

Fejfar, O. (1964). *The Lower Villafranchian vertebrates from Hajnáčka near Filákovo in Southern Slovakia*. Ustredni ustav geologicky, Praha.

Fejfar, O., & Sabol, M. (2004). Pliocene carnivores (Carnivora, Mammalia) from Ivanovce and Hajnacka (Slovakia). *Courier Forschungsinstitut Senckenberg*, *246*, 15–53.

Fejfar, O., **Schmidt-Kittler, N., & Zacharov, M.** (1987). *Lophocyon carpathicus* nov. gen. nov. sp. aus dem Jungtertiär der Ostslowakei und eine neue unterfamilie derschleikatzen (Viverridae). *Palaeontographica*, *199*(1–3), 1–22.

Filhol, M. H. (1879). Etude des mammiferes fossils de Saint-Gérand le Puy (Allier). *Annales des Sciences Geologiqués*, *10*, 1–252.

Filhol, M. H. (1881). Notes sur quelques mammifères fossiles de l'époque Miocéne. *Archives du Muséum d'Histoire Naturelle de Lyon*, *3*, 1–97.

Gaillard, C. (1899). Mammifères miocènes nouveaux ou peu connus de la Grive-Saint-Alban (Isère). *Archives du Muséum d'histoire naturelle de Lyon*, *7*, 1–11. https://doi.org/10.3406/mhnly.1899.957

García-Paredes, I., **Álvarez-Sierra, M. A.**, **Van den Hoek Ostende, L. W.**, **Hernández-Ballarín, V.**, **Hordijke, K.**, **López-Guerrero, P.**, **Oliver, A., & Peláez-Campomanes, P.** (2016). The Aragonian and Vallesian high-resolution micromammal succession from the Calatayud–Montalbán Basin (Aragón, Spain). *Comptes rendus de l'Académie des Sciences de Paris*, *15*(7), 781–789. https://doi.org/10.1016/j.crpv.2015.09.014

Gervais, P. (1859). *Zoologie et paléontologie françaises. Nouvelles recherches sur les animaux vertébrés*. Arthus Bertrand.

Gervais, P. (1872). Sur les mammifères dont les ossements accompagnent les dépots de chaux phosphatée des départements de Tarn-et-Garonne et du Lot. *Journal of Zoologie*, *1*, 356–380.

Gervais, P. (1873). Mammifères dont les ossements accompagnent les dépots de chaux phosphatée des départements de Tarn-et-Garonne et du Lot. *Journal of Zoologie*, *2*, 261–268.

Gervais, P. (1876). *Zoologie et paléontologie générales. Nouvelles recherches sur les animaux vertébrés*. Arthus Bertrand.

Ginsburg, L. (1961). La faune des carnivores Miocènes de Sansan (Gers). *Mémoires du Muséum National d'Histoire Naturelle*, *Paris*, *sér*. *C9*, 1–190.

Ginsburg, L. (1999). Order Carnivora. In G. E. Rössner, & K. Heissig (Eds.), *The Miocene land mammals of Europe* (pp. 109–148). Friedrich Pfeil.

Ginsburg, L. (2001). Les faunes de mammifères terrestres du Miocène moyen des Faluns du bassin de Savigné-sur-Lathan (France). *Geodiversitas*, *23*(3), 381–394.

Ginsburg, L., Maridet, O., & Mein, P. (2001). Un Ailurinae (Mammalia, Carnivora, Ailuridae) dans le Miocène moyen de Four (Isère, France). *Geodiversitas*, *23*(1), 81–85.

Ginsburg, L., Morales, J., Soria, D., & Herráez, E. (1997). Découverte d'une forme ancestrale du Petit Panda dans le Miocène moyen de Madrid (Espagne). *Comptes rendus de l'Académie des Sciences de Paris*, *325*(6), 447–451. https://doi.org/10.1016/S1251-8050(97)81163-9

Glatston, A. R., Princée, F., & de Boer, L. (2022). Are there two species of red panda? Are they equally threatened with extinction? In A. L. Glatston (Ed.). *Red panda biology and conservation of the first panda* (2nd ed., pp. 421–434). Academic Press. https://doi.org/10.1016/B978-0-12-823753-3.00031-4

Gray, J. E. (1843). *List of the specimens of Mammalia in the collection of the British Museum*. British Museum (Natural History) Publications, The Trustees.

Groves, C. (2022). The taxonomy and phylogeny of *Ailurus*. In A. L. Glatston (Ed.), *Red panda biology and conservation of the first panda* (2nd ed., pp. 95–117). Academic Press. https://doi.org/10.1016/B978-0-12-823753-3.00012-0

Hassanin, A., Veron, G., Ropiquet, A., van Vuuren, B. J., Lécu, A., Goodman, S. M., Haider, J., & Nguyen, T. T. (2021). Evolutionary history of Carnivora (Mammalia, Laurasiatheria) inferred from mitochondrial genomes. *PLoS ONE 16*(2), e0240770. https://doi.org/10.1371/journal.pone.0240770

Heizmann, E. P. J., & Morlo, M. (1994). *Amphictis schlosseri* n. sp. – eine neue Carnivoren-Art (Mammalia) aus dem Unter-Miozän von Südwestdeutschland. *Stuttgarter Beiträge zur Naturkunde A (Geol. Paläontol.)*, *216*, 1–25.

Helbing, H. (1928a). Carnivoren des oberen Stampien. *Abhandlungen der Schweizerischen Palaeontologischen Gesellschaft*, *50*, 1–36.

Helbing, H. (1928b). Carnivoren aus der miocänen Molasse der Schweiz. *Eclogae Geologia Helvetica*, *21*(1), 231–244.

Hernández-Ballarin, V., & Peláez-Campomanes, P. (2017). Impact of global climate in the diversity patterns of middle Miocene rodents from the Madrid Basin (Spain). *Palaeogeography, Palaeoclimatology, Palaeoecology*, *472*, 108–118. https://doi.org/10.1016/j.palaeo.2017.01.029

Herráez, E., García-Paredes, I., Peláez-Campomanes, P., & Morales, J. (2006). Los Nogales, nueva fauna de vertebrados del Mioceno medio de Madrid. *Estudios Geológicos*, *62*, 257–262. https://doi.org/10.3989/egeol.0662125

Herráez, E., Mena, P., & Nogueras, E. (2000). Los yacimientos paleontológicos dentro del término municipal de Madrid: El pasillo Verde Ferroviario, Cuña Alhambra-Latina y actuaciones limítrofes. In J. Morales (Ed.). *Patrimonio paleontológico de la Comunidad de Madrid. Arqueología, paleontología y etnografía. Monográfico 6* (pp. 47–55). Consejería de Educación de la Comunidad de Madrid.

Hu, Y., Wei, F., & Arjun, T. (2022). Red panda genomics and the evidence for two species. In A. L. Glatston (Ed.). *Red panda biology and conservation of the first panda* (2nd ed., pp. 413–420). Academic Press. https://doi.org/10.1016/B978-0-12-823753-3.00015-6

Hu, Y., Wu, Q., S. Ma, Shan, L., Wang, X., Niew Y., Ning, Z., Yan, L., Xiu, Y., & Wei, F. (2017). Comparative genomics reveals convergent evolution between the bamboo-eating giant and red pandas. *Proceedings of the National Academy of Sciences*, *114*(5), 1081–1086. https://doi.org/10.1073/pnas.1613870114

Kadić, O., & Kretzoi, M. (1927). Vorläufiger Bericht über die Ausgrabungen in der Csákvárer Höhlung. *Barlankutatós*, *14–15*, 1–21.

Kargopoulos, N., Valenciano, A., Abella, J., Kampouridis, P., Lechner, T., & Böhme, M. (2022). The exceptionally high diversity of small carnivorans from the Late Miocene hominid locality of Hammerschmiede (Bavaria, Germany). *PLoS One*, *17*(7), e0268968. https://doi.org/10.1371/journal.pone.0268968

Kaup, J. J. (1832). Vier neue Arten urweltlicher Raubthiere, welche im zoologischen Museum zu Darmstadt aufbewahrt werden. *Arch Mineral, Geognosie, Bergbau Hüttenkunde*, *5*, 150–158.

Koepfli, K-P., Dragoo, J. W., & Wang, X. (2017). The evolutionary history and molecular systematics of the Musteloidea. In: D. W. Macdonald, C. Newman, & L. A. Harrington (Eds.). *Biology and conservation of musteloids* (pp. 75–91). Oxford University Press. https://doi.org/10.1093/oso/9780198759805.003.0002

Kormos, T. (1934). Neue und wenig bekannte Musteliden aus dem ungarischen Oberpliozän. *Folia Zoologica et Hydrobiologica*, *5*(2), 129–158.

Kretzoi, M. (1929). Materialien zur phylogenetischen Klassifikation der Aeluroïdeen. *X Congres International de Zoologie*, *Budapest 1927*, *2*, 1293–1355.

Kretzoi, M. (1943). *Kochictis centennii* n. g. n. sp., ein altertümlicher Creodonte aus dem Oberoligozän Siebenbürgens. *Földtani Közlöny*, *73*, 180–195.

Kretzoi, M. (1947). New names for mammals. (Notes on nomenclature, No. 3). *Annales Historico Naturales Musei Nationalis Hungarici*, *40*, 285–287.

Kullmer, O., Morlo, M., Sommer, J., Lutz, H., Engel, T., Forman, M., & Holzförster, F. (2008). The second specimen of *Simocyon diaphorus* (Kaup, 1832) (Mammalia, Carnivora, Ailuridae) from the type-locality Eppelsheim (Early Late Miocene, Germany). *Journal of Vertebrate Paleontology*, *28*(3), 928–932. https://doi.org/10.1671/0272-4634(2008)28[928:TSSOSD]2.0.CO;2

Kundrát, M. (2022). Phenotypic and geographic diversity of the lesser panda *Parailurus*. In A. L. Glatston (Ed.). *Red panda biology and conservation of the first panda* (2nd

ed., pp. 53–79). Academic Press. https://doi.org/10.1016/B978-0-12-823753-3.00029-6

Lange, B. (1969). Un nouveau Mustéliné des phosphorites du Quercy *Mustelictis piveteaui*. *Comptes rendus de l'Académie des Sciences de Paris*, *D*, 268, 2870–2872.

Lange, B. (1970). *Mustelictis piveteaui*, mustelidd nouveau des phosphorites du Quercy. *Annales de Paléontologie, Vertébrés*, *56*, 73–91.

Law, C. J., Slater, G. J., & Mehta, R. S. (2018). Lineage diversity and size disparity in Musteloidea: Testing patterns of adaptive radiation using molecular and fossil-based methods. *Systematic Biology*, *67*(1), 127–144. https://doi.org/10.1093/sysbio/syx047

Lichtenstein, H. (1832). *Darstellung neuer oder wenig bekannter Säugethiere in Abbildungen und Beschreibungen: von fünf und sechzig Arten auf fünfzig colorirten Steindrucktafeln nach den Originalen des Zoologischen Museums der Universität zu Berlin*. C. G. Lüderitz.

Linnaeus, C. (1758). *Systema naturae per regna tria naturae, secundum classes, ordines, genera, species, cum characteribus, differentiis, synonymis, locis*. *Tomus*, vol *I*. Laurentius Salvius.

López-Martínez, N., Sesé, C., & Herráez, E. (1987). Los yacimientos de Micromamíferos del área de Madrid. *Boletín Geológico y Minero*, *98*, 159–176.

Lydekker, R. (1885). *Catalogue fossil Mammalia British Museum (Natural History)*. Taylor & Francis.

Mein, P. (1958). Les mammifères de la faune sidérolithique de Vieux-Collonges. *Nouvelles archives du Muséum d'histoire naturelle de Lyon*, *5*, 3–122. https://doi.org/10.3406/mhnly.1958.987

Mein, P. (1975). Biozonation du Néogène Méditerranéen à partir des Mammifères. *Proceedings VIth Congress of the RCMNS*, Bratislava, Slowakia, 18, table 1.

Merriam, C. H. (1890). Results of a biological survey of the San Francisco Mountain region and desert of the Little Colorado in Arizona. *North American Fauna*, *3*, 1–136.

Molina, J. I. (1782). *Saggio sulla storia naturale de Chili*. Stamperia di S. Tomaso d'Aquino.

Montes, M., Beaumud, B., Garcés, M., & Calvo J. P. (2006). Magnetoestratigrafía de las unidades Inferior e Intermedia del Mioceno de la Cuenca de Madrid. *Revista de la Sociedad Geológica de España*, *19*(3–4), 281–298.

Morales, J., Abella, J., Caballero, O., DeMiguel, D., Peláez-Campomanes, P., & Valenciano, A. (2025a). The enigmatic ailurid *Magerictis imperialensis* (Mammalia, Carnivora) unveiled: A systematic approach to the early Ailuridae [Dataset]. *MorphoBank*. https://doi.org/10.7934/P6014

Morales, J., Abella, J., Caballero, O., DeMiguel, D., Peláez-Campomanes, P., Valenciano, A. (2025b). The enigmatic ailurid *Magerictis imperialensis* (Mammalia, Carnivora) unveiled: A systematic approach to the early Ailuridae [Media list]. *MorphoSource*. https://doi.org/10.17602/M2/L780594

Morales, J., Mayda, S., Valenciano, A., DeMiguel, D., & Kaya, T. (2019). A new lophocyonid, *Izmirictis cani* gen. et sp. nov. (Carnivora: Mammalia), from the lower Miocene of Turkey. *Journal of Systematic Palaeontology*, *17*(16), 1347–1358. https://doi.org/10.1080/14772019.2018.1529000

Morlo, M. (1996). Carnivoren aus dem Unter-Miozan des Mainzer Beckens (2. Mustelida, Pinnipedia, Feliformia, Palaeogale). *Senckenbergiana lethaea*, *76*(1), 193–249. https://doi.org/10.1007/BF03042850

Morlo, M., & Kundrat, M. (2008). The first carnivoran fauna from the Ruscinian (Early Pliocene, MN 15) of Germany. *Paläontologische Zeitschrift*, *75*(2), 163–187. https://doi.org/10.1007/BF02988011

Morlo, M., & Peigné, S. (2010). Molecular and morphological evidence for Ailuridae and a review of its genera. In: A. Goswami & A. Friscia (Eds.), *Carnivoran evolution: New views on phylogeny, form, and function* (pp. 92–141). Cambridge University Press.

Nagel, D. (2003). Carnivora from the middle Miocene Hominoid locality of Çandir (Turkey). *Courier Forschungsinstitut Senckenberg*, *240*, 113–131.

Newton, E. F. (1890). On some new mammals from Red and Norwich Crags. *Quarterly Journal of the Geological Society of London*, *46*, 444–453. https://doi.org/10.1144/GSL.JGS.1890.046.01-04.29

Ogino, S., Nakaya, H., Nakai, M., Fukuchi, A., Maschenko, E. N., & Kalmykov, N. P. (2009). Mandible and lower dentition of *Parailurus baikalicus* (Ailuridae, Carnivora) from Transbaikal area, Russia. *Paleontological Research*, *13*(3), 259–264. https://doi.org/10.2517/1342-8144-13.3.259

Peigné, S. (2012). Les Carnivora de Sansan. In S. Peigné & S. Sen (Eds.), *Mammifères de Sansan* (pp. 559–660). Mémoires du Muséum national d'Histoire naturelle.

Peigné, S., Salesa, M. J., Antón, M., & Morales, J. (2005). Ailurid carnivoran mammal *Simocyon* from the late Miocene of Spain and the systematics of the genus. *Acta Palaeontologica Polonica*, *50*(2), 219–238.

Peláez-Campomanes, P., Morales, J., Álvarez-Sierra, M. A., Azanza, B., Fraile, S., García-Paredes, I., Hernández Fernández, M., Herráez, E., Nieto, M., Pérez, B., Quiralte, V., Salesa, M. J., Sánchez, I. M., & Soria, D. (2003). Updated biochronology of the Miocene mammal faunas from the Madrid basin (Spain). In J. W. F. Reumer, & W. Wessels (Eds.), *Distribution and migration of Tertiary mammals in Eurasia. A volume in honour of Hans de Bruijn* (pp. 431–441). Deinsea, 10.

Pesquero, M. D., Siliceo, G., Bárez, S., Salesa, M. J., & Morales, J. (2008). El Cañaveral: Un nuevo yacimiento del Aragoniense medio de Madrid. Libro de resúmenes. In J. I. Ruiz-Omeñaca, L. Piñuela, & J. C. García-Ramós (Eds.), *XXIV Jornadas de la Sociedad Española de Paleontología. Colunga (Asturias) 15–18 Octubre* (pp. 182–183). Museo del Jurásico de Asturias.

Pickford, M., & Laurent, Y. (2014). Valorisation of palaeontological collections: Nomination of a lectotype for *Conohyus simorrensis* (Lartet, 1851), Villefranche d'Astarac, France, and description of a new genus of tetraconodont. *Estudios Geológicos*, *70*, e002. https://doi.org/10.3989/egeol.41261.262

Pickford, M. & Morales, J. (2016). Basal middle Miocene Listriodontinae (Suidae, Artiodactyla) from Madrid, Spain. *Spanish Journal of Palaeontology*, *31*(2), 369–406. https://doi.org/10.7203/sjp.31.2.17162

Pilgrim, G. E. (1931). *Catalogue of the Pontian Carnivora of Europe in the Department of Geology*. British Museum (Natural History), London.

Pohle, H. (1917). *Pseudobassaris riggsi*, gen. nov., spec. nov. für *Amphictis* spec. Riggs. *Sitzungsberichte der Geselkchaft Naturforschender Freunde zu Berlin*, *1917*, 403–411.

Pomel, A. (1846). Mémoire pour servir à la géologie paléontologique des terrains tertiaires du département de

l'Ailier. *Bulletin de la Société Géologique de France, 2e ser., 3*, 353–373.

Pomel, A. (1853). Catalogue méthodique et descriptif des vertébrés fossiles découverts dans le bassin hydrographique supérieur de la Loire et surtout dans la vallée de son affluent principal l'Allier. In *Libraire de L'académie Impériale de Médecine*, *Paris* (pp. 3–193). Libraire de L'academie Imperiale de Medecine.

Roca, L. P., **Fraile, S.**, **Bernal, G.**, **Dumas, M.**, **Alonso, A.**, **Galindo, L., & Sánchez V. M.** (2009). Nuevos hallazgos Paleontologicos y Arqueologicos en el Intercambiador de Prıncipe Pıo. In *Plan de Intercambiadores* (pp. 172–179). Consorcio Regional de Transportes de Madrid.

Roth, C. (1987). *Die Raubtierfauna der miozänen Spaltenfüllungen Petersbuch 2 und Erkertshofen 2. Taxonomie – Stratigraphie – Ökologie*. [PhD dissertation, University of Mainz].

Roth, J., & Wagner, A. (1854). Die fossilen Knochen-Ueberreste von Pikermi in Griechenland. *Abh Königlich Bayer Akad Wiss, math-physikalische Kl*, *7*, 371–464.

Salesa, M. J., **Antón, M.**, **Peigné, S., & Morales, J.** (2006). Evidence of a false thumb in a fossil carnivore clarifies the evolution of pandas. *Proceedings of the National Academy of Sciences*, *103*(2), 379–382. https://doi.org/10.1073/pnas.0504899102

Salesa, M. J., **Antón, M.**, **Peigné, S., & Morales, J.** (2008). Functional anatomy and biomechanics of the postcranial skeleton of *Simocyon batalleri* (Viret, 1929) (Carnivora, Ailuridae) from the Late Miocene of Spain. *Zoological Journal of the Linnean Society*, *152*(3), 593–621. https://doi.org/10.1111/j.1096-3642.2007.00370.x

Salesa, M. J., **Gamarra, J.**, **Siliceo, G.**, **Antón, M. & Morales, J.** (2024). Unraveling the diversity of early felines: A new genus of Felinae (Carnivora, Felidae) from the Middle Miocene of Madrid (Spain). *Journal of Vertebrate Paleontology*, *43*(3), e2288924. https://doi.org/10.1080/02724634.2023.2288924

Salesa, M. J., **Peigné, S.**, **Antón, M., & Morales, J.** (2011). Evolution of the family Ailuridae: Origins and Old-World fossil record. In A. L. Glatston (Ed.). *Red panda biology and conservation of the first panda* (1st ed., pp. 27–41). Academic Press. https://doi.org/10.1016/B978-1-4377-7813-7.00003-3

Sánchez, I. M., **Salesa, M. J. & Morales, J.** (1998). Revisión Sistemática del género *Anchitherium* Meyer, 1834 (Equidae; Perrissodactyla) en España. *Estudios Geologicos*, *54*(1–2), 39–63. https://doi.org/10.3989/egeol.98541-2204

Sanisidro, O., **Alberdi, M. T., & Morales, J.** (2012). The first complete skull of *Hispanotherium matritense* (Prado, 1864) (Perissodactyla, Rhinocerotidae) from the middle Miocene of the Iberian Peninsula. *Journal of Vertebrate Paleontology*, *32*(2), 446–455. https://doi.org/10.1080/02724634.2012.639420

Sato, J. J., & Wolsan, M. (2012). Evolutionary origin of the red panda (*Ailurus fulgens*). *Honyurui Kagaku (Mammalian Science)*, *52*(1), 23–40. https://doi.org/10.11238/mammalianscience.52.23

Sato, J. J., **Wolsan, M.**, **Minami, S.**, **Hosoda, T.**, **Sinaga, M. H.**, **Hiyama, K.**, **Yamaguchi, Y., & Suzuki, H.** (2009). Deciphering and dating the red panda's ancestry and early adaptive radiation of Musteloidea. *Molecular Phylogenetics and Evolution*, *53*(3), 907–922. https://doi.org/10.1016/j.ympev.2009.08.019

Schaller, O. (2007). *Illustrated veterinary anatomical nomenclatures* (2nd ed.). Enke Verlag.

Schlosser, M. (1887). Die Affen, Lemuren Chiropteren, Insectivoren, Marsupialier, Creodonten und Carnivoren des europäischen Tertiärs, 1 Teil. *Beiträge zur Paläontologie Österreich-Ugarns und des Orients*, *6*(1–2), 1–224.

Schlosser, M. (1888). Die Affen, Lemuren Chiropteren, Insectivoren, Marsupialier, Creodonten und Carnivoren des europäischen Tertiärs, 1 Teil *Beiträge zur Paläontologie Österreich-Ugarns und des Orients*, *7*(1), 1–162.

Schlosser, M. (1899). *Parailurus anglicus* und *Ursus böckhi* aus den Ligniten von Baróth-Köpecz, Comitat Háromszék in Ungarn. *Mitt Jahrbuche Königlich Ungarischen Geol Anstalt*, *13*, 66–95.

Schmidt-Kittler, N. (1981). Zur Stammesgeschichte der marderverwandten Raubtiergruppen (Musteloidea, Carnivora). *Eclogae Geologicae Helvetiae*, *74*(3), 753–801.

Schreber, J. C. D. (1776). Die Saugthiere in Abbildungen nach der Natur, mit Beschreibungen. *Wolfgang Walther Erlangen*, *3*(17), 290–312.

Smith, J. B., & Dodson, P. (2003). A proposal for a standard terminology of anatomical notation and orientation in fossil vertebrate dentitions. *Journal of Vertebrate Paleontology*, *23*(1), 1–12. https://doi.org/10.1671/0272-4634(2003)23[1:APFAST]2.0.CO;2

Smith, K., **Czaplewski, N., & Cifelli, R. L.** (2016). Middle Miocene carnivorans from the Monarch Mill Formation, Nevada. *Acta Palaeontologica Polonica*, *61*(1), 231–252. https://doi.org/10.4202/app.00111.2014

Sotnikova, M. V. (2008). New species of lesser panda *Parailurus* (Mammalia, Carnivora) from Pliocene of Transbaikalia (Russia) and some aspects of ailurine phylogeny. *Paleontological Journal*, *42*(1), 90–99. https://doi.org/10.1134/S0031030108010152

Stock, C. (1947). A peculiar new carnivore from the Cuyama Miocene, California. *Southern California Academy of Sciences*, *46*, 84–89. https://doi.org/10.3160/0038-3872-46.2.84

Storr, G. C. C. (1780). *Prodromus methodi mammalium*. Reissian.

Swofford, D. L. (2002). *PAUP: Phylogenetic analysis using parsimony (and other methods), version 4*. Sinauer Associates, Sunderland, MA.

Tedford, R. H., **Albright III, L. B.**, **Barnosky, A. D.**, **Ferrusquía-Villafranca, I.**, **Hunt Jr., R. M.**, **Storer, J. E.**, **Swisher III, C. C.**, **Voorhies, M. R.**, **Webb, S. D.**, & **Whistler, D. P.** (2004). Mammalian biochronology of the Arikareean through Hemphillian interval (late Oligocene through early Pliocene epochs). In M. O. Woodburne (Ed.), *Late Cretaceous and Cenozoic mammals of North America: Biostratigraphy and geochronology* (pp. 169–231). Columbia University Press.

Tedford, R. H., & Gustafson, E. P. (1977). First North American record of the extinct panda *Parailurus*. *Nature*, *265*, 621–623. https://doi.org/10.1038/265621a0

Teilhard de Chardin, P. (1915). Les carnassiers des Phosphorites du Quercy. *Annales de Paléontologie*, *9*, 101–191.

Thenius, E. (1949a). Die Carnivoren von Göriach (Steiermark). Beiträge zur Kenntnis der Säugetierreste des steirischen Tertiärs IV. *Sitzungsberichten der Österreichischen Akademie der Wissenschaften, Mathematisch–Naturwissenschaftliche Klasse, Abteilung* **1**, 158, 695–762.

Thenius, E. (1949b). Zur Herkunft der Simocyoniden (Canidae, Mammalia). *Sitzungsberichten der Österreichischen Akademie der Wissenschaften, Mathematisch–Naturwissenschaftliche Klasse, Abteilung* **1**, 158, 799–810.

Thenius, E. (1977). Zur systematischen stellung von *Protursus* (Carnivora, Mammalia). *Anzeiger der Österreichischen Akademie der Wissenschaften, mathematisch – naturwissenschaflichen Klasse*, *3*, 37–41.

Thorpe, M. R. (1921). Two new fossil Carnivora. *American Journal of Science*, *1*(6), 477–483. https://doi.org/10.2475/ajs.s5-1.6.477

Toula, F. (1884). Ueber einige Säugethierreste von Göriach bei Turnau (Bruck, M.), Nord Steiermark. *Jahrbuch der kaiserlich-königlichen geologischen Reichsanstalt*, *34*, 385–401.

Valenciano, A., Baskin, J. A., Abella, J., Pérez-Ramos, A., Álvarez-Sierra, M. A., Morales, J., & Hartstone-Rose, A. (2016). *Megalictis*, the bone crushing giant mustelid (Carnivora, Mustelidae, Oligobuninae) from the lower Miocene of North America. *PLoS ONE*, *11*, e0152430. https://doi.org/10.1371/journal.pone.0152430

Van der Meulen, A. J., García-Paredes, I., Álvarez-Sierra, M. A., van den Hoek Ostende, L. W., Hordijk, K., Oliver, A., & Peláez-Campomanes, P. (2012). Updated Aragonian biostratigraphy: Small mammal distribution and its implications for the Miocene European chronology. *Geologica Acta*, *10*(2), 159–179. https://doi.org/10.1344/105.000001710

Viret, J. (1929a). *Cephalogale batalleri* carnassier du Pontien de Catalogne. *Bulletin de la Société d'Histoire Naturelle de Toulouse*, *58*, 567–68.

Viret, J. (1929b). Les faunes de mammiféres de l'Oligocène supérieur de la Limagne Bourbonnaise. *Annales de l'Université de Lyon*, *S. I. Sci. Med*, *47*, 1–328.

Viret, J. (1933). Contribution à l'étude des carnassiers Miocènes de la Grive-Saint-Alban (Isère). *Travaux du Laboratoire de Géologie de la Faculté des Sciences de Lyon*, *21*(18), 1–31.

Viret, J. (1951). Catalogue critique de la faune des mammifères miocènes de la Grive Saint-Alban. *Nouvelles Archives du Muséum d'Histoire Naturelle de Lyon*, *3*, 1–104.

Wagner, A. (1858). *Geschichte der Urwelt, mit besonderer Berücksichtigung der Menschenrassen und des mosaischen Schöpfungsberichtes* (2nd ed.). Leopold Voss.

Waibl, H., Gasse, H., Hashimoto, Y., Burdas, K. D., Constantinescu, G. M., Saber, A. S., Simoens, P., Salazar, I., Sotonyi, P., Augsburger, H., & Bragulla, H. (2005). *Nomina anatomica veterinaria* (5th ed.). Hannover, Columbia, Ghent and Sapporo: International Committee on Veterinary Gross Anatomical Nomenclature. World Association of Veterinary, Anatomists, Editorials Committee.

Wallace, S. C. (2011). Advanced members of the Ailuridae ('lesser' or red pandas subfamily Ailurinae). In A. L. Glatston (Ed.), *Red panda biology and conservation of the first panda* (1st ed., pp. 43–60). Academic Press. https://doi.org/10.1016/B978-1-4377-7813-7.00004-5

Wallace, S. C., & Lyon, L. M. (2022). Systematic revision of the Ailurinae (Mammalia: Carnivora: Ailuridae): With a new species from North America. In A. L. Glatston (Ed.), *Red panda biology and conservation of the first panda* (2nd ed., pp. 31–52). Academic Press. https://doi.org/10.1016/B978-0-12-823753-3.00011-9

Wallace, S. C., & Wang, X. (2004). Two new carnivores from an unusual late Tertiary forest biota in eastern North America. *Nature*, *431*(7008), 556–559. https://doi.org/10.1038/nature02819

Wang, X. (1997). New cranial material of *Simocyon* from China, and its implications for phylogenetic relationship to the red panda (*Ailurus*). *Journal of Vertebrate Paleontology*, *17*(1), 184–198. https://doi.org/10.1080/02724634.1997.10010963

Wang, X., Emry, R. J., Boyd, C. A., Person, J. J., White, S. C., & Tedford, R. H. (2023). An exquisitely preserved skeleton of *Eoarctos vorax* (nov. gen. et sp.) from Fitterer Ranch, North Dakota (early Oligocene) and systematics and phylogeny of North American early arctoids (Carnivora, Caniformia). Society of Vertebrate Paleontology Memoir 22. *Journal of Vertebrate Paleontology*, *42*(suppl. 1), 1–123. https://doi.org/10.1080/02724634.2022.2145900

Wang, X., Ye, J., Wu, W., Liu, L., & Bi, S. (1998). Carnivora from Middle Miocene of Northern Junggar Basin, Xinjiang Autonomous Region, China. *Vertebrata PalAsiatica*, *36*, 218–243.

Waterhouse, G. R. (1838). On the skull of the American badger. *Proceedings of the Zoological Society of London*, *6*, 153–154.

Webb, S. D. (1969). The Pliocene Canidae of Florida. *Bulletin of the Florida State Museum: Biological Science*, *14*(4), 273–308.

Wegner, R. N. (1913). Tertiär und umgelagerte Kreide bei Oppeln (Oberschlesien). *Palaeontographica*, *60*(3–4), 175–274.

Werdelin, L. (2005). The Carnivora of Rudabànya (MN 9, Late Miocene, Hungary). *Palaeontographia Italica*, *90*, 163–180.

Winge, H. (1895). *Jordfundne og nulevende rovdyr (Carnivora) fra Lagoa Santa, Minas Geraes, Brasilien: med udsigt over pungdyrenes slægtskab*. F. Dreyer. https://doi.org/10.5962/bhl.title.14825

Winter, S., Fennessy, J., Janke, A., & Nilsson, M. A. (2023). Northern olingo (*Bassaricyon gabbi*), zorilla (*Ictonyx striatus*), and honey badger (*Mellivora capensis*) mitochondrial genomes and a phylogeny of Musteloidea. *Frontiers in Ecology and Evolution*, *10*, 1089641. https://doi.org/10.3389/fevo.2022.1089641

Wolsan, M. (1993). Phylogeny and classification of early European Mustelida (Mammalia: Carnivora). *Acta Theriologica*, *38*(4), 345–384. https://doi.org/10.4098/AT.arch.93-29

Wolsan, M., & Lange-Badré, B. (1996). An arctomorph carnivoran skull from the Phosphorites du Quercy and the origin of procyonids. *Acta Palaeontologica Polonica*, *41*(3), 277–298.

Zapfe, H. (1950). Die Fauna der miozänen Spaltenfüllung von Neudorf an der March (CSR.). Carnivora. *Sitzungsberichte Der Akademie Der Wissenschaften Mathematisch-Naturwissenschaftliche Klasse*, *159*, 99–141.

Zdanzky, O. (1924). Jungtertiäre carnivoren Chinas. *Palaeontologia Sinica*, *2*(1), 1–149.

Associate Editor: Dr Stephan Spiekman